

7  
-25-939 S (2)



ORNL/TM-10701  
Dist. Category UC-535

OAK RIDGE  
NATIONAL  
LABORATORY

MARTIN MARIETTA

Analysis of the JASPER Program Radial  
Shield Attenuation Experiment

C. O. Slater

MASTER

MANAGED BY  
MARTIN MARIETTA ENERGY SYSTEMS, INC.  
FOR THE UNITED STATES  
DEPARTMENT OF ENERGY

DISTRIBUTION OF THIS DOCUMENT IS UNLIMITED

This report has been reproduced directly from the best available copy.

Available to DOE and DOE contractors from the Office of Scientific and Technical Information, P.O. Box 62, Oak Ridge, TN 37831; prices available from (615) 576-8401, FTS 626-8401.

This report was prepared as an account of work sponsored by an agency of the United States Government. Neither the United States Government nor any agency thereof, nor any of their employees, makes any warranty, express or implied, or assumes any legal liability or responsibility for the accuracy, completeness, or usefulness of any information, apparatus, product, or process disclosed, or represents that its use would not infringe privately owned rights. Reference herein to any specific commercial product, process, or service by trade name, trademark, manufacturer, or otherwise, does not necessarily constitute or imply its endorsement, recommendation, or favoring by the United States Government or any agency thereof. The views and opinions of authors expressed herein do not necessarily state or reflect those of the United States Government or any agency thereof.

ORNL/TM-10701  
Dist. Category UC-535

Engineering Physics and Mathematics

Analysis of the JASPER Program Radial Shield  
Attenuation Experiment

C. O. Slater

Date Published—January 1993

**DISCLAIMER**

This report was prepared as an account of work sponsored by an agency of the United States Government. Neither the United States Government nor any agency thereof, nor any of their employees, makes any warranty, express or implied, or assumes any legal liability or responsibility for the accuracy, completeness, or usefulness of any information, apparatus, product, or process disclosed, or represents that its use would not infringe privately owned rights. Reference herein to any specific commercial product, process, or service by trade name, trademark, manufacturer, or otherwise does not necessarily constitute or imply its endorsement, recommendation, or favoring by the United States Government or any agency thereof. The views and opinions of authors expressed herein do not necessarily state or reflect those of the United States Government or any agency thereof.

---

Prepared by the  
OAK RIDGE NATIONAL LABORATORY  
Oak Ridge, Tennessee 37831  
managed by  
MARTIN MARIETTA ENERGY SYSTEMS, INC.  
for the  
U.S. DEPARTMENT OF ENERGY  
under contract DE-AC05-84OR21400

**MASTER**

HH  
DISTRIBUTION OF THIS DOCUMENT IS UNLIMITED

11/11/18

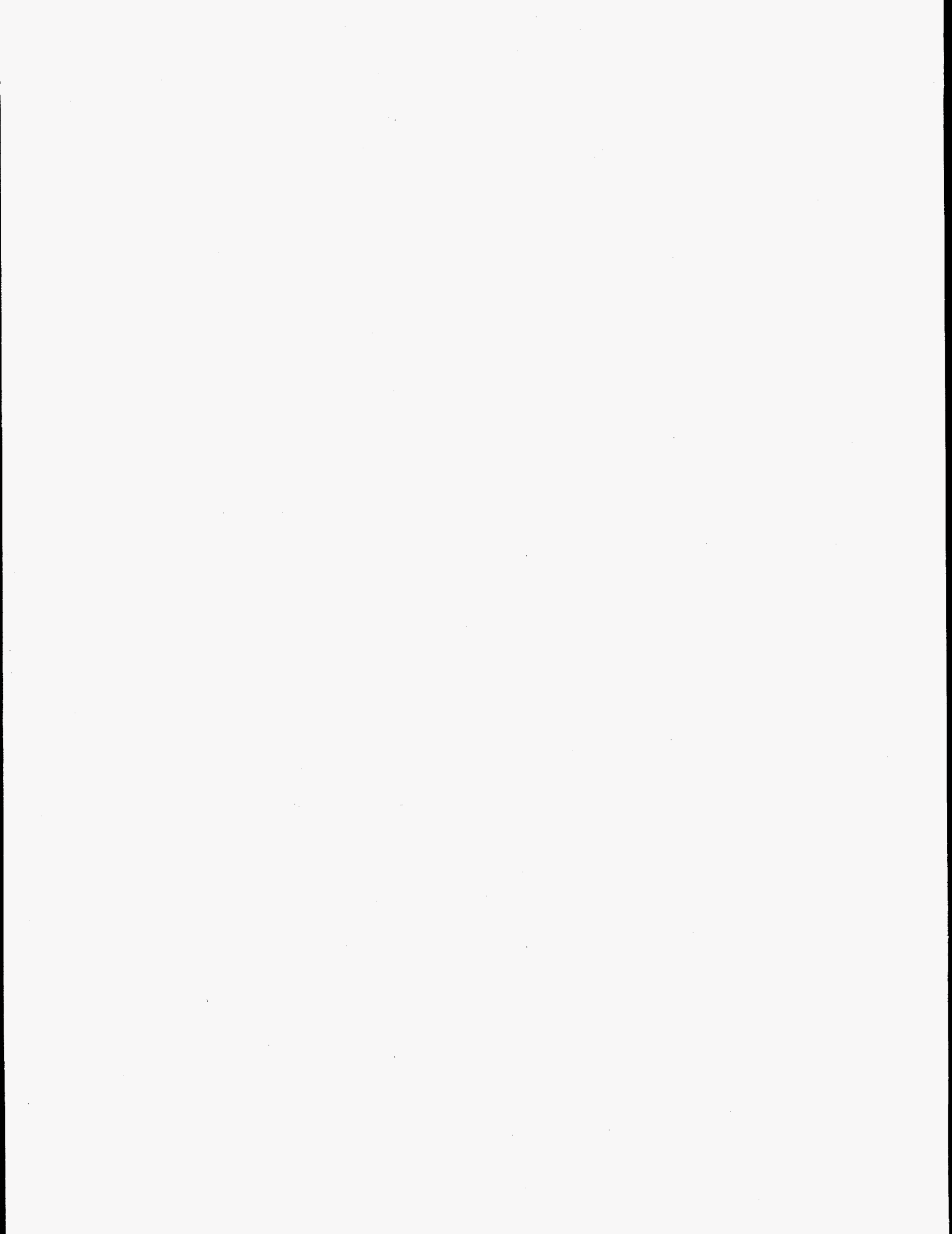
11/11/18

**DISCLAIMER**

**Portions of this document may be illegible in electronic image products. Images are produced from the best available original document.**

## TABLE OF CONTENTS

LIST OF FIGURES .....	v
LIST OF TABLES .....	ix
ABSTRACT .....	xii
ACKNOWLEDGMENTS .....	xiii
I. INTRODUCTION .....	1
2. EXPERIMENTAL DESIGN .....	3
3. ANALYSIS OF THE EXPERIMENT .....	7
4. CONCLUSIONS .....	59
APPENDIX A .....	61
APPENDIX B .....	79
APPENDIX C .....	103
REFERENCES .....	117



## LIST OF FIGURES

	<u>Page</u>
Fig. 1. The Tower Shielding Reactor-II (TSR-II) with its wide-beam collimator . . . . .	4
Fig. 2. Comparison of ENDF/B-V (Mat. 1160) and LLNL (Mat. 8811) <sup>11</sup> B total cross sections in the 61-group structure . . . . .	11
Fig. 3. Calculated versus measured E > 0.05 MeV neutron spectra on centerline 178.8 cm behind Configuration I.A . . . . .	13
Fig. 4. Calculated versus measured E > 0.05 MeV neutron spectra on centerline 47.3 cm behind Configuration II.D . . . . .	14
Fig. 5. Calculated versus measured E > 0.05 MeV neutron spectra on centerline 42.8 cm behind Configuration IV.C . . . . .	14
Fig. 6. Calculated versus measured E > 0.05 MeV neutron spectra on centerline 51.1 cm behind Configuration VI.A . . . . .	15
Fig. 7. Calculated versus measured E > 0.05 MeV neutron spectra on centerline 63.2 cm behind Configuration VI.F . . . . .	15
Fig. 8. Comparison of normalized calculated neutron spectra behind the two spectrum modifiers . . . . .	16
Fig. 9. Comparison of calculated and measured 5-in. Bonner ball count rates for a horizontal traverse 30 cm behind Configuration I.A (C/E range: 0.74-1.06) . . .	33
Fig. 10. Comparison of calculated and measured 5-in. Bonner ball count rates for a horizontal traverse 30 cm behind Configuration II.A (C/E range: 0.75-0.92) . .	34
Fig. 11. Comparison of calculated and measured 5-in. Bonner ball count rates for a horizontal traverse 30 cm behind Configuration II.D (C/E range: 0.28-0.58) . .	35
Fig. 12. Comparison of calculated and measured 5-in. Bonner ball count rates for a horizontal traverse 30 cm behind Configuration II.E (C/E range: 0.46-0.59) . .	36
Fig. 13. Comparison of calculated and measured 5-in. Bonner ball count rates for a horizontal traverse 30 cm behind Configuration III.A (C/E range: 0.96-1.09) . .	37
Fig. 14. Comparison of calculated and measured 5-in. Bonner ball count rates for a horizontal traverse 30 cm behind Configuration III.B (C/E range: 0.81-0.94) . .	38
Fig. 15. Comparison of calculated and measured 5-in. Bonner ball count rates for a horizontal traverse 30 cm behind Configuration III.C (C/E range: 0.77-0.89) . .	39



## LIST OF FIGURES (Cont'd)

	<u>Page</u>
Fig. 16. Comparison of calculated and measured 5-in. Bonner ball count rates for a horizontal traverse 30 cm behind Configuration III.E (C/E range: 0.66-0.82) . .	40
Fig. 17. Comparison of calculated and measured 5-in. Bonner ball count rates for a horizontal traverse 30 cm behind Configuration IV.A (C/E range: 0.76-0.87) . .	41
Fig. 18. Comparison of calculated and measured 5-in. Bonner ball count rates for a horizontal traverse 30 cm behind Configuration IV.C (C/E range: 0.71-0.95) . .	42
Fig. 19. Comparison of calculated and measured 5-in. Bonner ball count rates for a horizontal traverse 30 cm behind Configuration IV.G (C/E range: 0.32-0.61) . .	43
Fig. 20. Comparison of calculated and measured 5-in. Bonner ball count rates for a horizontal traverse 30 cm behind Configuration V.A (C/E range: 0.93-1.08) . .	44
Fig. 21. Comparison of calculated and measured 5-in. Bonner ball count rates for a horizontal traverse 30 cm behind Configuration V.B (C/E range: 0.90-1.02) . .	45
Fig. 22. Comparison of calculated and measured 5-in. Bonner ball count rates for a horizontal traverse 30 cm behind Configuration V.D (C/E range: 0.87-1.01) . .	46
Fig. 23. Comparison of calculated and measured 5-in. Bonner ball count rates for a horizontal traverse 30 cm behind Configuration V.G (C/E range: 0.87-1.06) . .	47
Fig. 24. Comparison of calculated and measured 5-in. Bonner ball count rates for a horizontal traverse 30 cm behind Configuration V.J (C/E range: 1.13-1.28) . . .	48
Fig. 25. Comparison of calculated and measured 5-in. Bonner ball count rates for a horizontal traverse 30 cm behind Configuration VI.A (C/E range: 0.72-0.87) . .	49
Fig. 26. Comparison of calculated and measured 5-in. Bonner ball count rates for a horizontal traverse 30 cm behind Configuration VI.B (C/E range: 0.79-0.89) . .	50
Fig. 27. Comparison of calculated and measured 5-in. Bonner ball count rates for a horizontal traverse 30 cm behind Configuration VI.D (C/E range: 0.79-0.87) . .	51
Fig. 28. Comparison of calculated and measured 5-in. Bonner ball count rates for a horizontal traverse 30 cm behind Configuration VI.F (C/E range: 0.80-0.89) . .	52
Fig. 29. Comparison of calculated and measured 5-in. Bonner ball count rates for a horizontal traverse 30 cm behind Configuration VII.A (C/E range: 0.70-0.82) . .	53
Fig. 30. Comparison of calculated and measured 5-in. Bonner ball count rates for a horizontal traverse 30 cm behind Configuration VII.B (C/E range: 0.65-0.76) . .	54

## LIST OF FIGURES (Cont'd)

	<u>Page</u>
Fig. 31. Comparison of calculated and measured 5-in. Bonner ball count rates for a horizontal traverse 30 cm behind Configuration VII.C (C/E range: 0.56-0.73) .	55
Fig. 32. Comparison of calculated 61-broad-group and 174-fine-group fast-neutron spectra with the measured spectrum on centerline 47.3 cm behind Configuration II.D . . . . .	57
Fig. 33. Comparison of calculated 61-broad-group and 174-fine-group fast-neutron spectra with the measured spectrum on centerline 63.2 cm behind Configuration VI.F . . . . .	57
Fig. B1. Sketch of the configuration for measurements under section I.A of the experimental program plan . . . . .	80
Fig. B2. Sketch of the configuration for measurements under section V.A of the experimental program plan . . . . .	81
Fig. B3. Sketch of the configuration for measurements under sections II.A-C,E and II.D (3-5) of the experimental program plan . . . . .	82
Fig. B4. Sketch of the configuration for measurements under sections II.D (1-2) of the experimental program plan . . . . .	83
Fig. B5. Sketches of the stainless steel containers used to form the B <sub>4</sub> C shield slabs . .	84
Fig. B6. Sketch of the configuration for measurements under sections III.A,C-E of the experimental program plan . . . . .	85
Fig. B7. Sketch of the configuration for measurements under section III.B of the experimental program plan . . . . .	86
Fig. B8. Sketch of the configuration for measurements under section IV.A of the experimental program plan . . . . .	87
Fig. B9. Sketch of the configuration for measurements under section IV.B of the experimental program plan . . . . .	88
Fig. B10. Sketch of the configuration for measurements under sections IV.C (1-2) of the experimental program plan . . . . .	89
Fig. B11. Sketch of the configuration for measurements under sections IV.C (3-5) through IV.I of the experimental program plan . . . . .	90

## LIST OF FIGURES (Cont'd)

	<u>Page</u>
Fig. B12. Sketch of the configuration for measurements under section IV.IA of the experimental program plan .....	91
Fig. B13. Sketch of the configuration for measurements under section IV.J of the experimental program plan .....	92
Fig. B14. Sketch of the configuration for measurements under section IV.K of the experimental program plan .....	93
Fig. B15. Sketch of the configuration for measurements under section IV.L of the experimental program plan .....	94
Fig. B16. Sketch of the configuration for measurements under section IV.M of the experimental program plan .....	95
Fig. B17. Sketch of the configuration for measurements under sections V.B-D of the experimental program plan .....	96
Fig. B18. Sketch of the configuration for measurements under sections V.E-G of the experimental program plan .....	97
Fig. B19. Sketch of the configuration for measurements under sections V.H-J of the experimental program plan .....	98
Fig. B20. Sketch of the configuration for measurements under sections VI.A (1-2) of the experimental program plan .....	99
Fig. B21. Sketch of the configuration for measurements under sections VI.A (3-5) through VI.E and VI.F (3-5) of the experimental program plan .....	100
Fig. B22. Sketch of the configuration for measurements under sections VI.F (1-2) of the experimental program plan .....	101
Fig. B23. Sketch of the configuration for measurements under sections VII.A-D of the experimental program plan .....	102

## LIST OF TABLES

	<u>Page</u>
Table 1. Atomic Densities ( $b^{-1} \cdot cm^{-1}$ ) for Constituents of Materials Used in the Experiment Calculations .....	9
Table 2. Bulk Densities for $B_4C$ Powder in Slabs .....	10
Table 3. Comparison of Calculated and Measured Bonner Ball Count Rates ( $s^{-1} \cdot W^{-1}$ ) at the Spectrum Measurement Locations .....	17
Table 4. Comparison of Calculated and Measured Bare $BF_3$ Detector Count Rates ( $s^{-1} \cdot W^{-1}$ ) Close Behind Configurations .....	19
Table 5. Comparison of Calculated and Measured Cd-Covered $BF_3$ Count Rates ( $s^{-1} \cdot W^{-1}$ ) Close Behind Configurations .....	20
Table 6. Comparison of Calculated and Measured 3-in Bonner Ball Count Rates ( $s^{-1} \cdot W^{-1}$ ) Close Behind Configurations .....	21
Table 7. Comparison of Calculated and Measured 5-in. Bonner Ball Count Rates ( $s^{-1} \cdot W^{-1}$ ) Close Behind Configurations .....	22
Table 8. Comparison of Calculated and Measured 8-in. Bonner Ball Count Rates ( $s^{-1} \cdot W^{-1}$ ) Close Behind Configurations .....	23
Table 9. Comparison of Calculated and Measured 10-in. Bonner Ball Count Rates ( $s^{-1} \cdot W^{-1}$ ) Close Behind Configurations .....	24
Table 10. Comparison of Calculated and Measured Bare $BF_3$ Detector Count Rates ( $s^{-1} \cdot W^{-1}$ ) Behind Configurations at Large Distances from the TSR-II Core Center .....	26
Table 11. Comparison of Calculated and Measured Cd-Covered $BF_3$ Detector Count Rates ( $s^{-1} \cdot W^{-1}$ ) Behind Configurations at Large Distances from the TSR-II Core Center .....	27
Table 12. Comparison of Calculated and Measured 3-in. Bonner Ball Count Rates ( $s^{-1} \cdot W^{-1}$ ) Behind Configurations at Large Distances from the TSR-II Core Center .....	28
Table 13. Comparison of Calculated and Measured 5-in. Bonner Ball Count Rates ( $s^{-1} \cdot W^{-1}$ ) Behind Configurations at Large Distances from the TSR-II Core Center .....	29

## LIST OF TABLES (Cont'd)

	<u>Page</u>
Table 14. Comparison of Calculated and Measured 8-in. Bonner Ball Count Rates ( $s^{-1} \cdot W^{-1}$ ) Behind Configurations at Large Distances from the TSR-II Core Center .....	30
Table 15. Comparison of Calculated and Measured 10-in. Bonner Ball Count Rates ( $s^{-1} \cdot W^{-1}$ ) Behind Configurations at Large Distances from the TSR-II Core Center .....	31
Table 16. Comparison of Calculated and Measured Bonner Ball Count Rates ( $s^{-1} \cdot W^{-1}$ ) in the Shielded Void Region of Several Configurations IV .....	32
Table 17. Sensitivities of Neutron Fluxes to Neutron Cross Sections of Various Elements Comprising the Shields of Configuration II.D (1-2) .....	58
Table 18. Sensitivities of Neutron Fluxes to Neutron Cross Sections of Various Elements Comprising the Shields of Configuration IV.H .....	58
Table C1. 51-Group Response Function for the Bare $BF_3$ Detector. Units are: (Counts $\cdot$ $cm^2$ /neutron) .....	104
Table C2. 51-Group Response Function for the Cd-Covered $BF_3$ Detector. Units are: (Counts $\cdot$ $cm^2$ /neutron) .....	105
Table C3. 51-Group Response Function for the 3-inch Bonner Ball. Units are: (Counts $\cdot$ $cm^2$ /neutron) .....	106
Table C4. 51-Group Response Function for the 5-inch Bonner Ball. Units are: (Counts $\cdot$ $cm^2$ /neutron) .....	107
Table C5. 51-Group Response Function for the 8-inch Bonner Ball. Units are: (Counts $\cdot$ $cm^2$ /neutron) .....	108
Table C6. 51-Group Response Function for the 10-inch Bonner Ball. Units are: (Counts $\cdot$ $cm^2$ /neutron) .....	109
Table C7. 61-Group Response Function for the Bare $BF_3$ Detector. Units are: (Counts $\cdot$ $cm^2$ /neutron) .....	110
Table C8. 61-Group Response Function for the Cd-Covered $BF_3$ Detector. Units are: (Counts $\cdot$ $cm^2$ /neutron) .....	111
Table C9. 61-Group Response Function for the 3-inch Bonner Ball. Units are: (Counts $\cdot$ $cm^2$ /neutron) .....	112

## LIST OF TABLES (Cont'd)

	<u>Page</u>
Table C10. 61-Group Response Function for the 5-inch Bonner Ball. Units are: (Counts · cm <sup>2</sup> /neutron) .....	113
Table C11. 61-Group Response Function for the 8-inch Bonner Ball. Units are: (Counts · cm <sup>2</sup> /neutron) .....	114
Table C12. 61-Group Response Function for the 10-inch Bonner Ball. Units are: (Counts · cm <sup>2</sup> /neutron) .....	115

## ABSTRACT

The results of the analysis of the JASPER Program Radial Shield Attenuation Experiment are presented. The experiment was performed in 1986 at the ORNL Tower Shielding Facility. It is the first of six experiments in this cooperative Japanese and American program in support of shielding designs for advanced sodium-cooled reactors. Six different shielding configurations and subconfigurations thereof were studied. The configurations were calculated with the DOT-IV two-dimensional discrete ordinates radiation transport computer code using the R-Z geometry option, a symmetric  $S_{12}$  quadrature (96 directions), and cross sections from ENDF/B versions IV and V in either a 51- or 61-group structure. Auxiliary codes were used to compute detector responses and prepare cross sections and source input for the DOT-IV calculations. Calculated detector responses were compared with measured responses and the agreement was good to excellent in many cases. However, the agreement for configurations having thick steel or  $B_4C$  regions or for some very large configurations was fair to poor. The disagreement was attributed to cross-section data, broad-group structure, or high background in the measurements. In particular, it is shown that two cross-section sets for  $^{11}B$  give very different results for neutron transmission through the thick  $B_4C$  regions used in one set of experimental configurations. Implications for design calculations are given.

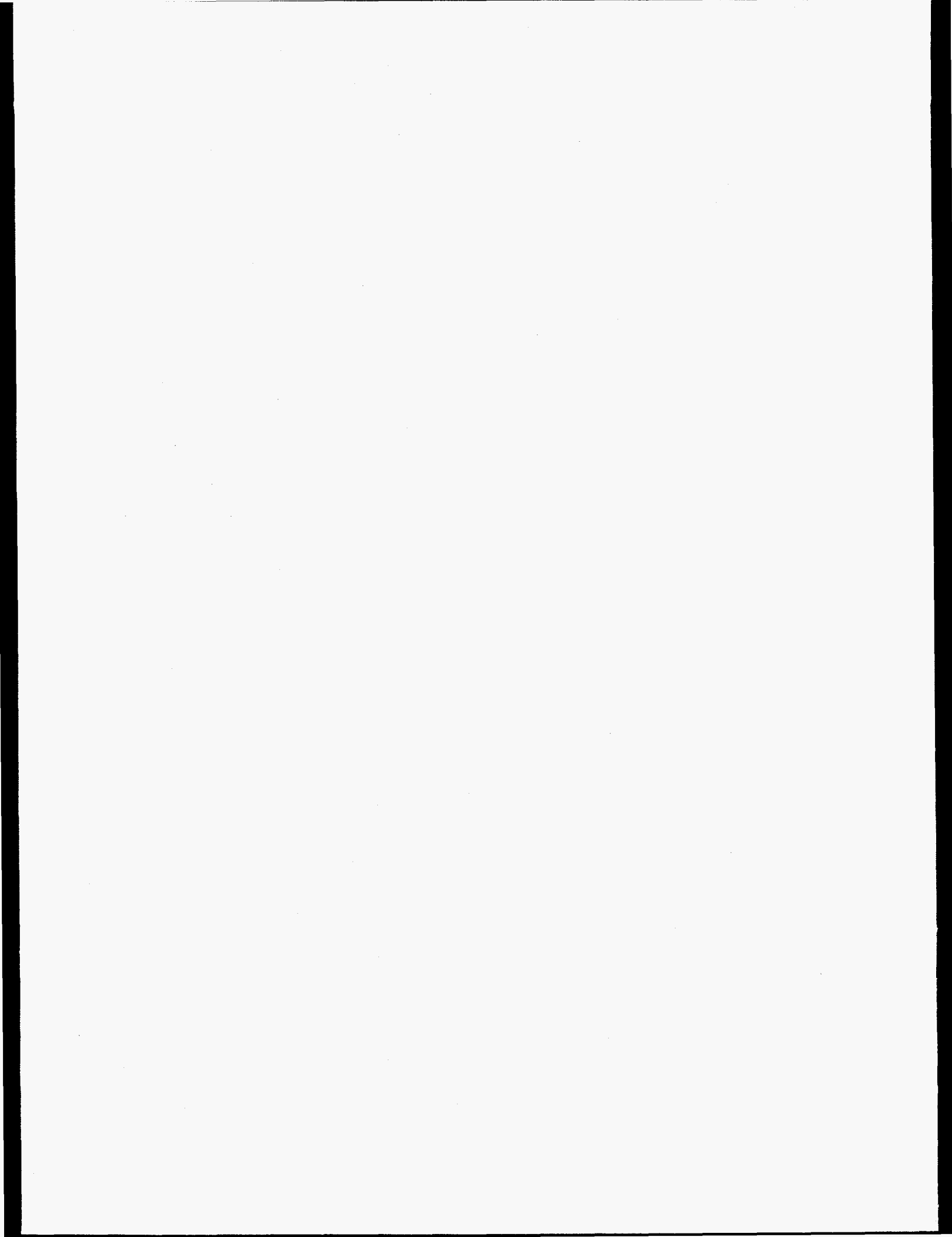
## ACKNOWLEDGMENTS

The author greatly appreciates the discussions with D. T. Ingersoll, W. W. Engle, Jr., and F. J. Muckenthaler during the analysis of this experiment. The reviewers (Larry Williams and Mark Smith) are thanked for their valuable services. The program direction of D. T. Ingersoll and W. W. Engle, Jr. is appreciated. Due to a shutdown of the JASPER Program for a 3-year period at the TSF, this report has been in production for several years. The author thanks A. C. Alford and Gail Marvin for their earlier work in preparing the manuscript and C. R. Householder for her work in completing the final manuscript.



## 1.0 INTRODUCTION

The shielding of components within liquid metal fast breeder reactor (LMFBR) designs is usually accomplished with combinations of stainless steel, boron carbide ( $B_4C$ ), and graphite, together with any thick sodium regions between the core and the component. Calculated radiation levels at those components can be quite uncertain due to: (1) the large number of mean-free-paths through which the radiation must be transported (deep penetration), (2) the three-dimensional complexities of the calculational geometry, and (3) the uncertainties associated with the methods and data used to calculate the radiation levels. A joint experimental program between the United States Department of Energy and the Japanese Power Reactor and Nuclear Fuel Development Corporation (PNC) was designed to address those concerns. The Japanese-American Shielding Program of Experimental Research (JASPER) consists of six experiments which would provide data that could be used to design LMFBR shields or verify calculational methods and data used to calculate radiation transport through those shields. Reported here are the results of the analysis of the first of the JASPER experiments, the Radial Shield Attenuation Experiment, which was performed in 1986 at the ORNL Tower Shielding Facility.<sup>1</sup>



## 2.0 THE EXPERIMENTAL DESIGN

The experiment consisted of slab mockups of six proposed LMFBR shield designs and sub-mockups thereof placed after a spectrum modifier that was positioned in front of the Tower Shielding Reactor, a schematic drawing of which is shown in Fig. 1. The sub-mockups were included to isolate the shielding effect of various portions of the shield and to provide checkpoints for the calculations. In this report, the configurations are identified by the section numbers in the Experimental Program Plan found in Appendix A. The configurations are described briefly.

Two spectrum modifiers were used. The first of the spectrum modifiers (SM1) is shown in Fig. B1. It consists of slabs of carbon steel (10 cm), aluminum (9 cm), and boral (2.5 cm) followed by two 10.1-cm-thick natural UO<sub>2</sub> blankets. This is Configuration IA of the experimental program plan. It is used for all except one set of configurations. The second of the spectrum modifiers (SM2) is shown in Fig. B2. It consists of carbon steel (10 cm), aluminum (9 cm), boral (2.5 cm), and sodium (183 cm plus 7.62 cm of aluminum in the walls of the six tanks) and is designated Configuration V.A in the experimental program plan. It is used only for configurations under section V of the plan.

Configurations II are shown in Figs. B3 and B4. These configurations represent near-core shields containing stainless steel and B<sub>4</sub>C, with a thick B<sub>4</sub>C region following a moderately thick stainless steel region. The five B<sub>4</sub>C slabs shown in Fig. B5 were used to create the three 15.2-cm-thick shield segments called for in the plan. Note that the experimental program plan gives nominal thicknesses for the slab combinations, while the figures show the actual thicknesses. Fig. B4 shows an arrangement required to measure the neutron spectrum behind configuration II.D. Because of a high gamma-ray field, 7.62 cm of lead had to be used behind the configuration in order to obtain good spectrum data. Other measurements were made without the lead slabs; therefore, there are two Configurations II.D, each being further defined by the measurement subsections pertaining to them [e.g. II.D(1,2) and II.D(3-5)]. The same applies to the other configurations for which lead was added in order to measure the neutron spectrum. Note also that the aluminum slabs in the shield mockups represent sodium-filled regions between shield components. The slabs are thinner than the sodium-filled regions they represent because aluminum is the better neutron attenuator.

Configurations III are shown in Figs. B6 and B7. These configurations are called benchmark and consist of stainless steel or stainless steel and B<sub>4</sub>C slabs following SM1.

Configurations IV are shown in Figs. B8-B16. These configurations represent the shield for a pool-type LMFBR and they consist of slabs of stainless steel, graphite, and B<sub>4</sub>C all following SM1. Many of these shields were so optically thick that radiation coming around the shield mockup created a large background problem for the measurements. Thus, beginning at section IV.I of the program plan, the plan was altered so that measurements would be made in a completely enclosed and shielded void region to reduce background interference (see Figs. B13-B16).

Configurations V are shown in Figs. B2 and B17-B19. They consist of SM2 and slabs of stainless steel, B<sub>4</sub>C, and sodium and represent the shield for the intermediate heat exchanger in a pool-type LMFBR. The thicknesses shown for the sodium tanks are centerline measurements. The tanks are nominally 31.75 cm thick with 0.635-cm end wall

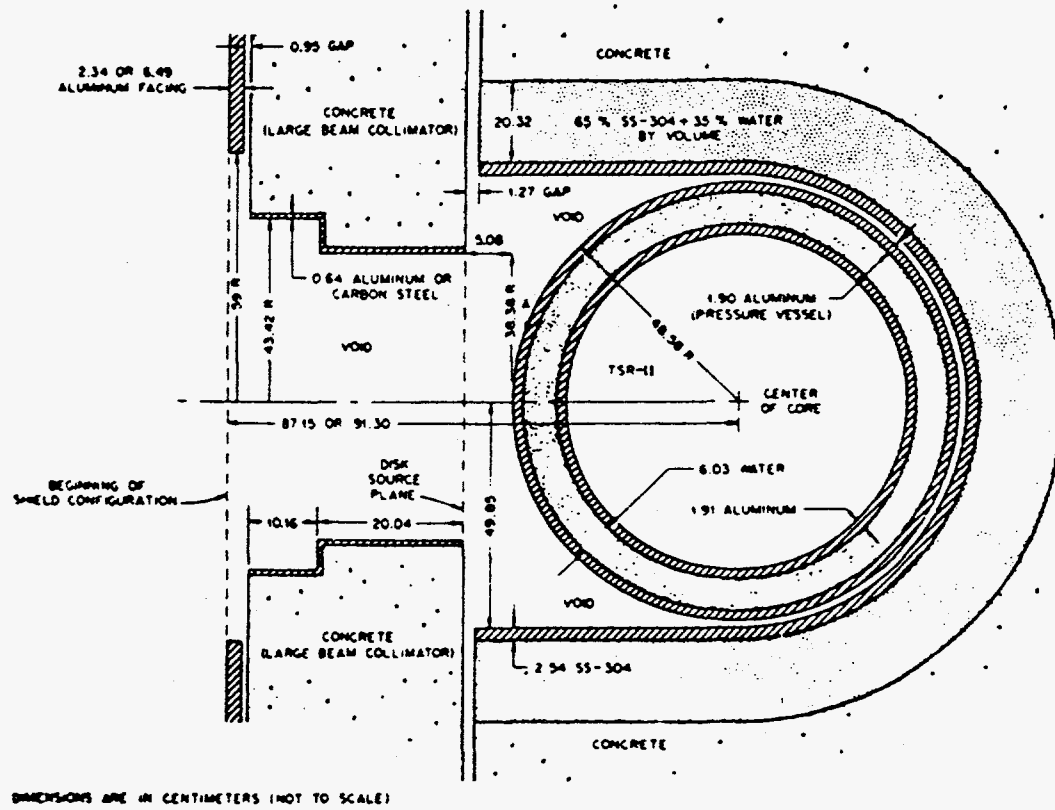


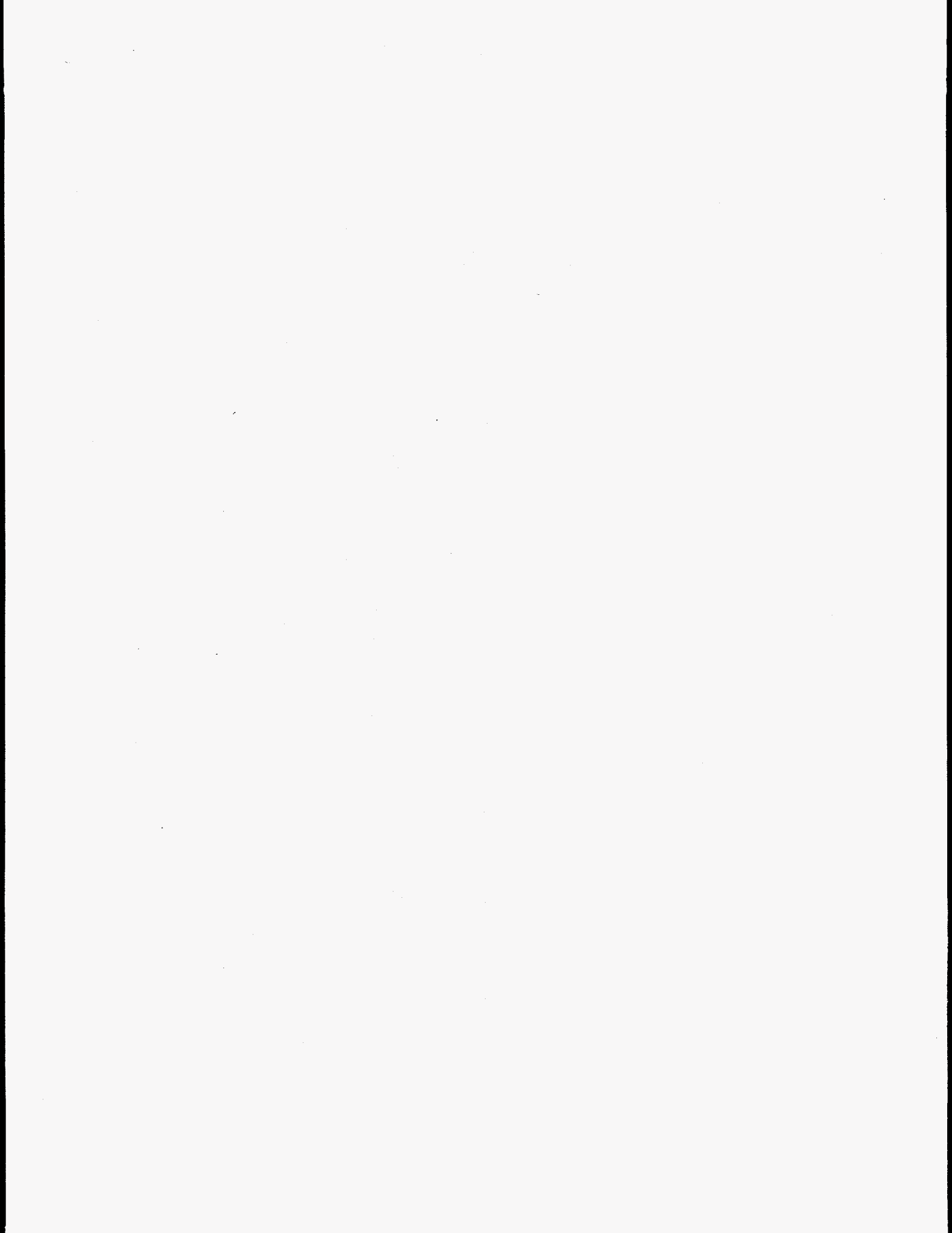
Fig. 1. The Tower Shielding Reactor-II (TSR-II) with its wide-beam collimator.

and 1.27-cm side wall thicknesses. Bulging, sagging, and bending of the tanks causes the wide variations in the thicknesses shown in the figures.

Configurations VI are shown in Figs. B20-B22 and are called the graphite benchmark. The configurations consist of SM1 followed by about 15 cm of stainless steel and various thicknesses of graphite. The two spectrum measurements required either lead alone or  $B_4C$  and lead to reduce the gamma-ray background.

Finally, Configurations VII are shown in Fig. B23. Like Configurations II, these also represent a near-core shield. However, the shield represented is one having a thick region of stainless steel followed by a moderately thick  $B_4C$  region and sodium. The mockups are preceded by SM1.

As the program plan shows (Appendix A), measurements were made with the bare and Cd-covered  $BF_3$  detectors, the 3-, 5-, 8-, and 10-in Bonner balls *in situ*, 30 cm behind configurations, at locations where spectra were measured (3-, 4-, 5-, and 10-in balls only), and behind configurations at large distances from the reactor center. The Bonner balls consist of cadmium-covered spherical shells of polyethylene around a 5.08-cm-diameter spherical  $BF_3$  chamber. Note that the bare and Cd-covered  $BF_3$  detectors are special cases of the Bonner balls having no polyethylene around them. Measurements were made with the PNC  $^3He$  detectors at the Bonner ball positions described above. Spectra were measured behind five configurations (I.A, II.D, IV.C, VI.A, and VI.F) with the NE-213 and Benjamin (hydrogen counter) spectrometers. The NE-213 spectrometer covers an energy range of 0.8 to 15.0 MeV and the three hydrogen counters (1, 3, and 10 atmospheres) cover the energy range 50 keV to 1.5 MeV.



## 3.0 ANALYSIS OF THE EXPERIMENT

### 3.1 Analysis Methods and Input Data

#### 3.1.1 Calculational Methods

Calculations of neutron transport through the configurations were performed mainly with the DOT-IV<sup>2</sup> two-dimensional discrete ordinates radiation transport computer code using the R-Z geometry option. (For the Cray computer, on which some of the calculations were performed, "DORT" is the analogous code.) DOT-IV was also used to calculate neutron fluxes in a limited void region behind the configurations when that void was not included in the geometry mockup for the configuration. The void region was one large enough to contain all the detector positions close behind the configurations (i.e., the 30-cm centerline and traverse measurements, other close-in measurements for Configurations IV, and all spectrum measurement positions except that for Configuration I.A). Diagnostic and parameter-study cases were run using the ANISN<sup>3</sup> one-dimensional discrete ordinates radiation transport code with the spherical geometry option. This code was used to check the effects of group structure, cross-section sets or versions, and material densities on calculated detector responses. It was also used to generate the forward and adjoint fluxes used in the limited sensitivity calculations which were performed with the SWANLAKE<sup>4</sup> code.

Calculated detector responses were obtained in one of three ways. First, the measured fast-neutron spectra were assumed to be point values; therefore, for comparisons with measured values, the DOT-IV-calculated fluxes were used without modification. Second, Bonner ball count rates close behind the configurations were obtained using the DOTWRTPN\* computer code (called DTWTPN on the Cray computer). This code calculates detector count rates by averaging DOT-IV point detector count rates over the reactor-side hemisphere of the Bonner balls. Third, Bonner ball count rates at detectors large distances behind the configurations were obtained using the DISKTRAN\* computer code (called DSKTRN on the Cray computer). DISKTRAN uses the DOT-IV angular fluxes from the top or bottom of a cylinder to calculate neutron fluxes at points in a void region outside the cylinder and folds those fluxes with detector response functions to give calculated detector count rates. Because the Bonner balls are not point detectors, the detector locations were adjusted forward of the ball centers to the "centers of detection"<sup>5</sup> for each of the balls. DISKTRAN was also used to calculate the neutron fluxes at the spectrum location behind Configuration I.A.

The DOT-IV calculations used boundary fluxes as sources and most of the time the fluxes required some processing in order to be used in a particular calculation. The boundary fluxes were processed by the BSPRP2\* and VFL2BDRY\* (called VFL2BD on the Cray computer) computer codes. The code BSPRP2 processes DOT-IV boundary flux files for input to subsequent DOT-IV calculations. The flux files may be altered to (1) select specific boundary fluxes from a multiple boundary flux file, (2) create a source for a different spatial mesh or quadrature, (3) normalize the source or correct it for

---

\*Computer codes written by the author.

streaming effects, or (4) combine several of the above features. The code VFL2BDRY reads top and bottom boundary fluxes from a DOT-IV R-Z flux and moments file and creates a top or bottom boundary source file for a subsequent DOT-IV calculation. While scale factors by group and interval can be applied to the boundary fluxes, no mesh or quadrature change is allowed. One may, however, follow up with BSPRP2 if such changes are desired. VFL2BDRY was used in this experiment to prepare boundary sources for follow-on DOT-IV calculations of neutron fluxes in the void region behind configurations, although some of the same sources could have been used as internal boundary sources for bootstrapped calculations of some of the larger configurations. When a change was made in the group structure used in the analysis, the previously generated boundary sources were converted to the new group structure using the Cray computer code CHBSGP written by the author. The code uses lethargy weighting to calculate boundary fluxes for the new group structure.

A final code used, TSFDISKS, is explained in Sect. 3.1.4.

### 3.1.2 Material Compositions

The material compositions used in the calculations are based on the material analyses given in Ref. 1 or data from reports on the analysis of previous Tower Shielding Facility (TSF) experiments. The atom densities of the various elements comprising the materials are shown in Table 1. The table lists the  $B_4C$  atom densities for a material density of  $1.0 \text{ g/cm}^3$ . Table 2 shows the material densities for the five  $B_4C$  slabs used in the experimental mockups. Mixtures for the slabs were formed by multiplying the  $B_4C$  mixture in Table 1 by the appropriate material density in Table 2.

### 3.1.3 Cross Sections and Detector Response Data

Initial calculations were performed with a 51-neutron-group structure using a cross-section library created in several steps for LMFBR reactor physics and shielding analyses. The data were mainly from ENDF/B-IV and were adequate for calculating some of the configurations as well as previous TSF experiments. However, the calculations showed very large underpredictions for Configurations II, which contained large amounts of  $B_4C$  and stainless steel. A study of various cross section sets led to data sets for Fe and  $^{11}\text{B}$  that gave results superior to any obtained with the old data or with data from libraries having other group structures. The important differences in the two  $^{11}\text{B}$  cross-section sets occur mainly above 0.4 MeV as the plot of the total cross section in Fig. 2 shows. The deeper cross-section window for the energy range 0.5-1.0 MeV and the lower cross section around 2 keV probably are responsible for the significantly increased neutron transmission through the  $B_4C$  slabs when using the newer  $^{11}\text{B}$  cross-section data. Because the new cross section data were available for a group structure different from that used in the original calculations, the group structure for the calculations was then changed to a 61-neutron-group structure for which a new cross-section library had been created.<sup>6</sup> Cross section data for Fe was obtained from a separate file created by C. Y. Fu.<sup>7</sup> This new Fe data has improved inelastic cross sections and generally gives more high-energy neutron transmission.



Table 1. Atomic densities ( $b^{-1} \cdot cm^{-1}$ ) for constituents of materials used in the experiment calculations

Element	Materials											
	Aluminum	SS304	Carbon steel	Boral	Lead	Block concrete	Lithiated paraffin	Sodium	B <sub>4</sub> C (1.0g/cm <sup>3</sup> )	UO <sub>2</sub> blanket	Graphite	Lithium hydride
H						6.400(-3)	5.930(-2)					5.610(-2)
<sup>6</sup> Li							5.625(-4)					4.163(-3)
<sup>7</sup> Li							6.938(-3)					5.194(-2)
<sup>10</sup> B				5.130(-3)					8.633(-3)			
<sup>11</sup> B				2.077(-2)					3.497(-2)			
C			9.820(-4)	6.450(-2)		1.010(-2)	3.340(-2)		1.090(-2)		8.124(-2)	
O						4.480(-2)	1.130(-2)			2.962(-2)		
Na								2.476(-2)		5.589(-3)		
Mg						2.180(-3)						
Al	6.050(-2) <sup>a</sup>			3.650(-2)		6.240(-4)				6.879(-3)		
Si						4.350(-3)						
S						5.780(-5)						
K						1.110(-4)						
Ca						9.890(-3)						
Cr		1.530(-2)										
Mn		1.760(-3)	1.550(-3)									
Fe	6.000(-4)	6.000(-2)	8.370(-2)	7.700(-4)		1.090(-4)						
Ni		7.800(-3)								2.000(-5)		
Pb					3.299(-2)					3.635(-5)		
<sup>235</sup> U										1.080(-4)		
<sup>238</sup> U										1.470(-2)		

<sup>a</sup>Read as  $6.050 \times 10^{-2}$ .

Table 2. Bulk densities for B<sub>4</sub>C powder in slabs.

Slab designation	Density (g/cm <sup>3</sup> )
1W	1.42
2W	1.39
3W	1.37
4W	1.41
5W	1.44

Bonner ball response functions in the 51 group structure were collapsed from Maerker's 100-group data.<sup>8</sup> These data are shown along with the group energy boundaries in Tables C1-C6. Data for the 61-group-structure were obtained from the 51-group-data using the AMP code.<sup>9</sup> These data are shown in Tables C7-C12 along with the group energy boundaries.

#### 3.1.4 Reactor Source Calculation

The source for the experiment was provided by the Tower Shielding Reactor II (TSR-II) with its wide-beam configuration as illustrated in Fig. 1. Maerker<sup>10</sup> calculated the absolute neutron source on the surface of the TSR-II and presented the results as one-dimensional (1-D) angular fluxes for the eight outward angles of an S<sub>16</sub> quadrature set and for the 51-group structure. The 1-D angular fluxes were projected onto a symmetric S<sub>12</sub> two-dimensional (2-D) quadrature (96 directions) on side and end cylindrical surfaces surrounding the core to form an equivalent internal boundary source for a DOT-IV calculation of neutron transport from the reactor through its collimator and onto the spectrum modifier. The projection of the source from the 1-D to the 2-D geometry was performed with the TSFDISKS code written by the author. The DOT-IV calculation was performed on a geometry model containing the TSR-II, its collimator, and the iron, aluminum and boral portion of the spectrum modifiers (Figs. B1 and B2) and boundary fluxes were saved at the interface between the reactor collimator and the spectrum modifier.<sup>11</sup> The output boundary fluxes were then used as the source for Configurations I.A, II.A, III.A-C, V.A, and VI.A. Boundary fluxes output from some of these calculations were then used as sources for larger configurations of which they are subsets. Configurations IV and VII at the outset used boundary fluxes from Configuration VI.A since they are identical out to the stainless steel slabs beyond the UO<sub>2</sub> blankets. The source, which is located on the surface of the aluminum beyond the blankets, should not be affected by shield mockups beyond the stainless steel slabs. Internal boundary fluxes output from two axial locations in Configuration IV.J were used to calculate smaller and larger Configurations IV in order to reduce calculational effort. Likewise, boundary fluxes at two locations in Configuration V.A were used to calculate larger Configurations V.

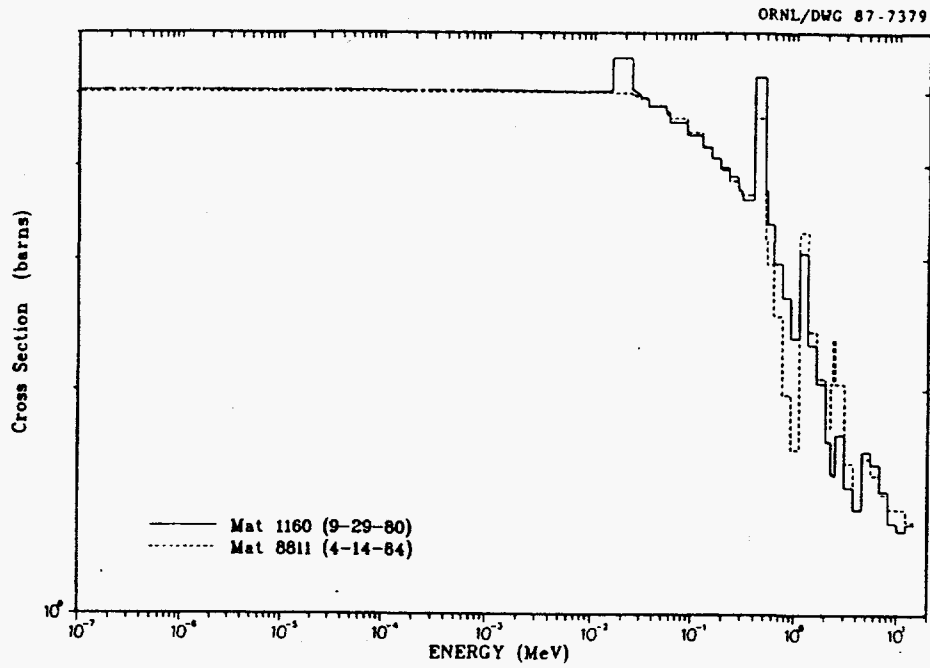


Fig. 2. Comparison of ENDF/B-V (Mat. 1160) and LLNL (Mat. 8811)  $^{11}\text{B}$  total cross sections in the 61-group structure.

### 3.2 Comparisons of Calculated and Measured Results

In comparing the calculated and measured results, qualitative judgments are made as to the agreement between the calculated and measured results. First of all, the results are generally compared according to the ratio of the calculated to the measured result. Since the quoted uncertainty for the Bonner ball measurements is  $\pm 10\%$ <sup>1</sup>, agreement is said to be excellent when calculation-to-experiment ratio ratios (C/E's) lie between 0.9 and 1.1. For this analysis, agreement is good for C/E's between 0.8 and 0.9 or 1.1 and 1.2; fair for C/E's between 0.6 and 0.8 or 1.2 and 1.4; and poor for C/E's less than 0.6 or greater than 1.4.

#### 3.2.1 Neutron Spectra Behind Configurations

Neutron spectra were measured behind five configurations: I.A, II.D, IV.C, VI.A, and VI.F. For all except Configuration I.A, lead or B<sub>4</sub>C and lead were used to reduce gamma-ray background in order to obtain good spectrum data. For Configuration I.A the spectrum was measured a great distance behind the configuration to reduce the gamma-ray interference. Calculated and measured E > 0.05 MeV neutron spectra are compared in Figs. 3-7. The calculated results are in good agreement with the measured results, with the integrals of the calculated spectra being 11-16% smaller than the integrals of the measured spectra. However, the calculation-to-experiment ratio (C/E) for Configuration II.D appears to better than the plot indicates, since the calculated spectrum is significantly above measured in the 3 to 10 MeV range and is below measured below 0.8 MeV. The compensating effects of the higher and lower fluxes probably gives Configuration II.D a higher C/E than that for some of the configurations where the shapes of the calculated and measured flux curves agree better. While the newer <sup>11</sup>B cross-section set causes a great improvement in the C/E for Configuration II.D (from 0.53 to 0.88), these results indicate that additional cross-section measurements or evaluations may be required to improve the high-energy cross sections. In the meantime, however, the newer set is recommended over the old for cases where the source incident on the shield is rather hard and the shield contains thick B<sub>4</sub>C regions. Calculations of the Alternate Shielding Materials Experiment<sup>11,12</sup> configurations containing B<sub>4</sub>C with the old and new cross-section sets showed little difference in the results, mainly because fast neutrons were only a small part of the source incident on the B<sub>4</sub>C. For Configuration II.D, the TSR-II neutron spectrum was hardened by the UO<sub>2</sub> blankets and thermalized little by the steel preceding the first B<sub>4</sub>C slab. The normalized neutron spectrum behind the blankets in the near-core spectrum modifier (Configuration I.A) is compared to that behind deep-pool sodium spectrum modifier (Configuration V.A) in Fig. 8. The configuration I.A spectrum is rather hard with most of the flux above 3 keV while the configuration V.A spectrum is much softer.

#### 3.2.2 Bonner Ball Count Rates at Spectrometer Locations

Calculated and Measured 3-, 4-, 5-, and 10-in Bonner ball count rates behind configurations at the same locations where spectrum measurements were taken are shown in Table 3. For Configuration I.A, the agreement is excellent for the 3- and 5-in Bonner balls and good for the 10-in Bonner ball. For the other configurations the agreement for the 4-, 5-, and 10-in Bonner balls is generally good, except for the fair agreement for the

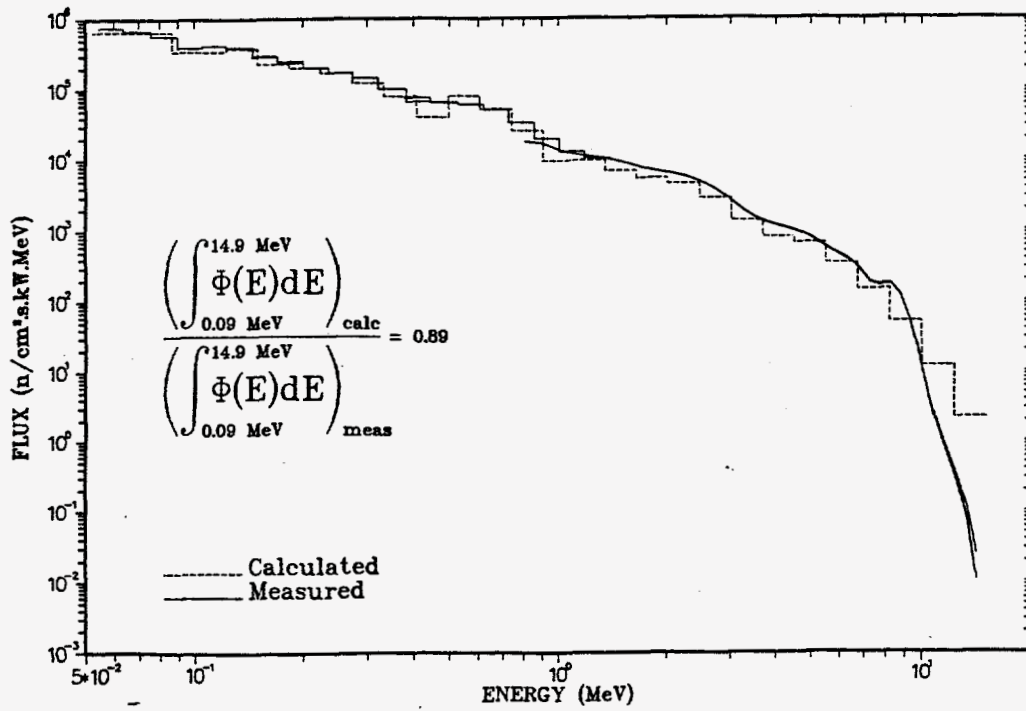


Figure 3. Calculated versus measured E > 0.05 MeV neutron spectra on centerline 178.8 cm behind Configuration I.A.

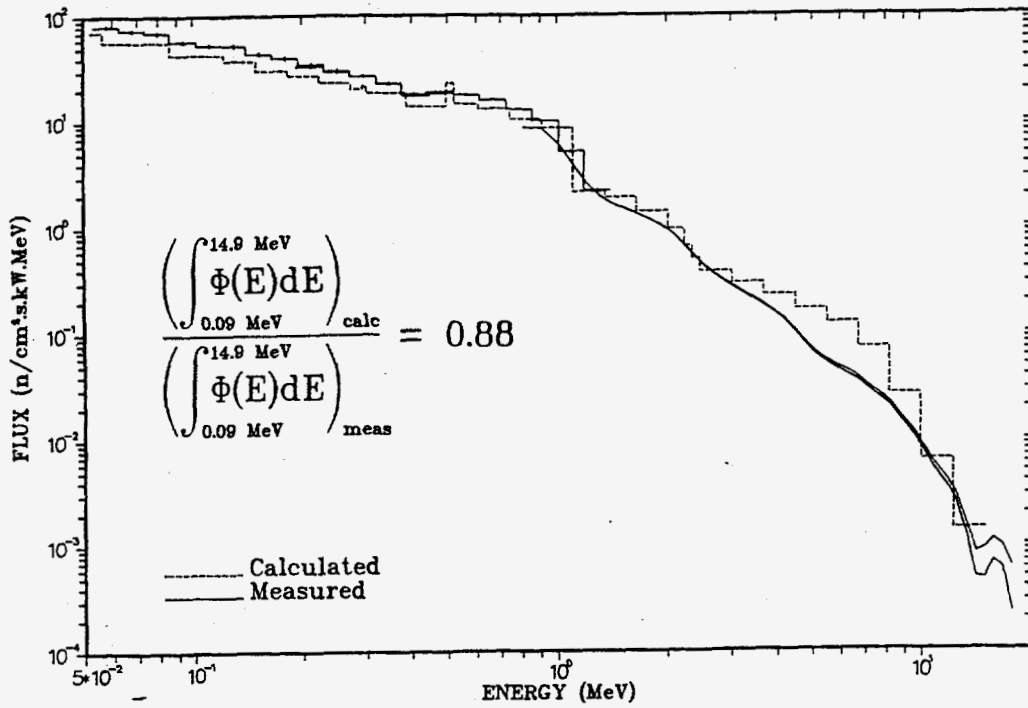


Fig. 4. Calculated versus measured E > 0.05 MeV neutron spectra on centerline 47.3 cm behind Configuration II.D.

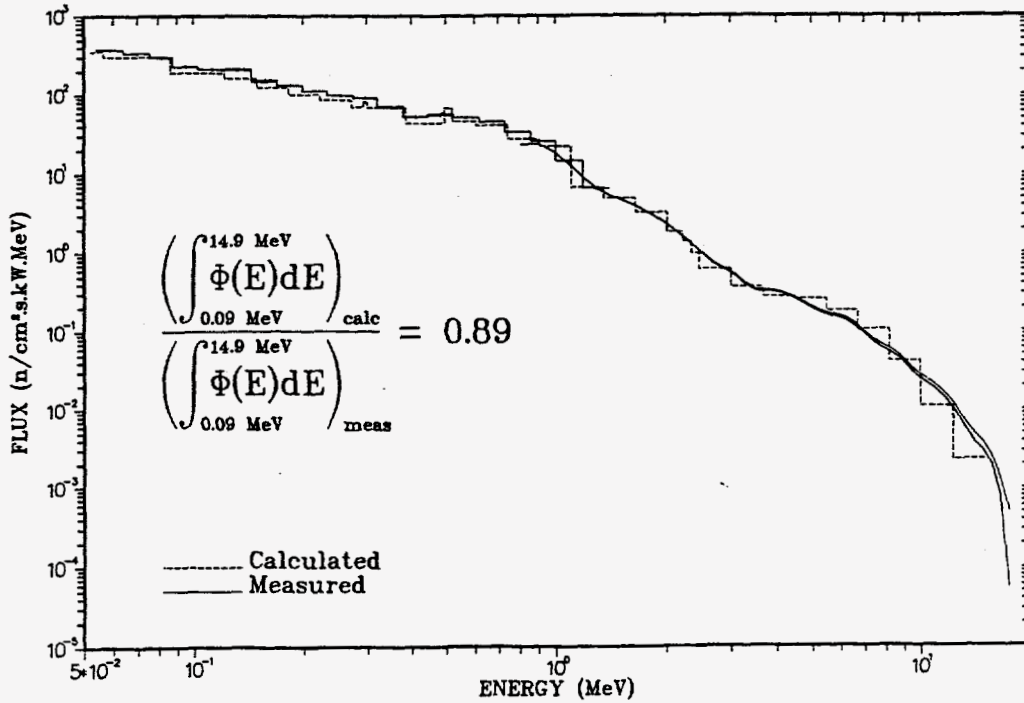


Fig. 5. Calculated versus measured E > 0.05 MeV neutron spectra on centerline 42.8 cm behind Configuration IV.C.

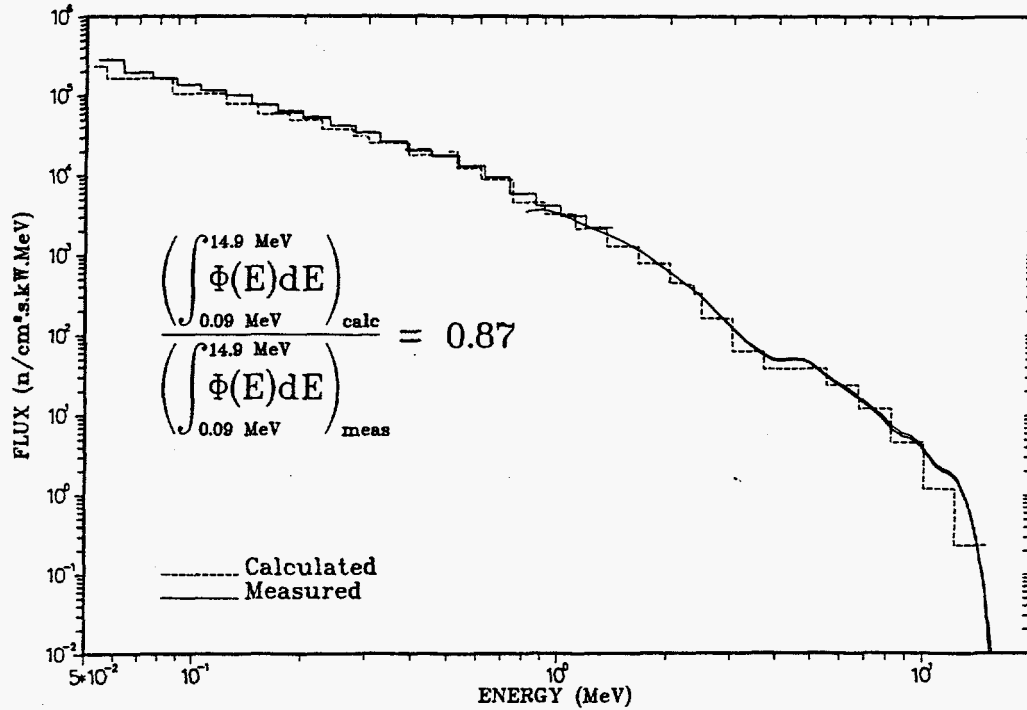


Fig. 6. Calculated versus measured  $E > 0.05$  MeV neutron spectra on centerline 51.1 cm behind Configuration VI.A.

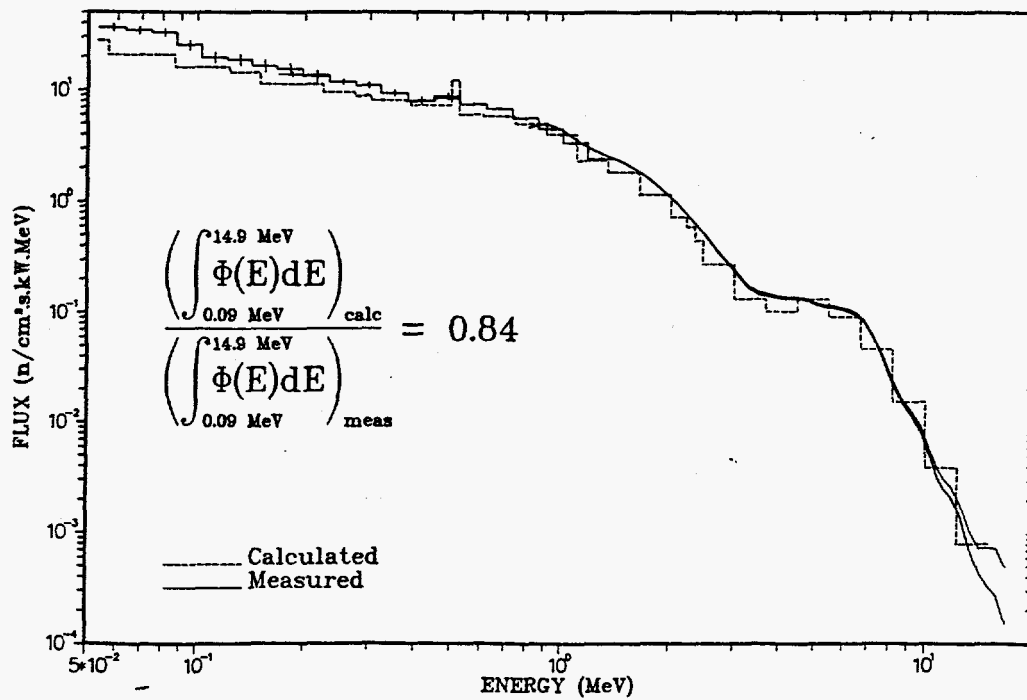


Fig. 7. Calculated versus measured  $E > 0.05$  MeV neutron spectra on centerline 63.2 cm behind Configuration VI.F.

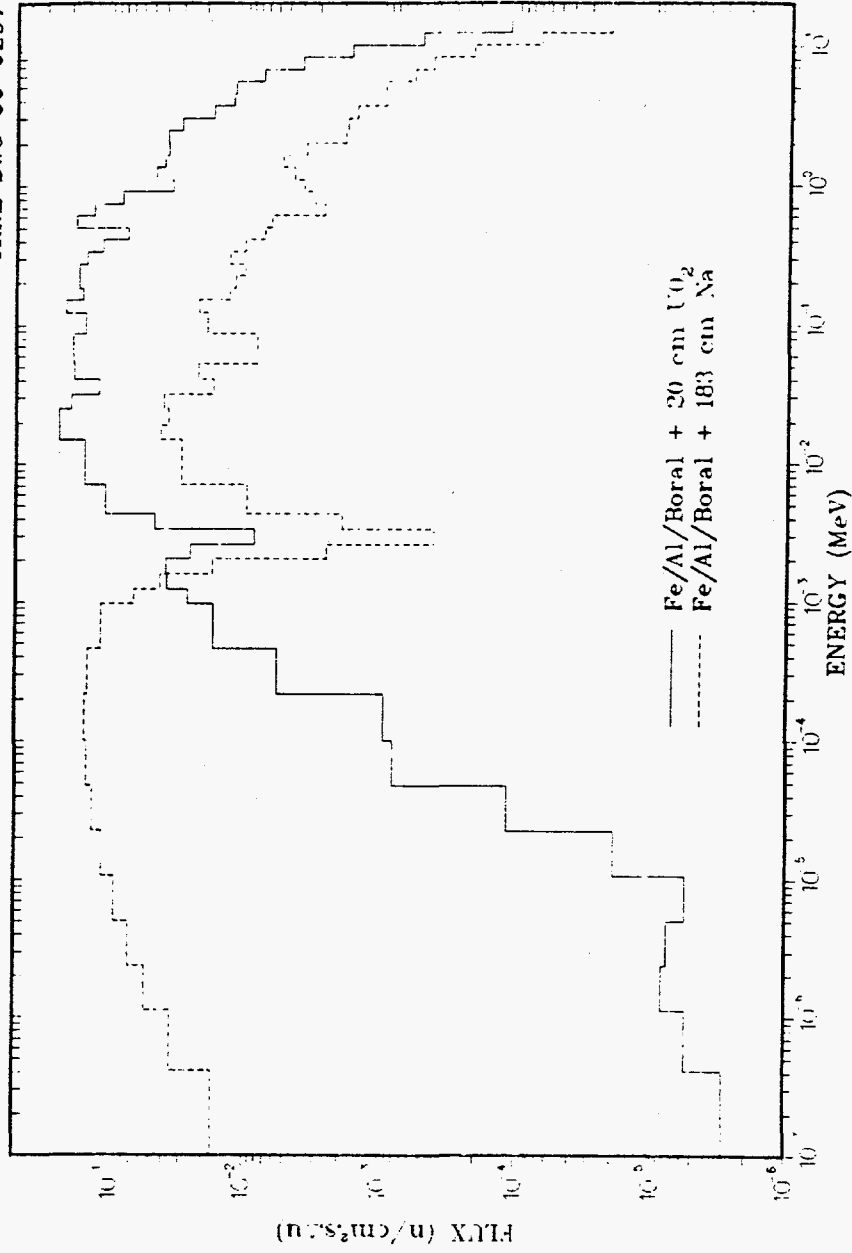


Figure 8. Comparison of normalized calculated neutron spectra behind the two spectrum modifiers.



Table 3. Comparison of Calculated and Measured Bonner Ball Count Rates ( $s^{-1} \cdot W^{-1}$ ) at the Spectrum Measurement Locations

Configuration	Detector			
	3-in. BB	4-in. BB	5-in. BB	10-in. BB
I.A				
Calculated	6.44(+1) <sup>a</sup>		3.03(+2)	1.02(+2)
Measured	6.86(+1)		3.13(+2)	1.20(+2)
C/E <sup>b</sup>	0.94		0.97	0.85
II.D				
Calculated	4.58(-3)		3.26(-2)	1.77(-2)
Measured	6.68(-3)		4.10(-2)	2.07(-2)
C/E	0.69		0.80	0.86
IV.C				
Calculated	2.61(-2)		1.44(-1)	5.90(-2)
Measured	3.36(-2)		1.76(-1)	6.95(-2)
C/E	0.78		0.82	0.85
VI.A				
Calculated		2.04(+2)	2.25(+2)	4.42(+1)
Measured		2.56(+2)	2.82(+2)	6.00(+1)
C/E		0.80	0.80	0.74
VI.F				
Calculated	3.34(-3)		1.80(-2)	9.54(-3)
Measured	4.51(-3)		2.22(-2)	1.12(-2)
C/E	0.74		0.81	0.85

<sup>a</sup>Read as  $6.44 \times 10^{+1}$ .

<sup>b</sup>Calculation-to-experiment ratio.

10-in Bonner ball behind Configuration VI.A. The agreement is fair for the 3-in Bonner ball behind Configurations II.D, IV.C, and VI.F. The reasons for the low C/E's is not understood, particularly since, as will be seen later, C/E's were much better at 30 cm behind those same configurations in the absence of the lead required to make the spectrum measurements. While this suggests the lead cross sections may be causing the problems, unaccounted background may also be contributing to the discrepancy. Configuration I.A results had background subtracted and the agreement was excellent. Background was not measured at the close-in detector positions because the configuration mockups are thought to shield the detector from radiation coming around the concrete peripheral shield. Yet measurements for some of the Configurations IV did show significant background even for detector positions close behind the configurations.

### 3.2.3 Bonner Ball Count Rates 30 cm Behind Configurations

Calculated and measured count rates are compared in Tables 4-9 for the bare and Cd-covered  $\text{BF}_3$  detectors and the 3-, 5-, 8-, and 10-in Bonner balls, respectively. Except for the special case for Configuration II.A, the calculated results for Configurations I, II, III, and V were obtained using the 51-group cross-section library. Thus, the results for the larger Configurations II are naturally low because of the  $^{11}\text{B}$  problem mentioned earlier. The results for the other configurations were obtained using the 61-group cross-section library.

The worst agreement between calculated and measured results is generally seen for the bare and Cd-covered  $\text{BF}_3$  detectors (Tables 4 and 5). For Configuration II.E, the agreement between the calculated and measured bare and Cd-covered  $\text{BF}_3$  detector count rates is very poor with C/E values of 0.06 and 0.28, respectively. The disagreement is attributed in part to the use of the old  $^{11}\text{B}$  cross sections as explained in section 3.2.2. Also, due to the presence of large amounts of  $\text{B}_4\text{C}$  in the configuration, the low-energy neutron flux transmitted through the shield is less than or comparable to that transmitted through the surrounding concrete or that air-scattered around the configuration. Therefore, background radiation can make the measured result considerably higher than the calculated result. The Configurations V containing  $\text{B}_4\text{C}$  also show low C/E values for these detectors for the same reasons given above. For Configuration VII.D, the low C/E values are attributed to unaccounted background.

For the other detectors, the agreement is good to excellent except for 1) the underpredictions behind some Configurations II and IV, 2) the overpredictions behind Configurations V.E-V.J, and 3) the fair-to-good agreement behind Configurations VII. Again, the underpredictions for Configurations II are attributed to the use of the old  $^{11}\text{B}$  cross sections and background problems. Some Configurations IV also have background problems as Tables 6-9 show C/E improvement for cases where background was removed from measurements close behind the configurations. A reason for the overprediction behind Configurations V.E-V.J is not apparent. Perhaps, some combination of peaks and valleys in the sodium and  $\text{B}_4\text{C}$  cross sections allow preferential transmission of neutrons in certain energy ranges and the multigroup cross sections do not model the cross sections well enough to accurately calculate the neutron transmission. The use of the broad-group structure to calculate neutron transport through the thick steel region probably causes the part of the problem for Configurations VII.

Table 4. Comparison of Calculated and Measured Bare BF<sub>3</sub> Detector Count Rates (s<sup>-1</sup>·W<sup>-1</sup>) Close Behind Configurations

Configuration	Distance (cm) behind configuration	Calculated	Measured	C/E <sup>a</sup>
I.A	30	7.73(-5) <sup>b</sup>	1.30(-3)	0.06
V.A	30	4.79(+0)	5.98(+0)	0.80
V.B	30	1.25(+0)	1.61(+0)	0.78
V.C	30	7.46(-1)	9.37(-1)	0.80
V.D	30	3.41(-1)	4.12(-1)	0.83
V.E	30	2.27(-3)	1.09(-2)	0.21
V.F	30	6.14(-3)	1.33(-2)	0.46
V.G	30	3.64(-3)	8.53(-3)	0.43
V.H	30	5.53(-4)	3.77(-3)	0.15
V.I	30	1.62(-3)	3.79(-3)	0.43
V.J	30	1.41(-3)	3.11(-3)	0.45
VI.A(3-5)	30	2.41(+1)	2.87(+1)	0.84
VI.B	30	7.65(+1)	8.40(+1)	0.91
VI.C	30	9.70(+1)	1.19(+2)	0.82
VI.D	30	8.76(+1)	1.13(+2)	0.78
VI.E	30	6.63(+1)	9.70(+1)	0.68
VI.F(3-5)	30	4.50(+1)	7.52(+1)	0.60
VII.D	30	3.78(-3)	1.01(-2)	0.37

<sup>a</sup>Calculation-to-experiment ratio.

<sup>b</sup>Read as 7.73 × 10<sup>-5</sup>.

Table 5. Comparison of Calculated and Measured Cd-Covered BF<sub>3</sub> Detector Count Rates (s<sup>-1</sup>.W<sup>-1</sup>) Close Behind Configurations

Configuration	Distance (cm) behind configuration	Calculated	Measured	C/E <sup>a</sup>
I.A	30	4.28(-5) <sup>b</sup>	1.53(-4)	0.28
V.A	30	2.73(+0)	2.92(+0)	0.93
V.B	30	9.97(-1)	1.11(+0)	0.90
V.C	30	4.72(-1)	5.23(-1)	0.90
V.D	30	2.01(-1)	2.21(-1)	0.91
V.E	30	2.22(-3)	4.32(-3)	0.51
V.F	30	3.20(-3)	4.91(-3)	0.65
V.G	30	2.38(-3)	3.49(-3)	0.68
V.H	30	5.12(-4)	1.02(-3)	0.50
V.I	30	9.35(-4)	1.18(-3)	0.79
V.J	30	8.73(-4)	9.23(-4)	0.95
VI.A(3-5)	30	9.28(+0)	1.25(+1)	0.74
VI.B	30	9.93(+0)	1.30(+1)	0.76
VI.C	30	5.68(+0)	7.42(+0)	0.77
VI.D	30	2.44(+0)	3.09(+0)	0.79
VI.E	30	8.61(-1)	1.08(+0)	0.80
VI.F(3-5)	30	2.65(-1)	3.39(-1)	0.78
VII.D	30	2.19(-3)	4.00(-3)	0.55

<sup>a</sup>Calculation-to-experiment ratio.

<sup>b</sup>Read as  $4.28 \times 10^{-5}$ .

Table 6. Comparison of Calculated and Measured 3-in Bonner Ball  
Count Rates ( $s^{-1} \cdot W^{-1}$ ) Close Behind Configurations

Configuration	Distance (cm) Behind Configuration	Calculated	Measured	C/E <sup>a</sup>
IA	30	6.06(+2) <sup>b</sup>	5.92(+2)	1.02
IIA <sup>c</sup>	30	1.91(+2)	2.00(+2)	0.96
IIA <sup>d</sup>	30	1.79(+2)	2.00(+2)	0.90
IIB	30	3.86(+0)	4.35(+0)	0.89
IIC	30	1.41(-1)	1.78(-1)	0.79
IID(3-5)	30	6.19(-3)	1.03(-2)	0.60
IIIE	30	3.10(-3)	5.20(-3)	0.60
IIIA	30	3.22(+2)	2.88(+2)	1.12
IIIB	30	7.07(+1)	7.26(+1)	0.97
IIIC	30	1.44(+2)	1.55(+2)	0.93
IIID	30	3.10(+1)	3.49(+1)	0.89
IIIE	30	9.10(+0)	1.07(+1)	0.85
IVA	30	9.65(+1)	1.06(+2)	0.91
IVB	30	2.15(+1)	2.40(+1)	0.90
IVC(3-5)	30	4.54(-2)	5.09(-2)	0.89
IVD	30	2.83(-2)	3.11(-2)	0.91
IVE	30	1.80(-2)	1.91(-2)	0.94
IVF	30	4.51(-3)	5.43(-3)	0.83
IVF <sup>e</sup>	72.4	2.08(-3)	2.41(-3)	0.86
IVG	30	7.68(-4)	1.26(-3)	0.61
IVG <sup>e</sup>	53.6	4.65(-4)	6.67(-4)	0.70
IVH	30	2.84(-4)	7.15(-4)	0.40
IVH <sup>e</sup>	52.1	1.78(-4)	2.95(-4)	0.60
IVJ	30	1.20(-4)	5.07(-4)	0.24
IVJ <sup>e</sup>	49.5	8.17(-5)	1.52(-4)	0.54
V.A	30	3.84(+1)	3.44(+1)	1.12
V.B	30	1.33(+1)	1.25(+1)	1.06
V.C	30	5.52(+0)	5.42(+0)	1.02
V.D	30	2.13(+0)	1.97(+0)	1.08
V.E	30	2.25(-1)	1.99(-1)	1.13
V.F	30	1.32(-1)	1.27(-1)	1.04
V.G	30	6.85(-2)	6.33(-2)	1.08
V.H	30	6.38(-2)	5.43(-2)	1.17
V.I	30	4.26(-2)	3.40(-2)	1.25
V.J	30	2.46(-2)	1.34(-2)	1.84
VIA(3-5)	30	1.89(+2)	2.01(+2)	0.94
VIB	30	1.25(+2)	1.35(+2)	0.93
VIC	30	5.70(+1)	6.30(+1)	0.90
VID	30	2.11(+1)	2.23(+1)	0.95
VIE	30	6.74(+0)	7.44(+0)	0.91
VIF(3-5)	30	1.93(+0)	2.10(+0)	0.92
VIIA	30	5.82(+1)	6.57(+1)	0.89
VILB	30	1.57(+1)	1.92(+1)	0.82
VILC	30	2.31(-1)	3.04(-1)	0.76
VILD	30	1.25(-1)	1.52(-1)	0.82

<sup>a</sup>Calculation-to-experiment ratio.

<sup>b</sup>Read as  $6.06 \times 10^{+2}$ .

<sup>c</sup>Calculated result obtained using 51 groups.

<sup>d</sup>Calculated result obtained using 61 groups.

<sup>e</sup>The measured result has background subtracted.

Table 7. Comparison of Calculated and Measured 5-in. Bonner  
Ball Count Rates ( $s^{-1} \cdot W^{-1}$ ) Close Behind Configurations

Configuration	Distance (cm) behind configuration	Calculated	Measured	C/E <sup>a</sup>
IA	30	2.94(+3) <sup>b</sup>	2.86(+3)	1.08
IIA <sup>c</sup>	30	7.64(+2)	8.31(+2)	0.92
IIA <sup>d</sup>	30	7.50(+2)	8.31(+2)	0.90
II.B	30	2.18(+1)	2.64(+1)	0.83
II.C	30	8.65(-1)	1.26(+0)	0.69
IID(3-5)	30	4.20(-2)	7.16(-2)	0.59
II.E	30	1.47(-2)	2.47(-2)	0.60
III.A	30	1.32(+3)	1.33(+3)	0.99
III.B	30	3.76(+2)	4.12(+2)	0.91
III.C	30	5.59(+2)	6.26(+2)	0.89
III.D	30	1.68(+2)	2.02(+2)	0.83
III.E	30	5.07(+1)	6.13(+1)	0.83
IV.A	30	2.18(+2)	2.45(+2)	0.89
IV.B	30	3.81(+1)	4.42(+1)	0.86
IV.C(3-5)	30	2.61(-1)	2.98(-1)	0.88
IV.D	30	1.44(-1)	1.64(-1)	0.88
IV.E	30	4.45(-2)	4.93(-2)	0.90
IV.F	30	8.55(-3)	1.08(-2)	0.79
IV.F <sup>e</sup>	72.4	3.97(-3)	4.72(-3)	0.84
IV.G	30	1.30(-3)	2.20(-3)	0.59
IV.G <sup>e</sup>	53.6	7.98(-4)	1.14(-3)	0.70
IV.H	30	5.42(-4)	1.32(-3)	0.41
IV.H <sup>e</sup>	52.1	3.44(-4)	5.57(-4)	0.62
IV.I	30	2.08(-4)	8.95(-4)	0.23
IV.I <sup>e</sup>	49.5	1.42(-4)	2.91(-4)	0.49
V.A	30	6.04(+1)	5.61(+1)	1.08
V.B	30	2.08(+1)	2.03(+1)	1.02
V.C	30	7.97(+0)	7.66(+0)	1.04
V.D	30	2.88(+0)	2.68(+0)	1.07
V.E	30	1.03(+0)	9.02(-1)	1.14
V.F	30	4.16(-1)	3.91(-1)	1.06
V.G	30	1.69(-1)	1.50(-1)	1.13
V.H	30	3.37(-1)	2.83(-1)	1.19
V.I	30	1.47(-1)	1.19(-1)	1.24
V.J	30	6.31(-2)	4.94(-2)	1.28
VIA(3-5)	30	4.58(+2)	5.15(+2)	0.89
VIB	30	2.16(+2)	2.46(+2)	0.88
VIC	30	8.23(+1)	9.45(+1)	0.87
VID	30	2.71(+1)	2.97(+1)	0.91
VIE	30	8.00(+0)	9.04(+0)	0.88
VIF(3-5)	30	2.19(+0)	2.42(+0)	0.90
VII.A	30	2.13(+2)	2.61(+2)	0.82
VII.B	30	5.59(+1)	7.69(+1)	0.73
VII.C	30	1.20(+0)	1.61(+0)	0.75
VII.D	30	4.36(-1)	5.46(-1)	0.80

<sup>a</sup>Calculation-to-experiment ratio.

<sup>b</sup>Read as  $2.94 \times 10^{+3}$ .

<sup>c</sup>Calculated result obtained using 51 groups.

<sup>d</sup>Calculated result obtained using 61 groups.

<sup>e</sup>The measured result has background subtracted.

Table 8. Comparison of Calculated and Measured 8-in. Bonner  
Ball Count Rates ( $s^{-1} \cdot W^{-1}$ ) Close Behind Configurations

Configuration	Distance (cm) behind configuration	Calculated	Measured	C/E <sup>a</sup>
I.A	30	2.01(+3) <sup>b</sup>	2.10(+3)	0.96
II.A <sup>c</sup>	30	4.95(+2)	5.68(+2)	0.87
II.A <sup>d</sup>	30	5.02(+2)	5.68(+2)	0.88
II.B	30	1.62(+1)	2.04(+1)	0.79
II.C	30	6.94(-1)	1.02(+0)	0.68
II.D(3-5)	30	3.73(-2)	6.68(-2)	0.56
II.E	30	1.08(-2)	1.85(-2)	0.58
III.A	30	8.65(+2)	9.17(+2)	0.94
III.B	30	2.71(+2)	3.17(+2)	0.85
III.C	30	3.60(+2)	4.24(+2)	0.85
III.D	30	1.18(+2)	1.47(+2)	0.80
III.E	30	3.61(+1)	4.57(+1)	0.79
IV.A	30	1.06(+2)	1.25(+2)	0.85
IV.B	30	1.60(+1)	1.87(+1)	0.86
IV.C(3-5)	30	2.03(-1)	2.15(-1)	0.94
IV.D	30	1.06(-1)	1.21(-1)	0.88
IV.E	30	2.34(-2)	2.64(-2)	0.89
IV.F	30	3.86(-3)	4.82(-3)	0.80
IV.F <sup>e</sup>	72.4	1.82(-3)	2.20(-3)	0.83
IV.G	30	5.52(-4)	9.34(-4)	0.59
IV.G <sup>c</sup>	53.6	3.44(-4)	4.90(-4)	0.70
IV.H	30	2.52(-4)	5.83(-4)	0.43
IV.H <sup>e</sup>	52.1	1.63(-4)	2.48(-4)	0.66
IV.I	30	8.67(-5)	3.73(-4)	0.23
IV.I	49.5	6.03(-5)	1.20(-4)	0.50
V.A	30	2.20(+1)	2.12(+1)	1.04
V.B	30	7.86(+0)	7.94(+0)	0.99
V.C	30	2.85(+0)	2.79(+0)	1.02
V.D	30	9.88(-1)	9.37(-1)	1.05
V.E	30	7.06(-1)	5.93(-1)	1.19
V.F	30	2.35(-1)	2.12(-1)	1.11
V.G	30	8.16(-2)	7.20(-2)	1.13
V.H	30	2.58(-1)	2.11(-1)	1.22
V.I	30	9.01(-2)	7.18(-2)	1.25
V.J	30	3.22(-2)	2.52(-2)	1.28
VI.A(3-5)	30	2.25(+2)	2.61(+2)	0.86
VI.B	30	8.76(+1)	1.03(+2)	0.85
VI.C	30	3.03(+1)	3.62(+1)	0.84
VI.D	30	9.46(+0)	1.06(+1)	0.89
VI.E	30	2.72(+0)	3.08(+0)	0.88
VI.F(3-5)	30	7.44(-1)	8.44(-1)	0.88
VII.A	30	1.34(+2)	1.69(+2)	0.79
VII.B	30	3.38(+1)	4.64(+1)	0.73
VII.C	30	7.90(-1)	1.08(+0)	0.73
VII.D	30	2.37(-1)	3.11(-1)	0.76

<sup>a</sup>Calculation-to-experiment ratio.

<sup>b</sup>Read as  $2.01 \times 10^{+3}$ .

<sup>c</sup>Calculated result obtained using 51 groups.

<sup>d</sup>Calculated result obtained using 61 groups.

<sup>e</sup>The measured result has background subtracted.

Table 9. Comparison of Calculated and Measured 10-in. Bonner  
Ball Count Rates ( $s^{-1} \cdot W^{-1}$ ) Close Behind Configurations

Configuration	Distance (cm) behind configuration	Calculated	Measured	C/E <sup>a</sup>
I.A	30	1.00(+3) <sup>b</sup>	1.13(+3)	0.89
II.A <sup>c</sup>	30	2.37(+2)	2.71(+2)	0.87
II.A <sup>d</sup>	30	2.44(+2)	2.71(+2)	0.90
II.B	30	8.23(+0)	1.07(+1)	0.77
II.C	30	3.75(-1)	5.76(-1)	0.65
II.D(3-5)	30	2.17(-2)	3.89(-2)	0.56
II.E	30	5.76(-3)	9.63(-3)	0.60
III.A	30	4.18(+2)	4.59(+2)	0.91
III.B	30	1.35(+2)	1.63(+2)	0.83
III.C	30	1.71(+2)	2.13(+2)	0.80
III.D	30	5.68(+1)	7.36(+1)	0.77
III.E	30	1.75(+1)	2.37(+1)	0.74
IV.A	30	4.59(+1)	5.42(+1)	0.85
IV.B	30	6.64(+0)	7.94(+0)	0.84
IV.C(3-5)	30	1.09(-1)	1.16(-1)	0.94
IV.D	30	5.48(-2)	6.35(-2)	0.86
IV.E	30	1.07(-2)	1.20(-2)	0.89
IV.F	30	1.67(-3)	2.10(-3)	0.80
IV.Fe <sup>e</sup>	72.4	7.97(-4)	9.41(-4)	0.85
IV.G	30	2.36(-4)	3.95(-4)	0.60
IV.G <sup>e</sup>	53.6	1.49(-4)	2.03(-4)	0.73
IV.H	30	1.11(-4)	2.48(-4)	0.45
IV.H <sup>e</sup>	52.1	7.26(-5)	1.04(-4)	0.70
IV.I	30	3.60(-5)	1.55(-4)	0.23
IV.I <sup>e</sup>	49.5	2.53(-5)	4.70(-5)	0.54
V.A	30	8.67(+0)	8.24(+0)	1.05
V.B	30	3.19(+0)	3.20(+0)	1.00
V.C	30	1.13(+0)	1.09(+0)	1.04
V.D	30	3.86(-1)	3.65(-1)	1.06
V.E	30	3.57(-1)	2.98(-1)	1.20
V.F	30	1.09(-1)	9.76(-2)	1.12
V.G	30	3.54(-2)	3.13(-2)	1.13
V.H	30	1.39(-1)	1.14(-1)	1.22
V.I	30	4.38(-2)	3.51(-2)	1.25
V.J	30	1.44(-2)	1.16(-2)	1.24
VI.A(3-5)	30	9.66(+1)	1.10(+2)	0.88
VI.B	30	3.57(+1)	4.25(+1)	0.84
VI.C	30	1.21(+1)	1.47(+1)	0.82
VI.D	30	3.78(+0)	4.32(+0)	0.88
VI.E	30	1.10(+0)	1.25(+0)	0.88
VI.F(3-5)	30	3.07(-1)	3.58(-1)	0.86
VII.A	30	6.21(+1)	7.77(+1)	0.80
VII.B	30	1.52(+1)	2.13(+1)	0.71
VII.C	30	3.62(-1)	5.03(-1)	0.72
VII.D	30	1.00(-1)	1.37(-1)	0.73

<sup>a</sup>Calculation-to-experiment ratio.

<sup>b</sup>Read as  $1.00 \times 10^{+3}$ .

<sup>c</sup>Calculated result obtained using 51 groups.

<sup>d</sup>Calculated result obtained using 61 groups.

<sup>e</sup>The measured result has background subtracted.



### 3.2.4 Bonner Ball Count Rates Behind Configurations at Large Distances from the TSR-II Core Center

Calculated bare and Cd-covered  $\text{BF}_3$  detector and 3-, 5-, 8-, and 10-in Bonner ball count rates behind configurations at large distances from the TSR-II core center are compared to measured count rates respectively in Tables 10-15. The agreement is similar to that 30 cm behind the configurations but slightly worse. The agreement for those Configurations V that were largely overpredicted at 30 cm is much better. The general downward trend in the C/E values seems to indicate some underprediction of the fluxes at the distant detectors.

### 3.2.5 Bonner Ball Count Rates Inside Configurations

Because of high background behind the very large Configurations IV, measurements for those configurations were made with Bonner balls in a void region within the configuration mockup and completely surrounded by shielding. Configuration IV.I was measured both with and without the shielding around the detectors, while Configurations IV.J through IV.M were all measured *in situ*. Calculated and measured Bonner ball count rates are compared in Table 16. Poor agreement is shown for the bare  $\text{BF}_3$  detector, while fair to good agreement is shown for the Cd-covered  $\text{BF}_3$  detector and good to excellent agreement is shown for the 3-, 5-, 8-, and 10-in Bonner balls. If Configuration IV.J is excluded, one sees improved C/E values with increasing configuration size for all detectors except the bare detector. Boundary sources for all configurations except Configuration IV.J were derived from output from the Configuration IV.J DOT-IV calculation. This would be an explanation for higher C/E values for Configuration IV.IA and lower C/E values for Configurations IV.K through IV.M, but not the trend shown in Table 16. A possible explanation for the upward trend in the C/E values is an overprediction of the transport through sodium. As the thickness of sodium preceding the void increases, the C/E also increases.

### 3.2.6 5-in Bonner Ball Horizontal Traverses 30 cm Behind Configurations

Plotted curves of calculated and measured count rates for 5-in Bonner ball horizontal traverses 30 cm behind configurations are shown in Figs. 9-31. The calculated and measured curve shapes are in reasonably good agreement, although the calculated results tend to be more underpredictive at the outer edges of the traverse. The 2-D modeling of the square slabs probably affects the comparisons at the outer edges of the traverses. The top-of-range C/E values are good to excellent except for Configurations II.D and II.E, for which calculations were performed with the 51-group structure and the old  $^{11}\text{B}$  cross section set; Configuration IV.G, for which background was high; and for Configurations VII.B and VII.C, for which agreement was fair. Note that the traverses behind Configurations V (Figs. 20-24) indicate little effect on the radial variation of the count rate due to the nonuniformity of the sodium tanks.

Table 10. Comparison of Calculated and Measured Bare BF<sub>3</sub> Detector Count Rates (s<sup>-1</sup> · W<sup>-1</sup>) Behind Configurations at Large Distances from the TSR-II Core Center

Configuration	Distance (cm) from TSR-II core center	Calculated	Measured	C/E <sup>a</sup>
I.A	304.8	8.23(-5) <sup>b</sup>	3.80(-4)	0.22
V.A	501.3	7.10(-1)	9.40(-1)	0.76
V.B	501.3	1.75(-1)	2.32(-1)	0.75
V.C	501.3	1.71(-1)	1.94(-1)	0.88
V.D	501.3	1.07(-1)	1.45(-1)	0.74
V.E	501.3	5.00(-4)	3.70(-3)	0.14
V.F	501.3	2.12(-3)	3.70(-3)	0.57
V.G	501.3	1.51(-3)	3.21(-3)	0.47
V.H	501.3	1.53(-4)	1.66(-3)	0.09
V.I	501.3	5.87(-4)	9.40(-4)	0.62
V.J	501.3	6.94(-4)	9.00(-4)	0.77
VI.A(3-5)	304.8	3.94(+0)	4.98(+0)	0.79
VI.B	304.8	1.51(+1)	1.69(+1)	0.89
VI.C	304.8	2.12(+1)	2.79(+1)	0.76
VI.D	304.8	2.19(+1)	3.07(+1)	0.71
VI.E	304.8	1.93(+1)	3.10(+1)	0.62
VI.F(3-5)	304.8	1.55(+1)	2.87(+1)	0.54
VII.D	304.8	3.00(-3)	6.44(-3)	0.47

<sup>a</sup>Calculation-to-experiment ratio.

<sup>b</sup>Read as 8.23 × 10<sup>-5</sup>.

Table 11. Comparison of Calculated and Measured Cd-Covered BF<sub>3</sub> Detector Count Rates (s<sup>-1</sup> · W<sup>-1</sup>) Behind Configurations at Large Distances from the TSR-II Core Center

Configuration	Distance (cm) from TSR-II core center	Calculated	Measured	C/E <sup>a</sup>
I.A	304.8	3.95(-5) <sup>b</sup>	8.30(-5)	0.48
V.A	501.3	3.53(-1)	4.34(-1)	0.81
V.B	501.3	1.32(-1)	1.58(-1)	0.84
V.C	501.3	8.91(-2)	1.13(-1)	0.79
V.D	501.3	5.80(-2)	7.14(-2)	0.81
V.E	501.3	3.60(-4)	1.20(-3)	0.30
V.F	501.3	8.34(-4)	1.40(-3)	0.60
V.G	501.3	8.41(-4)	1.34(-3)	0.63
V.H	501.3	9.79(-5)	3.85(-4)	0.25
V.I	501.3	2.61(-4)	3.56(-4)	0.73
V.J	501.3	3.51(-4)	3.65(-4)	0.96
VI.A(3-5)	304.8	1.49(+0)	2.27(+0)	0.66
VI.B	304.8	1.90(+0)	2.72(+0)	0.70
VI.C	304.8	1.23(+0)	1.79(+0)	0.69
VI.D	304.8	6.06(-1)	8.48(-1)	0.71
VI.E	304.8	2.50(-1)	3.51(-1)	0.71
VI.F(3-5)	304.8	9.11(-2)	1.27(-1)	0.72
VII.D	304.8	1.64(-3)	2.77(-3)	0.59

<sup>a</sup>Calculation-to-experiment ratio.

<sup>b</sup>Read as  $3.95 \times 10^{-5}$ .

Table 12. Comparison of Calculated and Measured 3-in. Bonner Ball Count Rates ( $s^{-1} \cdot W^{-1}$ ) Behind Configurations at Large Distances from the TSR-II Core Center

Configuration	Distance (cm) behind configuration	Calculated	Measured	C/E <sup>a</sup>
I.A	304.8	7.39(+1) <sup>b</sup>	7.11(+1)	1.04
I.A	457.2	2.15(+1)	2.12(+1)	1.01
II.A <sup>c</sup>	304.8	2.94(+1)	3.25(+1)	0.90
II.A <sup>d</sup>	304.8	2.77(+1)	3.25(+1)	0.85
II.B	304.8	7.95(-1)	9.80(-1)	0.81
II.C	304.8	3.90(-2)	5.35(-2)	0.73
II.D(3-5)	304.8	2.47(-3)	4.26(-3)	0.58
II.E	304.8	2.43(-3)	3.53(-3)	0.69
III.A	304.8	4.84(+1)	4.34(+1)	1.12
III.B	304.8	1.20(+1)	1.26(+1)	0.95
III.C	304.8	2.41(+1)	2.64(+1)	0.91
III.D	304.8	5.88(+0)	6.92(+0)	0.85
III.E	304.8	1.87(+0)	2.26(+0)	0.83
IV.A	304.8	1.72(+1)	2.07(+1)	0.83
IV.B	304.8	4.74(+0)	6.00(+0)	0.79
IV.C(3-5)	304.8	1.49(-2)	1.81(-2)	0.82
IV.C(3-5)	457.2	2.65(-3)	3.72(-3)	0.71
IV.D	457.2	1.75(-3)	2.36(-3)	0.74
IV.E	457.2	1.31(-3)	1.68(-3)	0.78
IV.F	457.2	3.92(-4)	5.06(-4)	0.77
V.A	501.3	4.77(+0)	5.00(+0)	0.95
V.B	501.3	1.72(+0)	1.76(+0)	0.98
V.C	501.3	1.02(+0)	1.12(+0)	0.91
V.D	501.3	6.09(-1)	6.22(-1)	0.98
V.E	501.3	3.11(-2)	3.52(-2)	0.88
V.F	501.3	2.77(-2)	3.08(-2)	0.90
V.G	501.3	2.21(-2)	2.24(-2)	0.99
V.H	501.3	9.61(-3)	1.11(-2)	0.87
V.I	501.3	9.48(-3)	8.50(-3)	1.12
V.J	501.3	8.76(-3)	6.86(-3)	1.28
VI.A(3-5)	304.8	3.01(+1)	3.68(+1)	0.82
VI.B	304.8	2.37(+1)	2.78(+1)	0.85
VI.C	304.8	1.23(+1)	1.50(+1)	0.82
VI.D	304.8	5.26(+0)	6.05(+0)	0.87
VI.E	304.8	1.96(+0)	2.38(+0)	0.82
VI.F(3-5)	304.8	6.65(-1)	7.92(-1)	0.84
VII.A	304.8	1.15(+1)	1.37(+1)	0.84
VII.B	304.8	3.81(+0)	5.11(+0)	0.75
VII.C	304.8	7.97(-2)	1.18(-1)	0.68
VII.D	304.8	8.44(-2)	1.01(-1)	0.84

<sup>a</sup>Calculation-to-experiment ratio.

<sup>b</sup>Read as  $7.39 \times 10^{+1}$ .

<sup>c</sup>Calculated result obtained using 51 groups.

<sup>d</sup>Calculated result obtained using 61 groups.

Table 13. Comparison of Calculated and Measured 5-in. Bonner Ball Count Rates ( $s^{-1} \cdot W^{-1}$ ) Behind Configurations at Large Distances from the TSR-II Core Center

Configuration	Distance (cm) behind		Calculated	Measured	C/E <sup>a</sup>
	Configuration				
IA	304.8		3.48(+2) <sup>b</sup>	3.63(+2)	0.96
IA	457.2		9.99(+1)	1.13(+2)	0.88
II.A <sup>c</sup>	304.8		1.15(+2)	1.35(+2)	0.85
II.A <sup>d</sup>	304.8		1.13(+2)	1.35(+2)	0.84
II.B	304.8		4.38(+0)	5.94(+0)	0.74
II.C	304.8		2.41(-1)	3.81(-1)	0.63
II.D(3-5)	304.8		1.68(-2)	2.98(-2)	0.56
II.E	304.8		1.16(-2)	1.74(-2)	0.67
III.A	304.8		1.83(+2)	1.93(+2)	0.95
III.B	304.8		5.96(+1)	7.15(+1)	0.83
III.C	304.8		8.88(+1)	1.08(+2)	0.82
III.D	304.8		3.03(+1)	3.90(+1)	0.78
III.E	304.8		1.02(+1)	1.36(+1)	0.75
IV.A	304.8		3.84(+1)	4.85(+1)	0.79
IV.B	304.8		8.40(+0)	1.10(+1)	0.76
IV.C(3-5)	304.8		8.66(-2)	1.07(-1)	0.81
IV.C(3-5)	457.2		1.51(-2)	2.21(-2)	0.68
IV.D	457.2		8.79(-3)	1.23(-2)	0.71
IV.E	457.2		3.20(-3)	4.26(-3)	0.75
IV.F	457.2		7.39(-4)	1.07(-3)	0.69
V.A	501.3		7.37(+0)	8.18(+0)	0.90
V.B	501.3		2.67(+0)	2.75(+0)	0.97
V.C	501.3		1.45(+0)	1.61(+0)	0.90
V.D	501.3		8.18(-1)	8.17(-1)	1.00
V.E	501.3		1.43(-1)	1.46(-1)	0.98
V.F	501.3		8.46(-2)	8.71(-2)	0.97
V.G	501.3		5.36(-2)	5.15(-2)	1.04
V.H	501.3		5.08(-2)	5.05(-2)	1.01
V.I	501.3		3.19(-2)	2.93(-2)	1.09
V.J	501.3		2.20(-2)	1.79(-2)	1.23
VI.A(3-5)	304.8		7.33(+1)	9.29(+1)	0.79
VI.B	304.8		4.09(+1)	5.10(+1)	0.80
VI.C	304.8		1.78(+1)	2.24(+1)	0.79
VI.D	304.8		6.76(+0)	7.94(+0)	0.85
VI.E	304.8		2.34(+0)	2.89(+0)	0.81
VI.F(3-5)	304.8		7.54(-1)	9.70(-1)	0.78
VII.A	304.8		4.10(+1)	5.48(+1)	0.75
VII.B	304.8		1.35(+1)	2.00(+1)	0.68
VII.C	304.8		4.19(-1)	6.07(-1)	0.69
VII.D	304.8		2.95(-1)	3.64(-1)	0.81

<sup>a</sup>Calculation-to-experiment ratio.

<sup>b</sup>Read as  $3.48 \times 10^{+2}$ .

<sup>c</sup>Calculated result obtained using 51 groups.

<sup>d</sup>Calculated result obtained using 61 groups.

Table 14. Comparison of Calculated and Measured 8-in. Bonner Ball Count Rates ( $s^{-1} \cdot W^{-1}$ ) Behind Configurations at Large Distances from the TSR-II Core Center

Configuration	Distance (cm) behind		Measured	C/E <sup>a</sup>
	configuration	Calculated		
I.A	304.8	2.36(+2) <sup>b</sup>	2.64(+2)	0.89
I.A	457.2	6.68(+1)	8.05(+1)	0.81
II.A <sup>c</sup>	304.8	7.38(+1)	9.18(+1)	0.80
II.A <sup>d</sup>	304.8	7.49(+1)	9.18(+1)	0.82
II.B	304.8	3.30(+0)	4.61(+0)	0.72
II.C	304.8	1.98(-1)	3.17(-1)	0.62
II.D(3-5)	304.8	1.53(-2)	2.84(-2)	0.54
II.E	304.8	8.92(-3)	1.32(-2)	0.68
III.A	304.8	1.18(+2)	1.36(+2)	0.87
III.B	304.8	4.27(+1)	5.46(+1)	0.78
III.C	304.8	5.67(+1)	7.35(+1)	0.77
III.D	304.8	2.13(+1)	2.94(+1)	0.72
III.E	304.8	7.31(+0)	1.00(+1)	0.73
IV.A	304.8	1.87(+1)	2.45(+1)	0.76
IV.B	304.8	3.57(+0)	4.72(+0)	0.76
IV.C(3-5)	304.8	6.94(-2)	7.91(-2)	0.88
IV.C(3-5)	457.2	1.19(-2)	1.67(-2)	0.71
IV.D	457.2	6.52(-3)	9.40(-3)	0.69
IV.E	457.2	1.70(-3)	2.35(-3)	0.72
IV.F	457.2	3.37(-4)	4.72(-4)	0.71
V.A	501.3	2.68(+0)	3.10(+0)	0.86
V.B	501.3	1.01(+0)	1.10(+0)	0.92
V.C	501.3	5.20(-1)	5.86(-1)	0.89
V.D	501.3	2.82(-1)	2.92(-1)	0.97
V.E	501.3	1.01(-1)	9.90(-2)	1.02
V.F	501.3	4.85(-2)	4.94(-2)	0.98
V.G	501.3	2.63(-2)	2.55(-2)	1.03
V.H	501.3	4.00(-2)	3.81(-2)	1.05
V.I	501.3	1.98(-2)	1.79(-2)	1.11
V.J	501.3	1.13(-2)	9.50(-3)	1.19
VI.A(3-5)	304.8	3.65(+1)	4.81(+1)	0.76
VI.B	304.8	1.68(+1)	2.15(+1)	0.78
VI.C	304.8	6.61(+0)	8.65(+0)	0.76
VI.D	304.8	2.39(+0)	2.93(+0)	0.82
VI.E	304.8	8.08(-1)	1.00(+0)	0.81
VI.F(3-5)	304.8	2.61(-1)	3.18(-1)	0.82
VII.A	304.8	2.55(+1)	3.50(+1)	0.73
VII.B	304.8	8.23(+0)	1.25(+1)	0.66
VII.C	304.8	2.83(-1)	4.16(-1)	0.68
VII.D	304.8	1.65(-1)	2.05(-1)	0.80

<sup>a</sup>Calculation-to-experiment ratio.

<sup>b</sup>Read as  $2.36 \times 10^{+2}$ .

<sup>c</sup>Calculated result obtained using 51 groups.

<sup>d</sup>Calculated result obtained using 61 groups.

Table 15. Comparison of Calculated and Measured 10-in. Bonner Ball Count Rates ( $s^{-1} \cdot W^{-1}$ ) Behind Configurations at Large Distances from the TSR-II Core Center

Configuration	Distance (cm) behind		Calculated	Measured	C/E <sup>a</sup>
	Configuration				
I.A	304.8		1.17(+2) <sup>b</sup>	1.32(+2)	0.89
I.A	457.2		3.29(+1)	4.08(+1)	0.81
II.A <sup>c</sup>	304.8		3.53(+1)	4.39(+1)	0.80
II.A <sup>d</sup>	304.8		3.64(+1)	4.39(+1)	0.83
II.B	304.8		1.70(+0)	2.44(+0)	0.70
II.C	304.8		1.09(-1)	1.81(-1)	0.60
ILD(3-5)	304.8		9.07(-3)	1.65(-2)	0.55
II.E	304.8		4.96(-3)	6.88(-3)	0.72
III.A	304.8		5.71(+1)	6.91(+1)	0.83
III.B	304.8		2.15(+1)	2.69(+1)	0.80
III.C	304.8		2.69(+1)	3.63(+1)	0.74
III.D	304.8		1.04(+1)	1.44(+1)	0.72
III.E	304.8		3.59(+0)	5.27(+0)	0.68
IV.A	304.8		8.18(+0)	1.05(+1)	0.78
IV.B	304.8		1.49(+0)	1.97(+0)	0.76
IV.C(3-5)	304.8		3.79(-2)	4.35(-2)	0.87
IV.C(3-5)	457.2		6.45(-3)	9.12(-3)	0.71
IV.D	457.2		3.41(-3)	4.94(-3)	0.69
IV.E	457.2		7.82(-4)	1.05(-3)	0.74
IV.F	457.2		1.48(-4)	1.94(-4)	0.76
V.A	501.3		1.05(+0)	1.18(+0)	0.89
V.B	501.3		4.14(-1)	4.42(-1)	0.94
V.C	501.3		2.08(-1)	2.29(-1)	0.91
V.D	501.3		1.11(-1)	1.17(-1)	0.95
V.E	501.3		5.23(-2)	4.99(-2)	1.05
V.F	501.3		2.30(-2)	2.28(-2)	1.01
V.G	501.3		1.16(-2)	1.10(-2)	1.05
V.H	501.3		2.23(-2)	2.08(-2)	1.07
V.I	501.3		9.90(-3)	8.85(-3)	1.12
V.J	501.3		5.17(-3)	4.33(-3)	1.19
VI.A(3-5)	304.8		1.59(+1)	2.09(+1)	0.76
VI.B	304.8		6.89(+0)	8.92(+0)	0.77
VI.C	304.8		2.67(+0)	3.49(+0)	0.77
VI.D	304.8		9.67(-1)	1.17(+0)	0.83
VI.E	304.8		3.31(-1)	4.02(-1)	0.82
VI.F(3-5)	304.8		1.10(-1)	1.34(-1)	0.82
VII.A	304.8		1.19(+1)	1.61(+1)	0.74
VII.B	304.8		3.74(+0)	5.63(+0)	0.66
VII.C	304.8		1.31(-1)	1.98(-1)	0.66
VII.D	304.8		7.14(-2)	9.03(-2)	0.79

<sup>a</sup>Calculation-to-experiment ratio.

<sup>b</sup>Read as  $1.17 \times 10^{+2}$ .

<sup>c</sup>Calculated result obtained using 51 groups.

<sup>d</sup>Calculated result obtained using 61 groups.

Table 16. Comparison of Calculated and Measured Bonner Ball Count Rates ( $s^{-1} \cdot W^{-1}$ ) in the Shielded Void Region of Several Configurations IV

Detector	Configuration				
	IV.IA	IV.J	IV.K	IV.L	IV.M
<b>Bare BF<sub>3</sub></b>					
Calculated	3.28(-5) <sup>a</sup>	1.59(-5)	6.84(-6)	2.90(-6)	1.24(-6)
Measured	6.54(-5)	2.92(-5)	1.38(-5)	6.18(-6)	3.00(-6)
C/E <sup>b</sup>	0.50	0.54	0.50	0.47	0.41
<b>Cd-cov. BF<sub>3</sub></b>					
Calculated	1.95(-5)	8.54(-6)	3.56(-6)	1.45(-6)	6.07(-7)
Measured	2.85(-5)	1.12(-5)	4.85(-6)	1.92(-6)	7.34(-7)
C/E	0.68	0.76	0.73	0.76	0.83
<b>3-in. BB<sup>c</sup></b>					
Calculated	2.50(-4)	1.02(-4)	4.02(-5)	1.54(-5)	6.08(-6)
Measured	3.12(-4)	1.14(-4)	4.83(-5)	1.76(-5)	6.60(-6)
C/E	0.80	0.89	0.83	0.88	0.92
<b>5-in. BB</b>					
Calculated	4.24(-4)	1.59(-4)	5.85(-5)	2.12(-5)	7.88(-6)
Measured	5.40(-4)	1.82(-4)	7.04(-5)	2.51(-5)	8.50(-6)
C/E	0.79	0.87	0.83	0.84	0.93
<b>8-in. BB</b>					
Calculated	1.71(-4)	5.98(-5)	2.08(-5)	7.21(-6)	2.59(-6)
Measured	2.11(-4)	6.60(-5)	2.40(-5)	8.20(-6)	2.66(-6)
C/E	0.81	0.91	0.87	0.88	0.97
<b>10-in. BB</b>					
Calculated	6.93(-5)	2.35(-5)	8.01(-6)	2.75(-6)	9.83(-7)
Measured	8.82(-5)	2.48(-5)	9.34(-6)	3.12(-6)	1.04(-6)
C/E	0.79	0.95	0.86	0.88	0.95

<sup>a</sup>Read as  $3.28 \times 10^{-5}$ .

<sup>b</sup>Calculation-to-experiment ratio.

<sup>c</sup>Bonner ball.



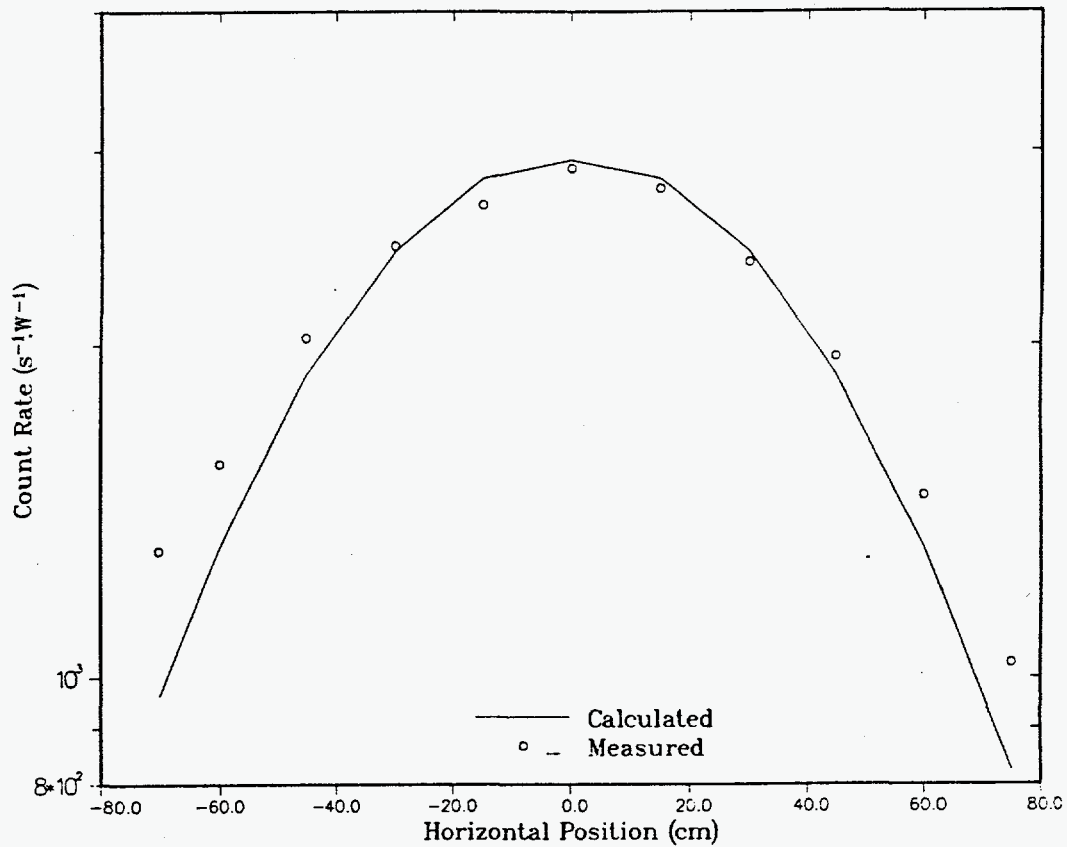


Fig. 9. Comparison of calculated and measured 5-in. Bonner ball count rates for a horizontal traverse 30 cm behind Configuration I.A (C/E range: 0.74-1.06)

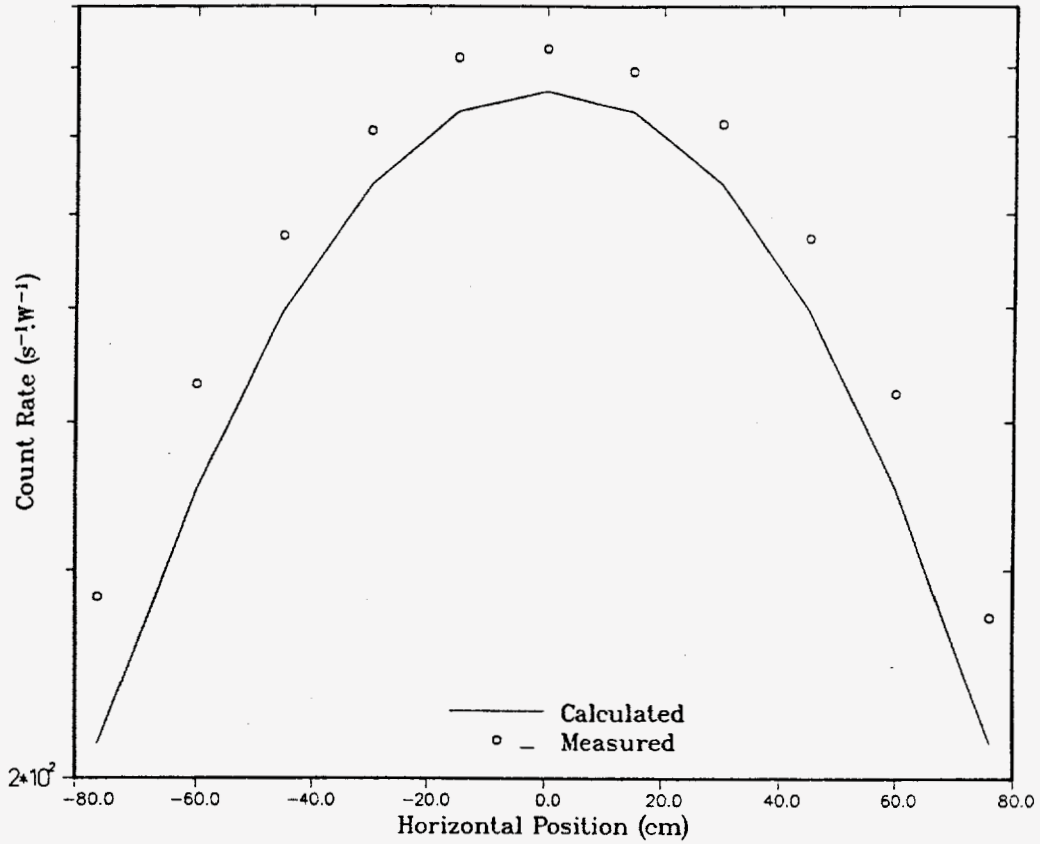


Fig. 10. Comparison of calculated and measured 5-in. Bonner ball count rates for a horizontal traverse 30 cm behind Configuration II.A (C/E range: 0.75-0.92)

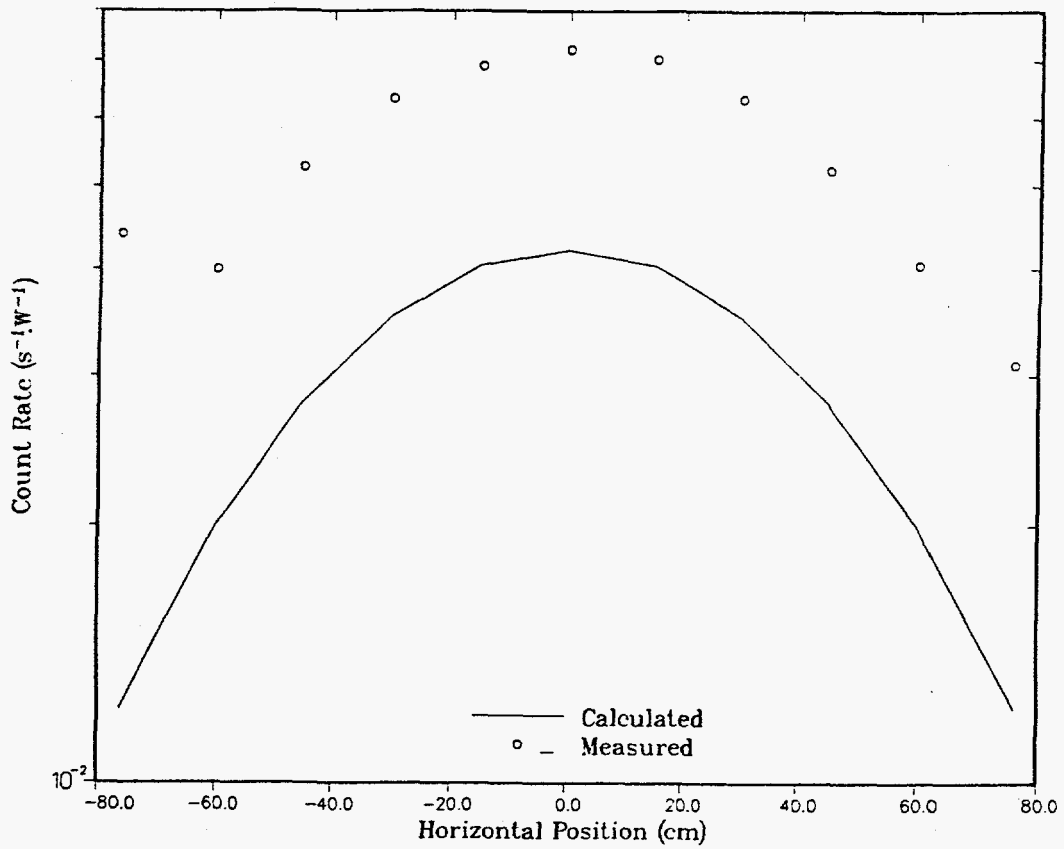


Fig. 11. Comparison of calculated and measured 5-in. Bonner ball count rates for a horizontal traverse 30 cm behind Configuration II.D (C/E range: 0.28-0.58)

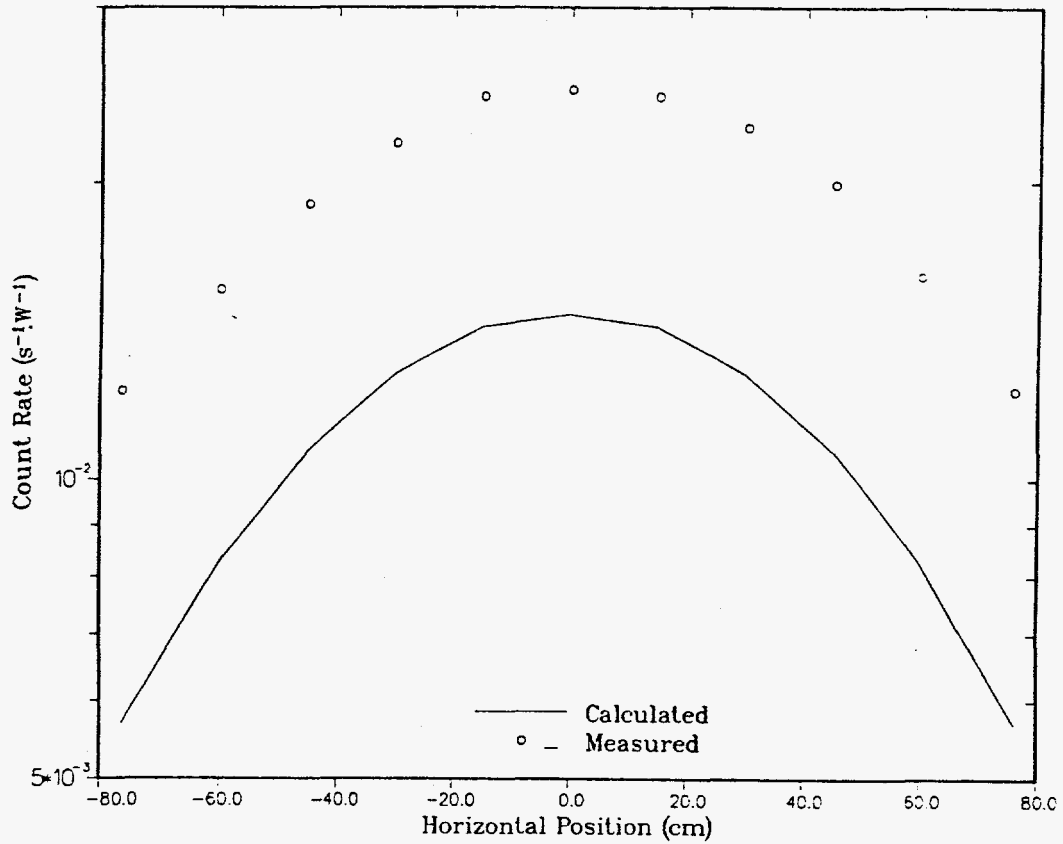


Fig. 12. Comparison of calculated and measured 5-in. Bonner ball count rates for a horizontal traverse 30 cm behind Configuration II.E (C/E range: 0.46-0.59)

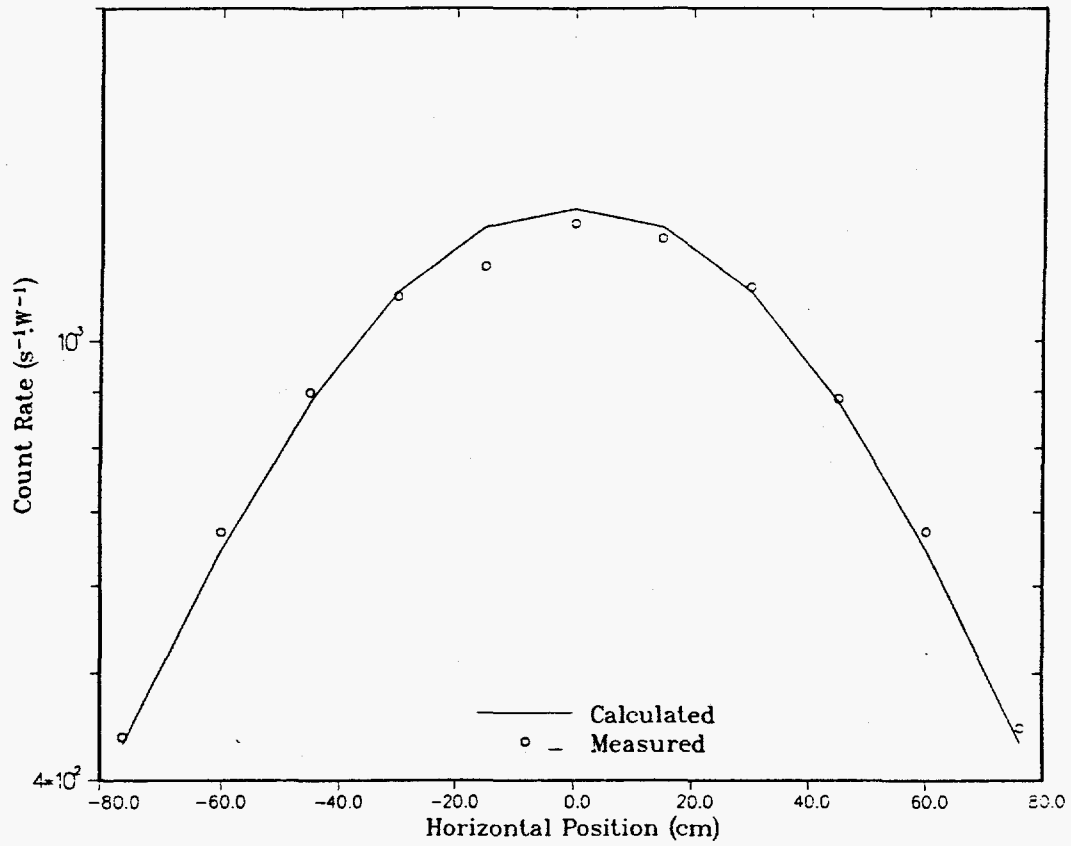


Fig. 13. Comparison of calculated and measured 5-in. Bonner ball count rates for a horizontal traverse 30 cm behind Configuration III.A (C/E range: 0.96-1.09)

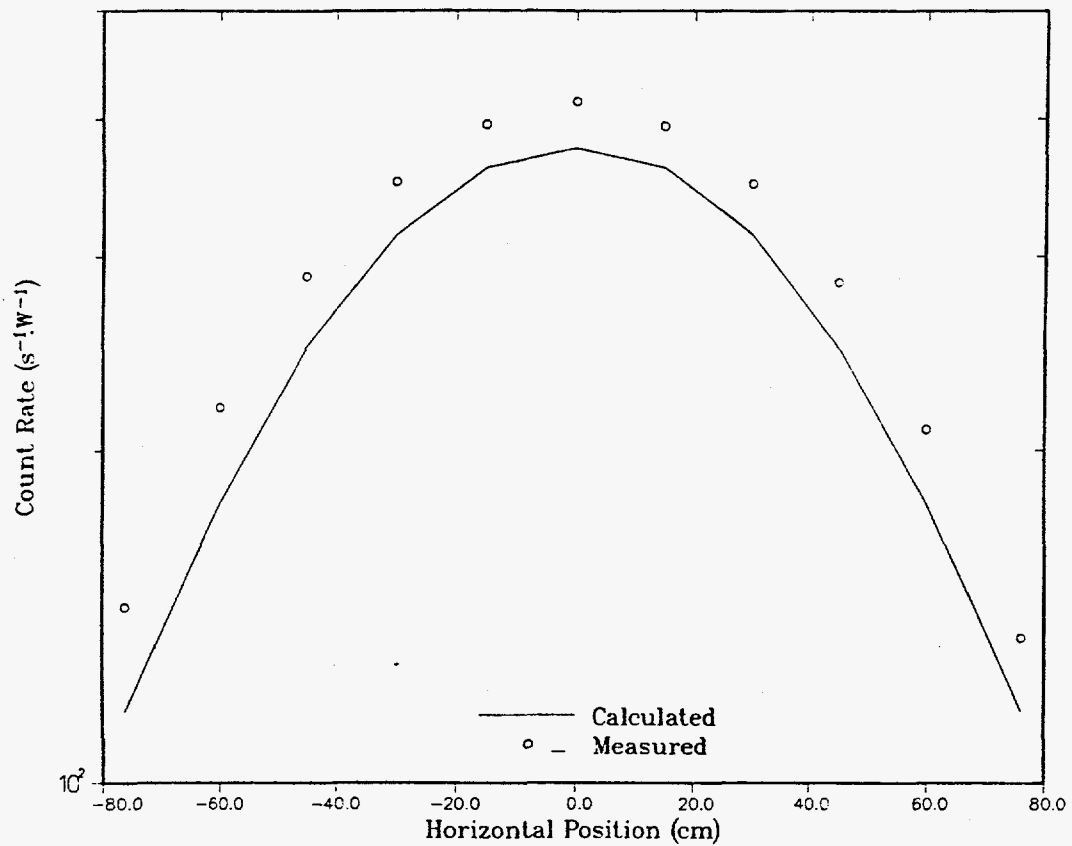


Fig. 14. Comparison of calculated and measured 5-in. Bonner ball count rates for a horizontal traverse 30 cm behind Configuration III.B (C/E range: 0.81-0.94)

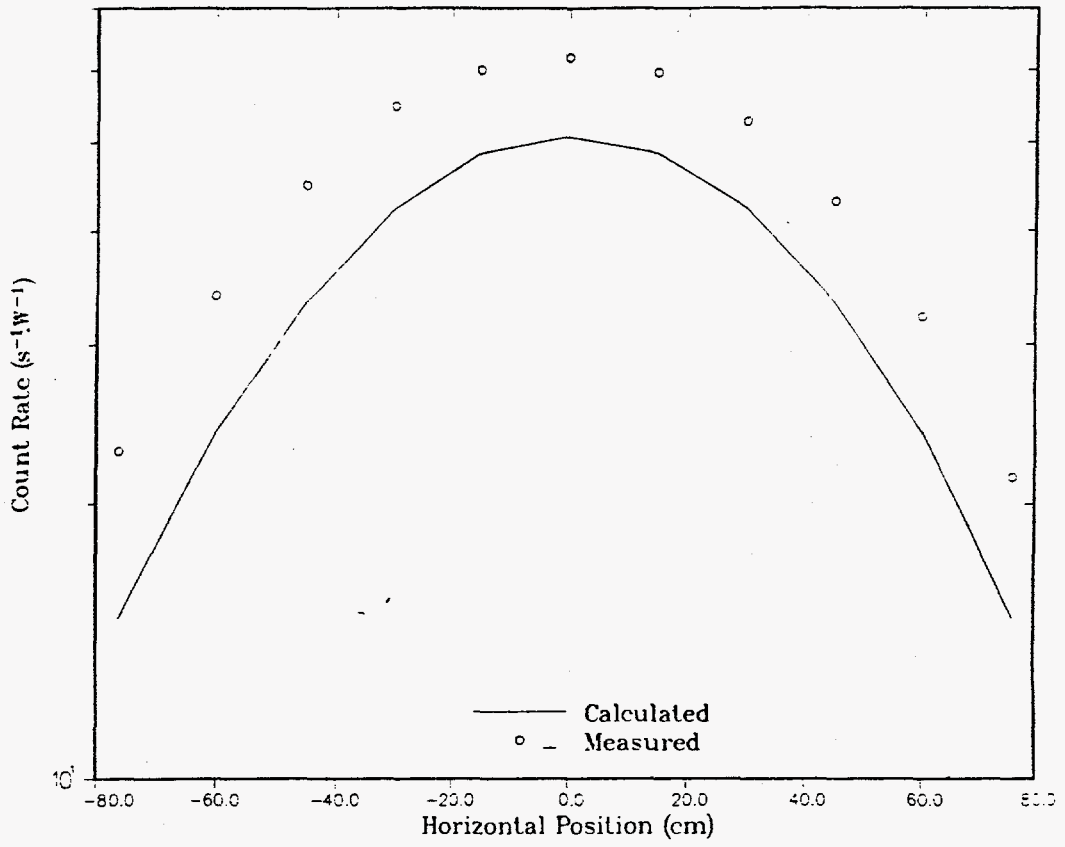


Fig. 15. Comparison of calculated and measured 5-in. Bonner ball count rates for a horizontal traverse 30 cm behind Configuration III.C (C/E range: 0.77-0.89)

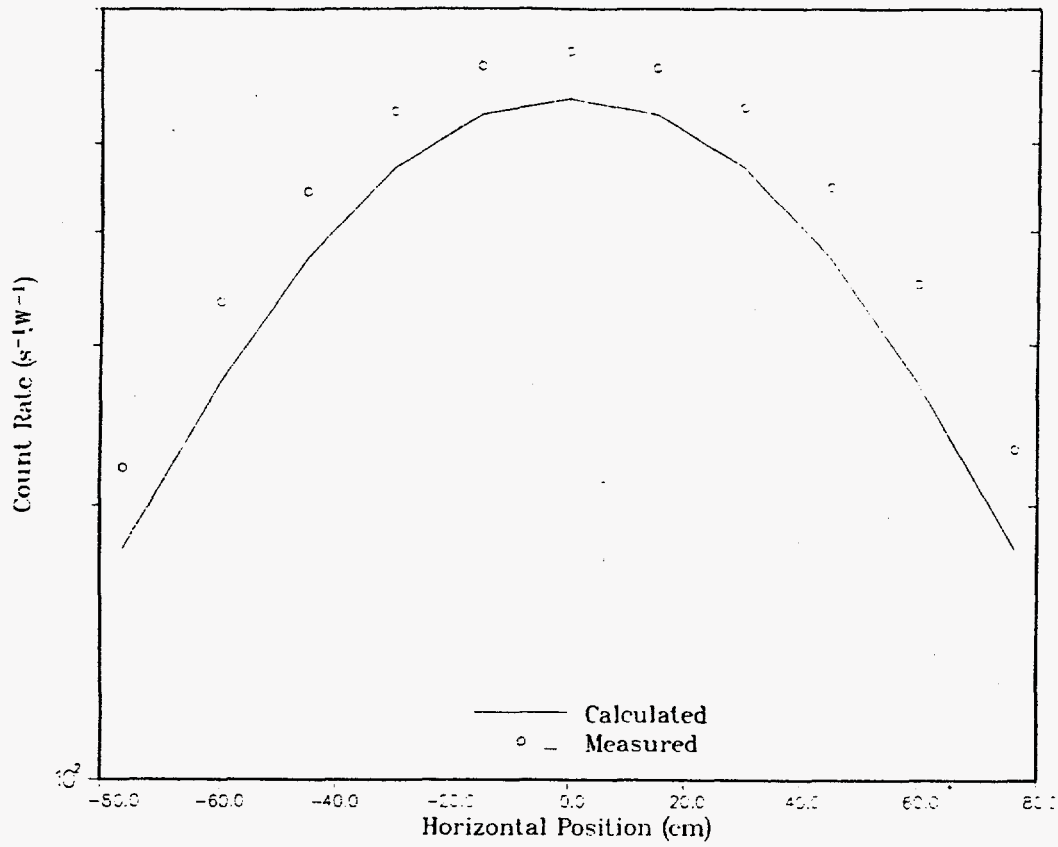


Fig. 16. Comparison of calculated and measured 5-in. Bonner ball count rates for a horizontal traverse 30 cm behind Configuration III.E (C/E range: 0.66-0.82)



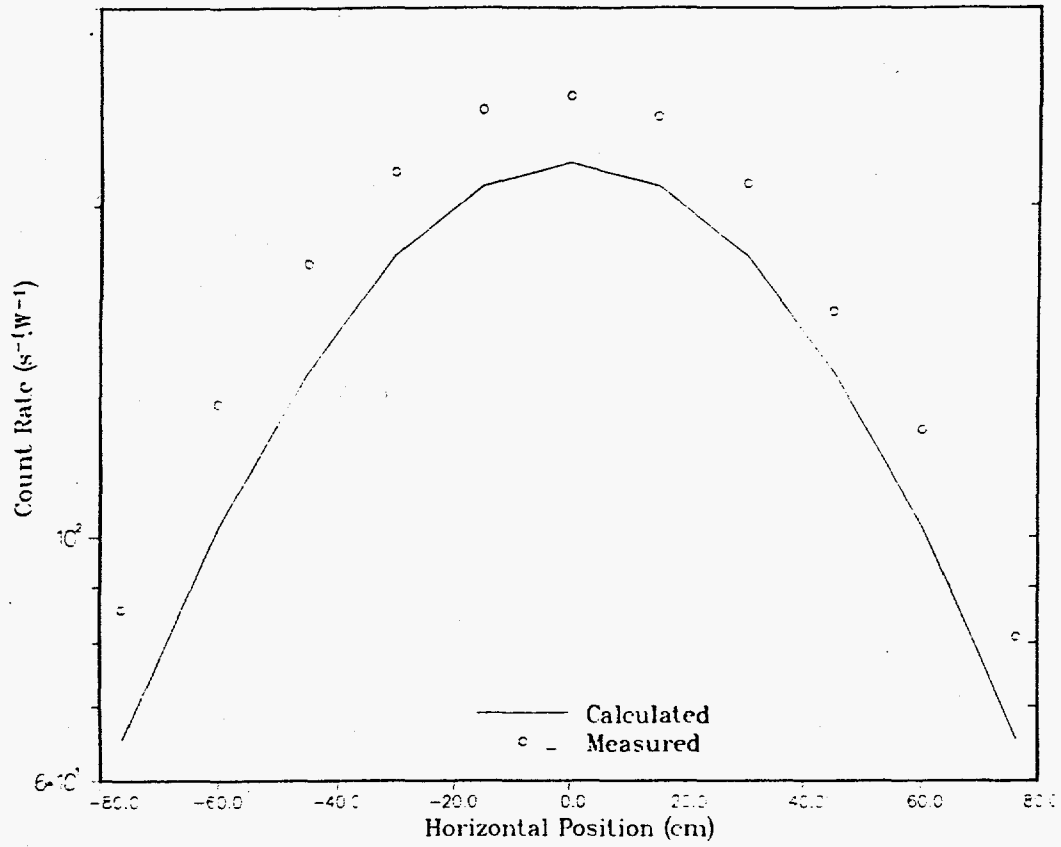


Fig. 17. Comparison of calculated and measured 5-in. Bonner ball count rates for a horizontal traverse 30 cm behind Configuration IV.A (C/E range: 0.76-0.87)

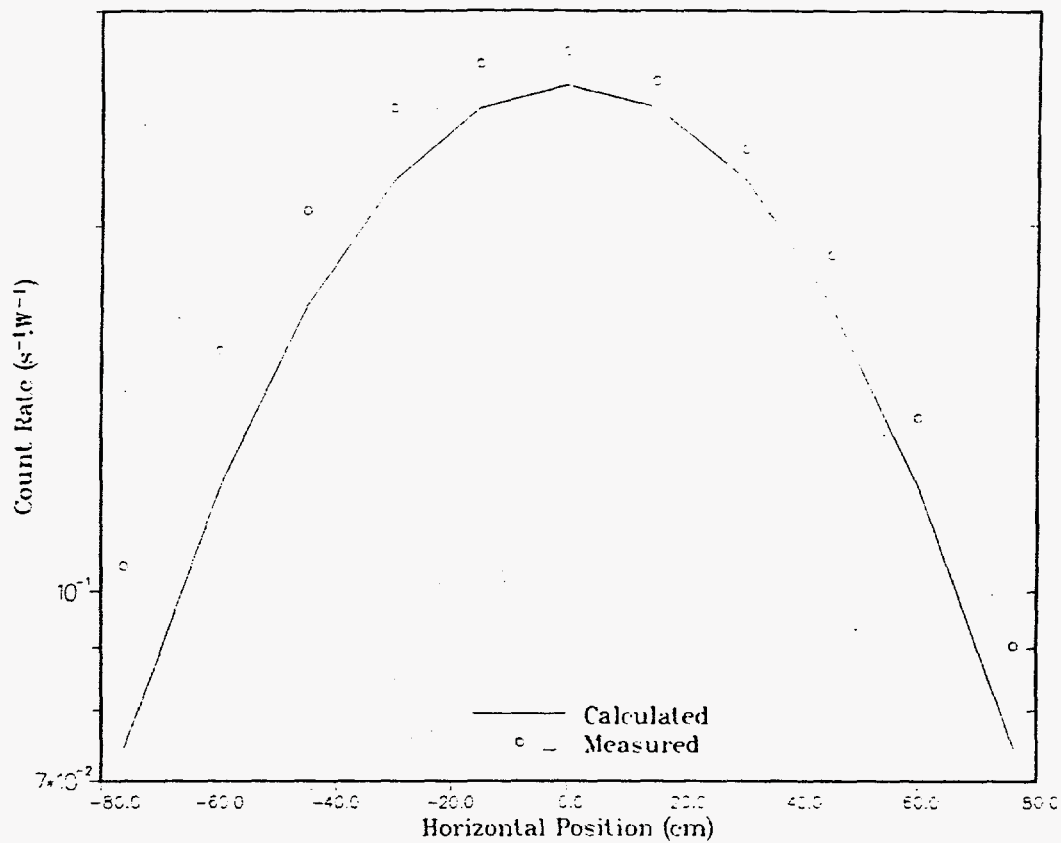


Fig. 18. Comparison of calculated and measured 5-in. Bonner ball count rates for a horizontal traverse 30 cm behind Configuration IV.C (C/E range: 0.71-0.95)

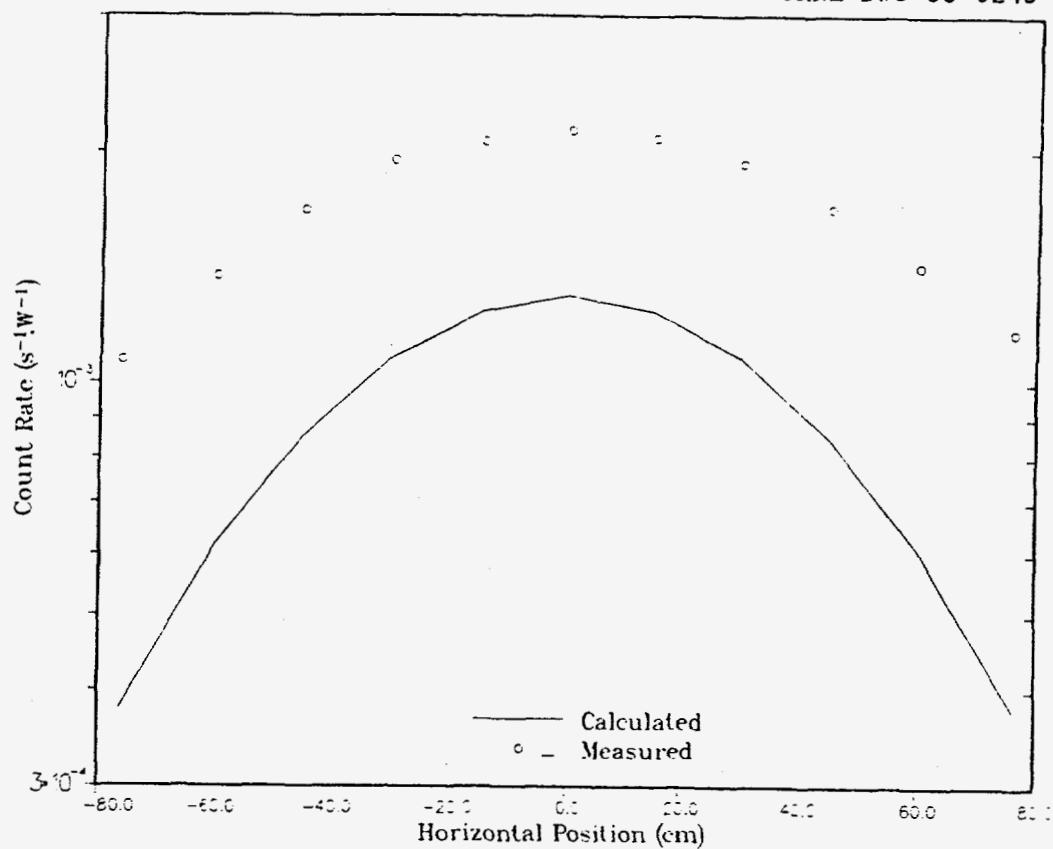


Fig. 19. Comparison of calculated and measured 5-in. Bonner ball count rates for a horizontal traverse 30 cm behind Configuration IV.G (C/E range: 0.32-0.61)

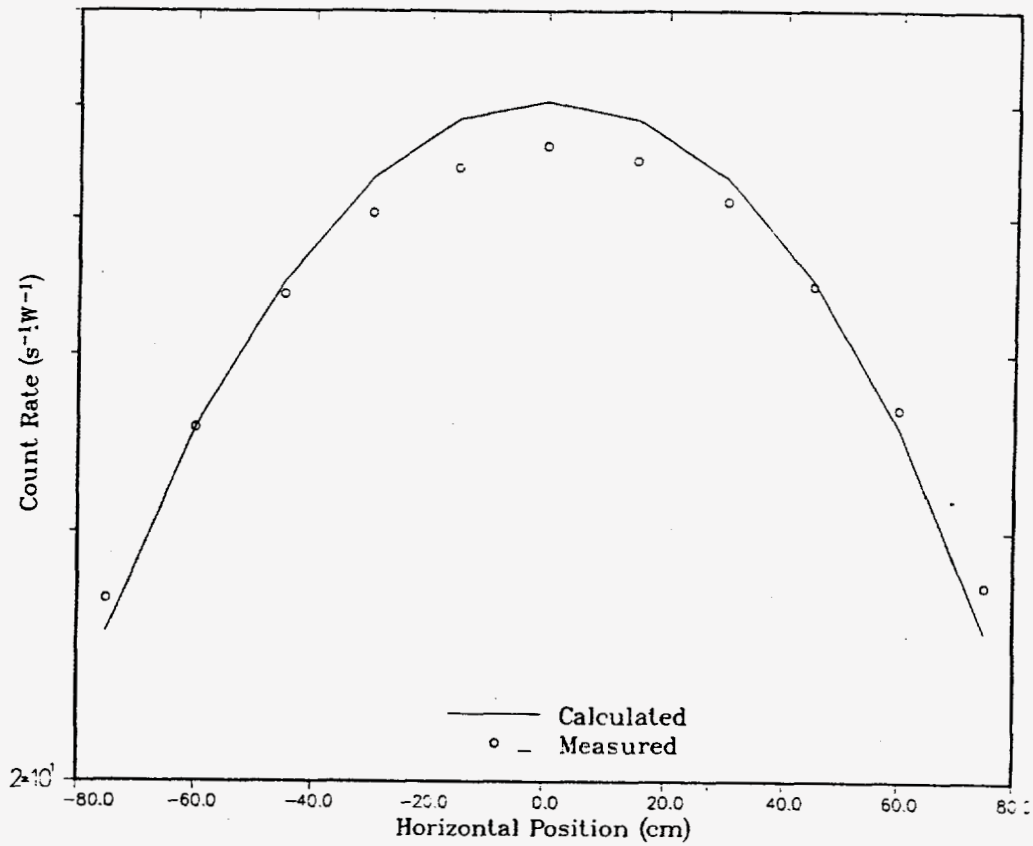


Fig. 20. Comparison of calculated and measured 5-in. Bonner ball count rates for a horizontal traverse 30 cm behind Configuration V.A (C/E range: 0.93-1.08)

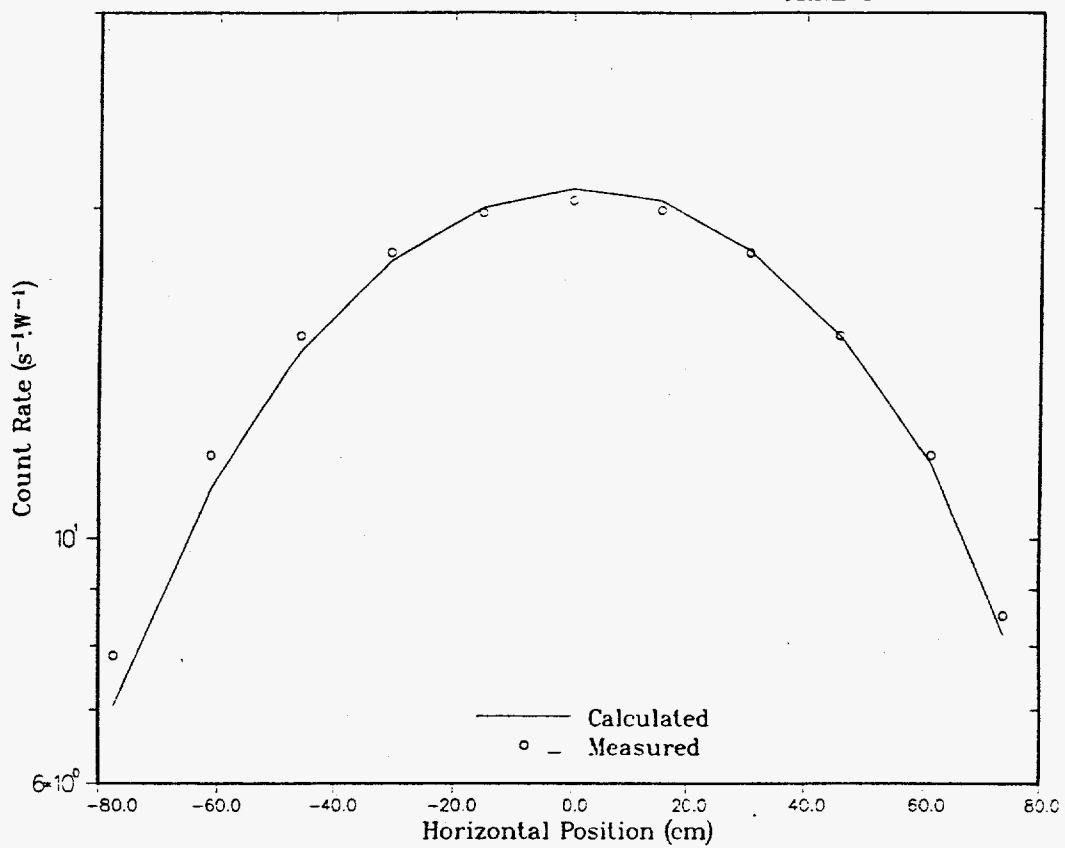


Fig. 21. Comparison of calculated and measured 5-in. Bonner ball count rates for a horizontal traverse 30 cm behind Configuration V.B (C/E range: 0.90-1.02)

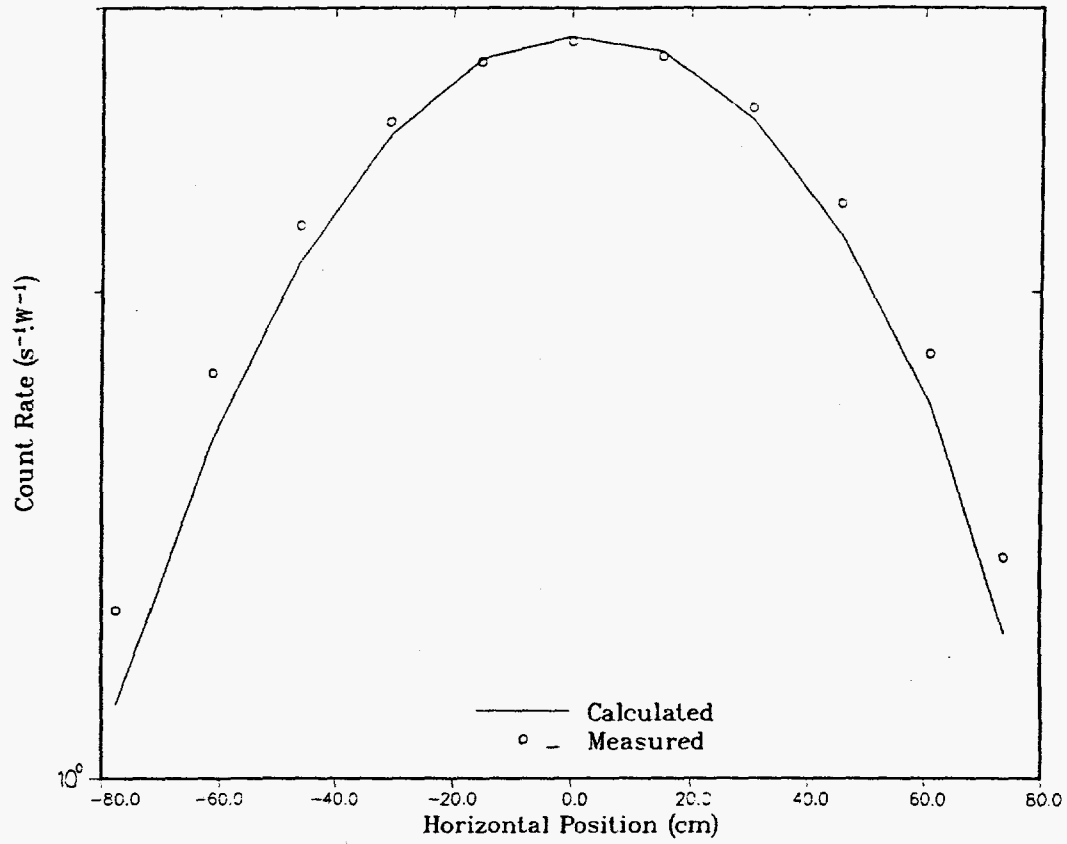


Fig. 22. Comparison of calculated and measured 5-in. Bonner ball count rates for a horizontal traverse 30 cm behind Configuration V.D (C/E range: 0.87-1.01)

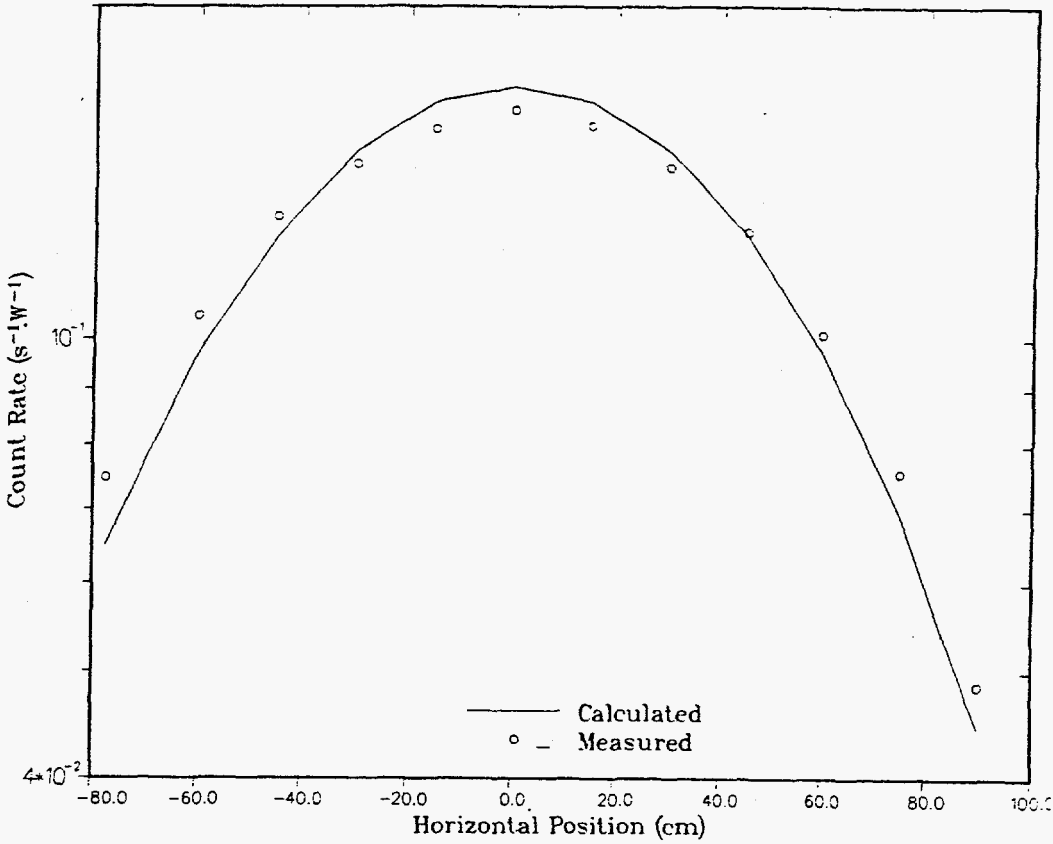


Fig. 23. Comparison of calculated and measured 5-in. Bonner ball count rates for a horizontal traverse 30 cm behind Configuration V.G (C/E range: 0.87-1.06)

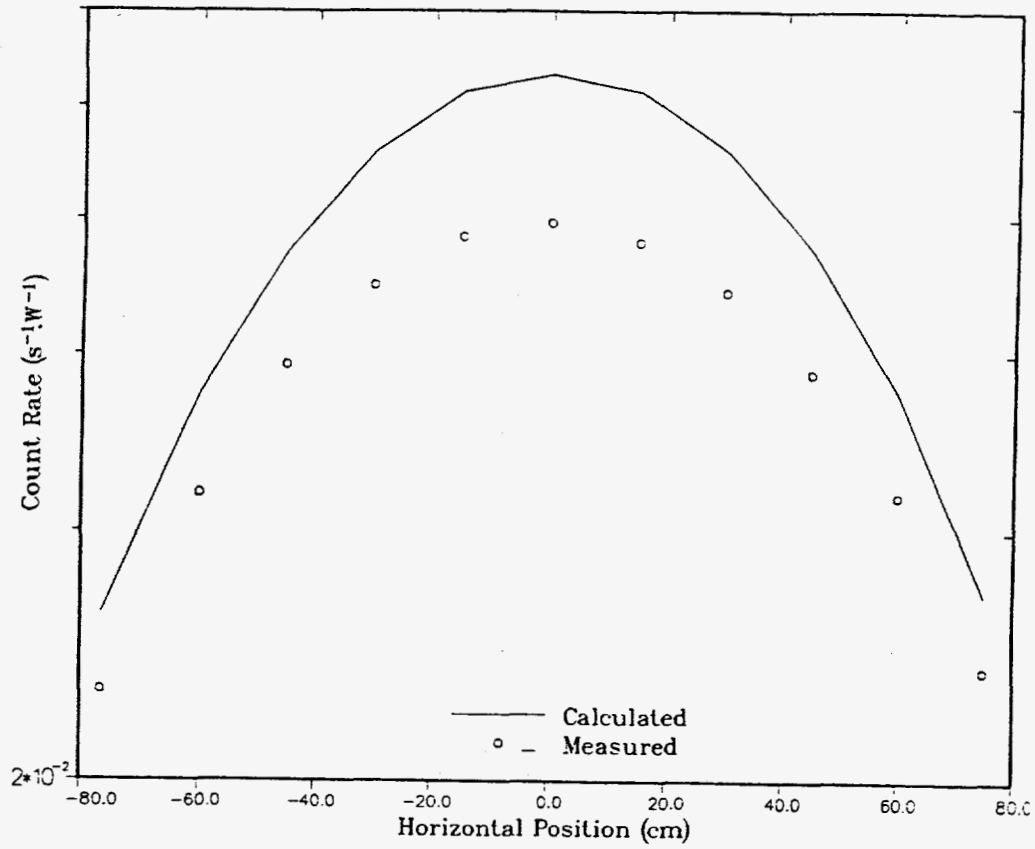


Fig. 24. Comparison of calculated and measured 5-in. Bonner ball count rates for a horizontal traverse 30 cm behind Configuration V.J (C/E range: 1.13-1.28)



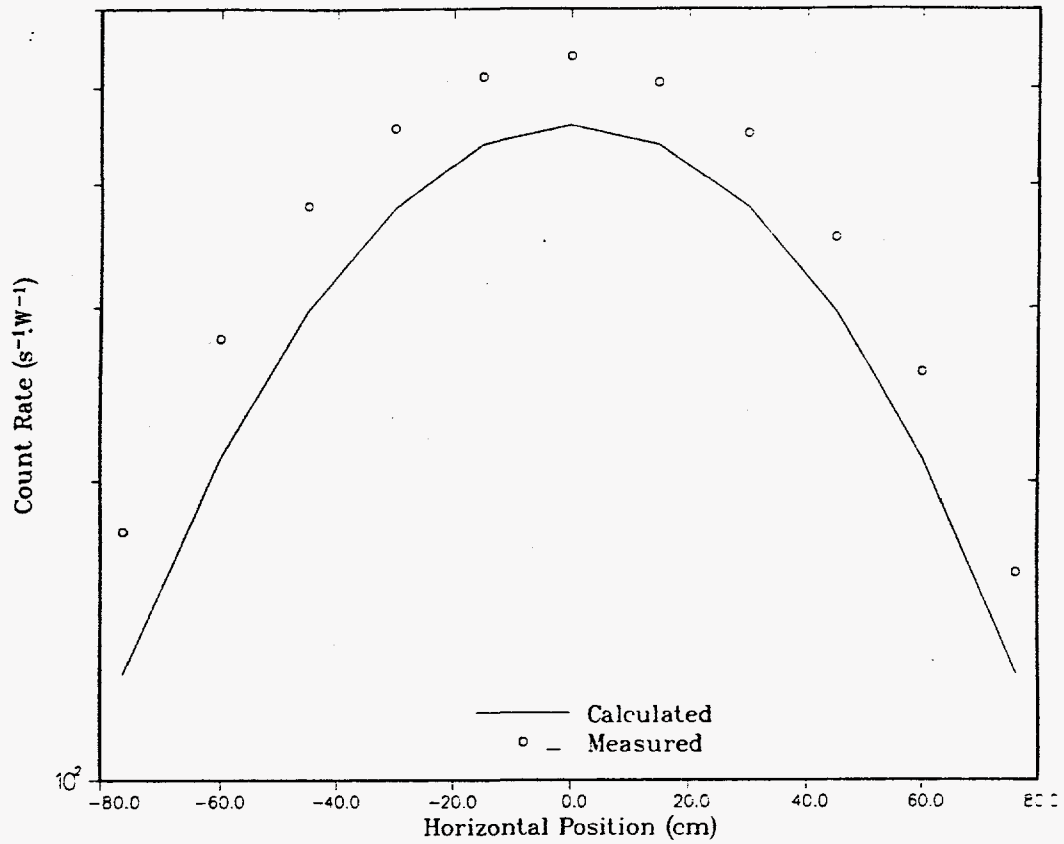


Fig. 25. Comparison of calculated and measured 5-in. Bonner ball count rates for a horizontal traverse 30 cm behind Configuration VI.A (C/E range: 0.72-0.87)

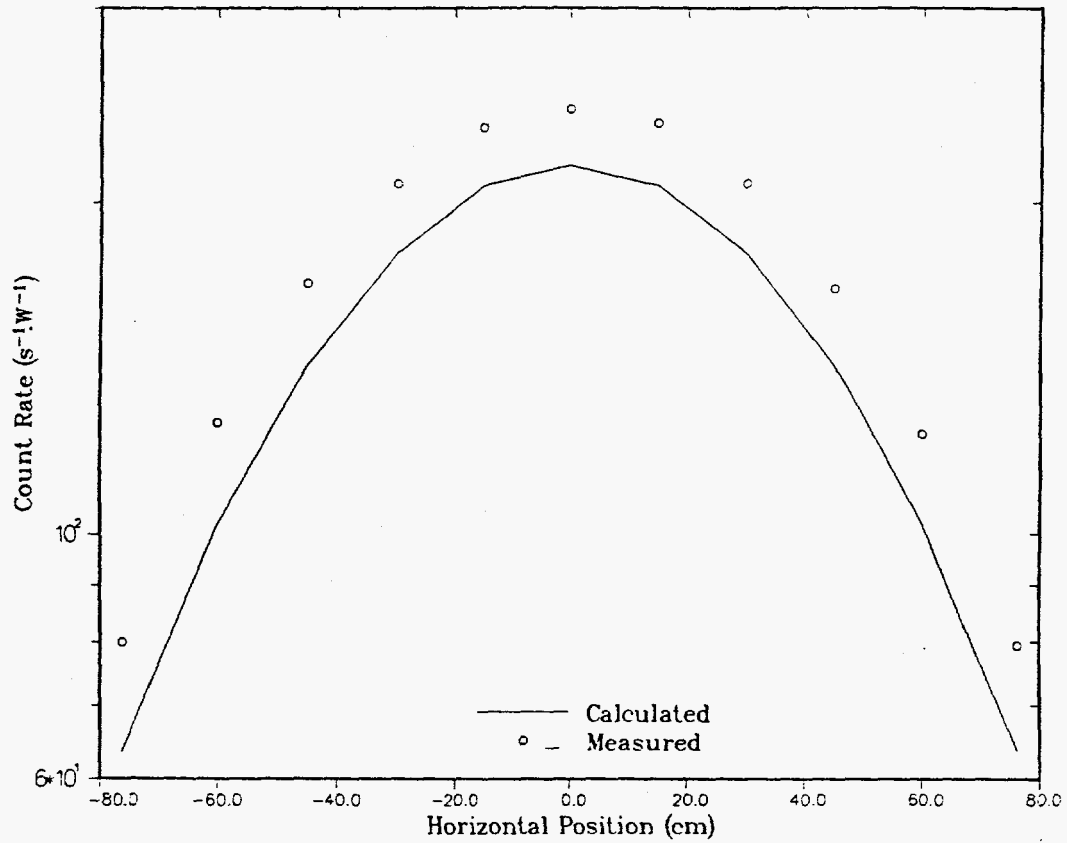


Fig. 26. Comparison of calculated and measured 5-in. Bonner ball count rates for a horizontal traverse 30 cm behind Configuration VI.B (C/E range: 0.79-0.89)

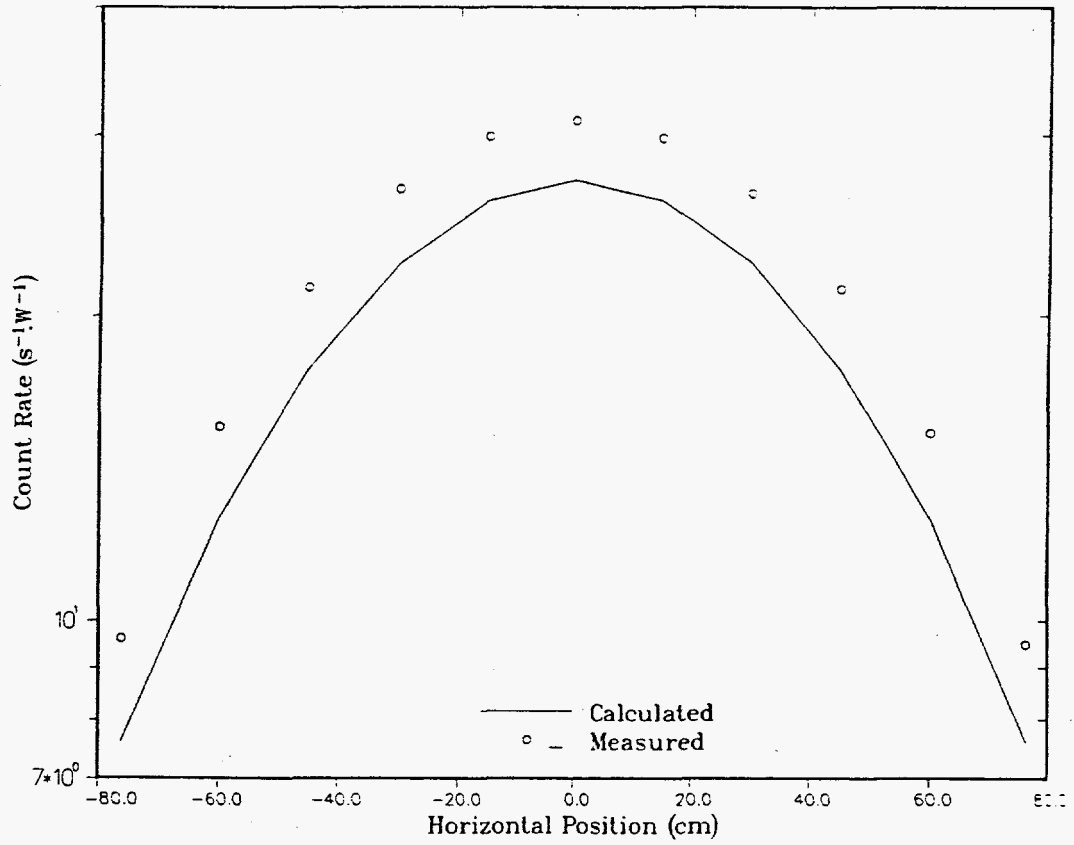


Fig. 27. Comparison of calculated and measured 5-in. Bonner ball count rates for a horizontal traverse 30 cm behind Configuration VI.D (C/E range: 0.79-0.87)

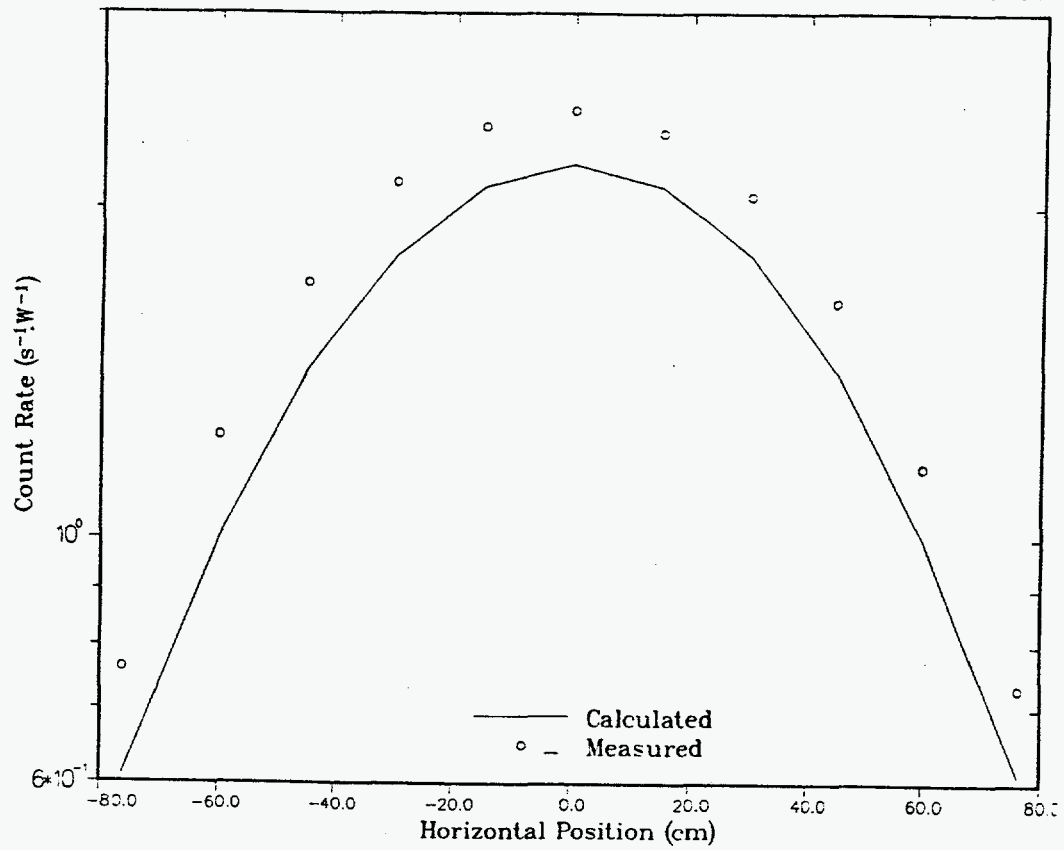


Fig. 28. Comparison of calculated and measured 5-in. Bonner ball count rates for a horizontal traverse 30 cm behind Configuration VI.F (C/E range: 0.80-0.89)

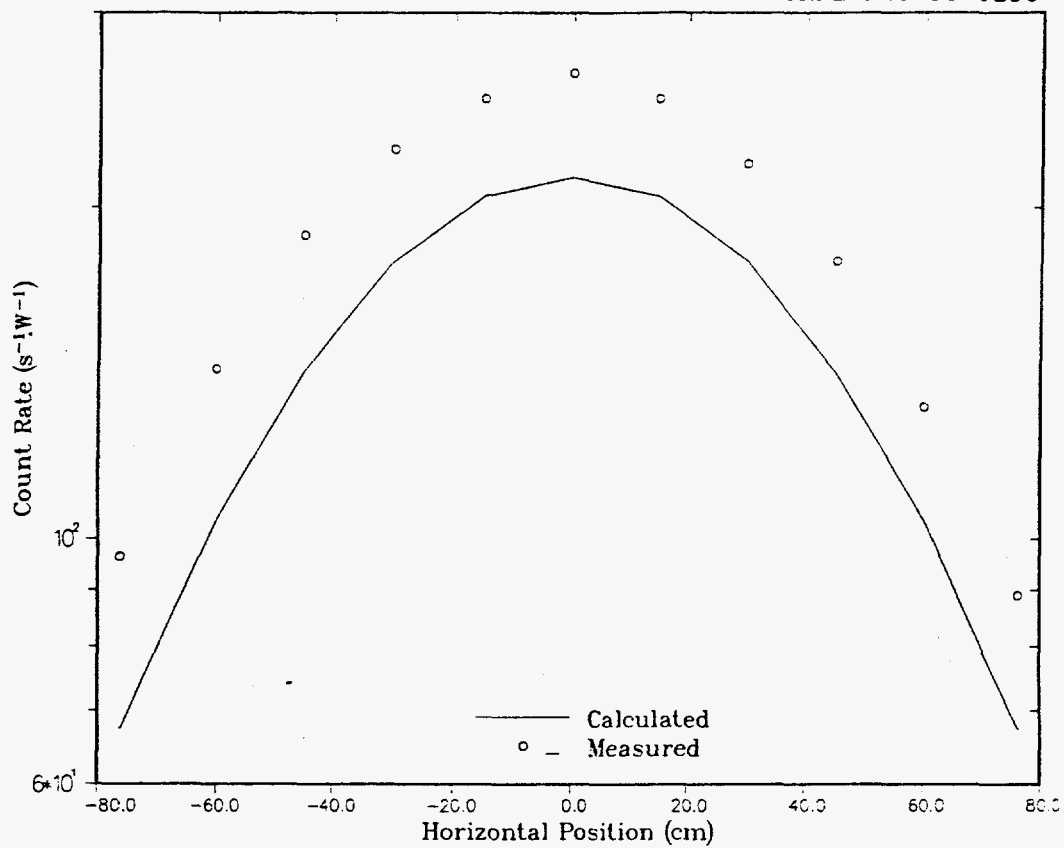


Fig. 29. Comparison of calculated and measured 5-in. Bonner ball count rates for a horizontal traverse 30 cm behind Configuration VII.A (C/E range: 0.70-0.82)

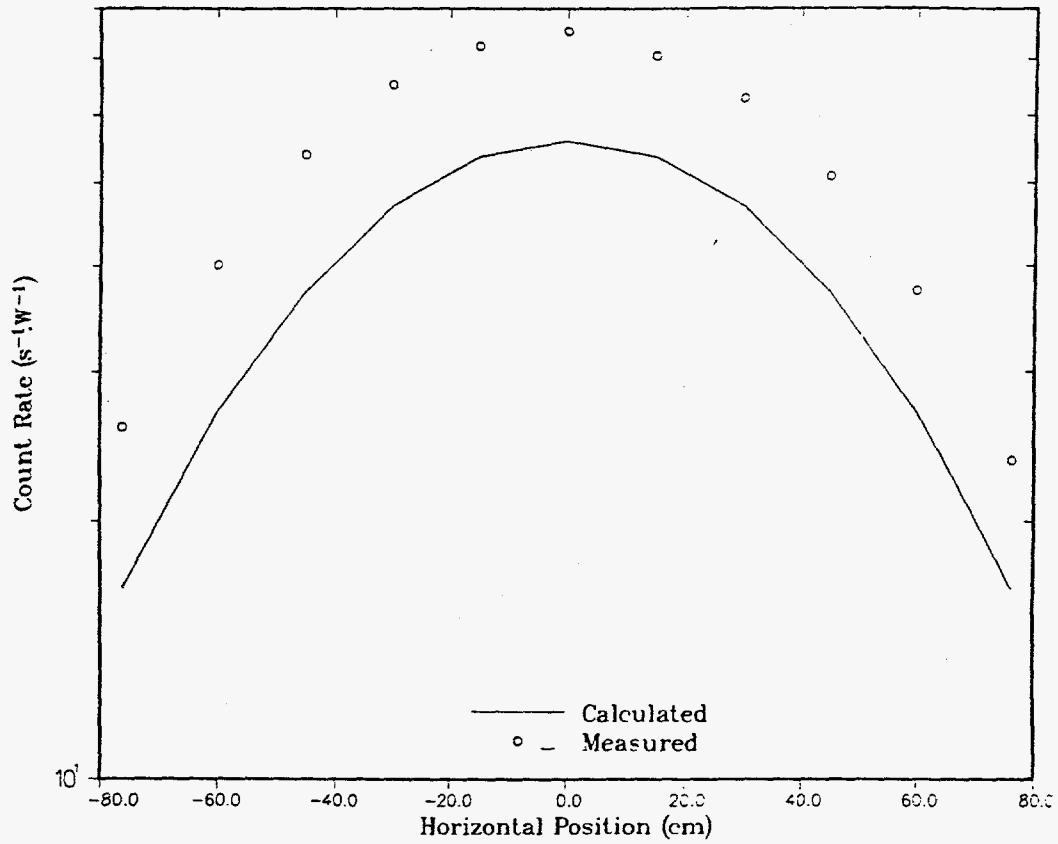


Fig. 30. Comparison of calculated and measured 5-in. Bonner ball count rates for a horizontal traverse 30 cm behind Configuration VII.B (C/E range: 0.65-0.76)

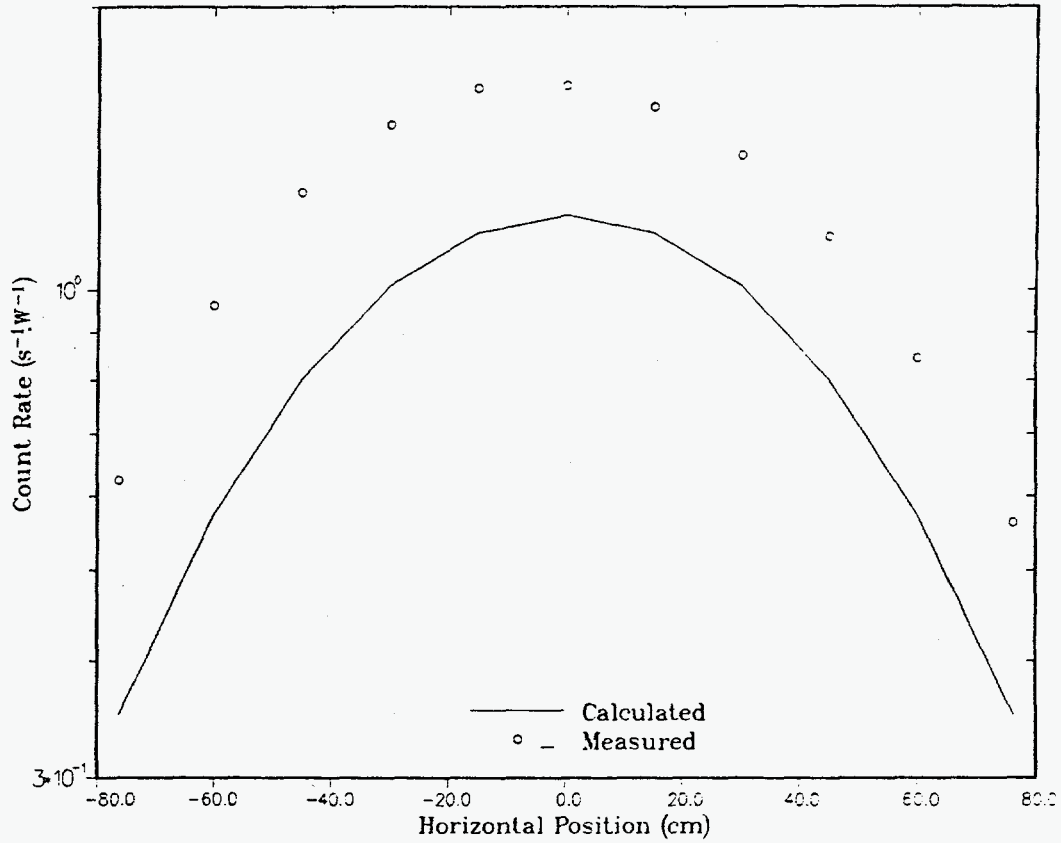


Fig. 31. Comparison of calculated and measured 5-in. Bonner ball count rates for a horizontal traverse 30 cm behind Configuration VII.C (C/E range: 0.56-0.73)

### 3.3 Discrepancies Between Calculated and Measured Spectra

The group structure was analyzed as a possible cause of the discrepancy between the calculated and measured neutron spectra. ANISN 1-D spherical geometry calculations were performed for Configurations II.D(1,2) and VI.F(1,2) using the 61-group library and the 174-group library from which it was derived. The 61-group spectra were normalized to the DOT-IV spectra and the 174-group spectra were scaled upward by the factors used to normalize the 61-group spectra (this factor was about 1.25 for both configurations). The two calculated spectra are compared with the measured spectra in Figs. 32 and 33 for Configurations II.D(1,2) and VI.F(1,2), respectively. The integrated fast-neutron flux for the 174-group calculations was found to be a factor of 1.03 higher for Configuration II.D(1,2) and a factor of 1.26 higher for Configuration VI.F(1,2). Thus, the group structure shows little effect for Configuration II.D(1,2) but a significant improvement in radiation transmission for Configuration VI.F(1,2). The C/E for Configuration II.D(1,2) would increase from 0.88 to 0.91, while that for Configuration VI.F(1,2) would increase from 0.84 to 1.06, probably due to the better representation of the carbon cross section with the fine-group structure.

### 3.4 Cross-Section Sensitivities

Because of the discrepancies between the calculated and measured detector responses, cross-section sensitivities were studied in order to determine the importance of the cross sections of various elements to calculated radiation levels. Two configurations, II.D(1,2) and IV.H, were studied. Configuration II.D(1,2) contained large amounts of steel and B<sub>4</sub>C while Configuration IV.H contained large amounts of steel and graphite. Sensitivities were calculated for the neutron flux in three energy ranges:  $E > 1.1$  MeV,  $E > 0.12$  MeV, and total ( $E > 0.0$  MeV). The results are shown in Table 17 for Configuration II.D(1,2) and Table 18 for Configuration IV.H. Cross sections for Fe, <sup>11</sup>B, Al, and <sup>238</sup>U are most important for Configuration II.D(1,2). Iron shows a high-energy effect while boron shows mostly a low-energy effect. For Configuration IV.H, the most important cross sections are those for Fe, C, Al, Cr, and <sup>238</sup>U. The only positive sensitivity shown is for <sup>235</sup>U, which is responsible the fission neutron source in the blankets.



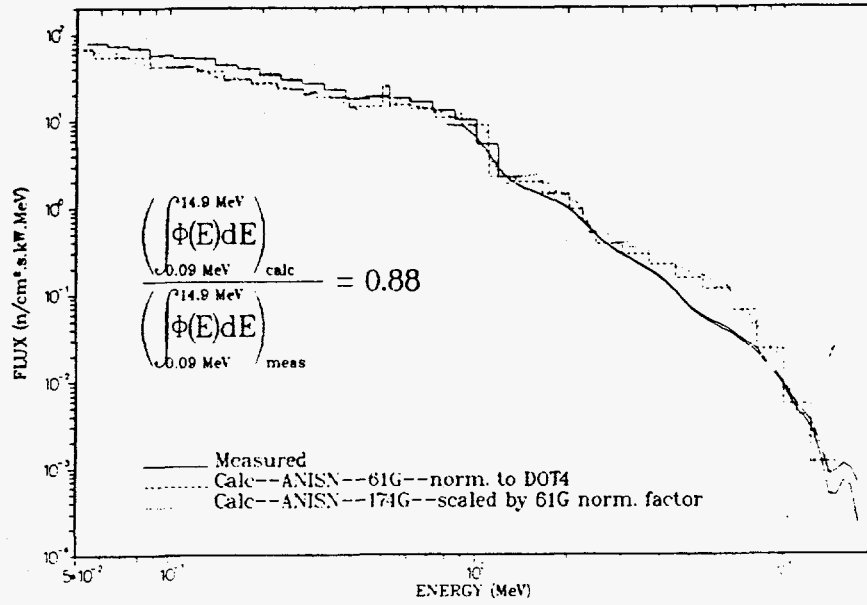


Fig. 32. Comparison of calculated 61-broad-group and 174-fine-group fast-neutron spectra with the measured spectrum on centerline 47.3 cm behind Configuration II.D

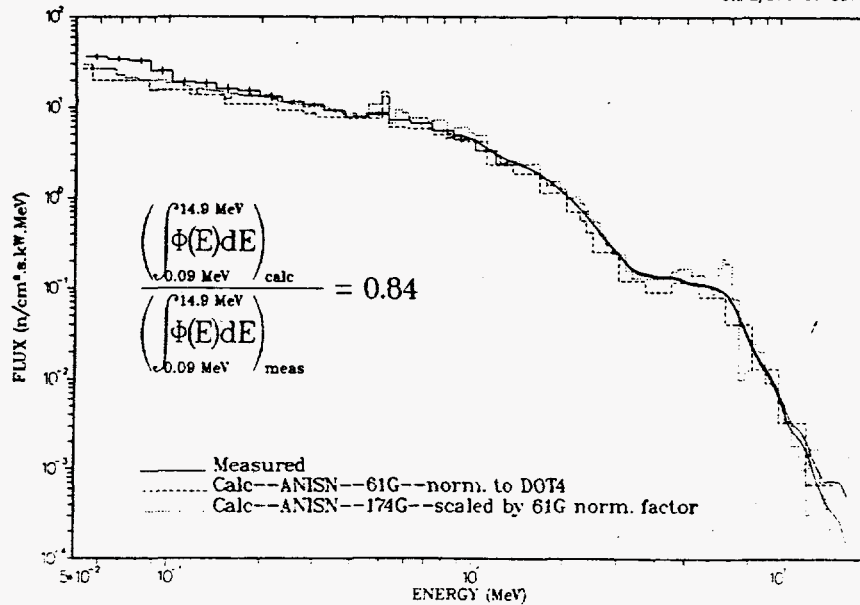


Fig. 33. Comparison of calculated 61-broad-group and 174-fine-group fast-neutron spectra with the measured spectrum on centerline 63.2 cm behind Configuration VI.F

Table 17. Sensitivities of Neutron Fluxes to Neutron Cross Sections of Various Elements Comprising the Shields of Configuration II.D (1-2)

Element	Response		Total Flux
	E > 1.1 MeV Flux	E > 0.12 MeV Flux	
B-10	-0.859	-1.285	-1.623
B-11	-2.585	-3.147	-3.218
C	-0.766	-1.037	-1.029
O	-0.543	-0.602	-0.631
Na	-0.158	-0.158	-0.161
Al	-1.478	-1.434	-1.433
Pb	-0.576	-0.366	-0.357
U-235	0.238	0.263	0.264
U-238	-1.237	-1.246	-1.238
Cr	-0.842	-0.675	-0.635
Ni	-0.436	-0.351	-0.341
Mn	-0.127	-0.115	-0.114
Fe	-4.811	-4.057	-3.861

Table 18. Sensitivities of Neutron Fluxes to Neutron Cross Sections of Various Elements Comprising the Shields of Configuration IV.H

Element	Response		Total Flux
	E > 1.1 MeV Flux	E > 0.12 MeV Flux	
B-10	-0.301	-0.377	-0.635
B-11	-0.849	-1.021	-1.393
C	-4.891	-6.551	-7.780
O	-0.579	-0.567	-0.683
Na	-0.165	-0.163	-0.183
Al	-2.112	-2.067	-2.112
U-235	0.213	0.247	0.299
U-238	-1.269	-1.287	-1.431
Cr	-1.858	-1.543	-1.500
Ni	-0.974	-0.823	-1.092
Mn	-0.260	-0.244	-0.410
Fe	-8.814	-7.282	-7.602

## 4.0 CONCLUSIONS

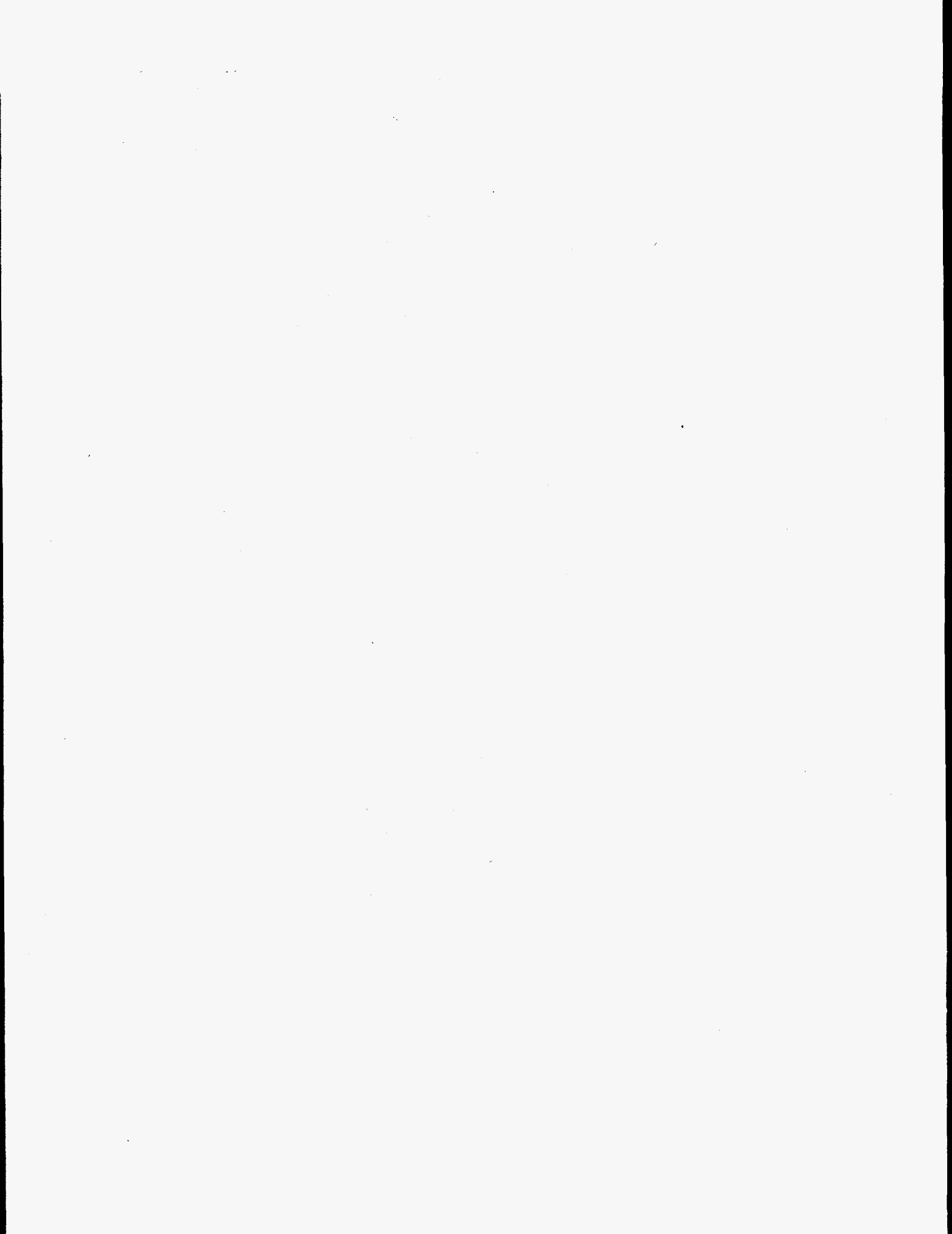
Measured data from the Radial Shield Attenuation Experiment have been analyzed. Calculations were performed with the DOT-IV two-dimensional discrete ordinates radiation transport code for each of the experimental configurations of the Radial Shield Attenuation Experiment and calculated results were compared with measured results. In general, the calculated results were in good agreement with the measured results. Some cases of disagreement were attributed to a high background contribution to the measured results. However, in other cases, the data appeared to be lacking. Configurations containing large amounts of  $B_4C$  gave low calculated results because of over-attenuation by the ENDF/B versions IV and V  $^{11}B$  data set. A LENDL set, which differed from the ENDF set mainly at high energies, gave much improved results but substantially overpredicted portions of the neutron spectra and substantially underpredicted others. It is preferable to the ENDF set, but the need for better high-energy cross-section definition for this set is indicated by the results obtained even with a fine-group structure. The broad-group structure was found to be partially responsible for the underprediction of radiation transmission through graphite. The integrated fast-neutron spectrum obtained using a fine-group structure indicated much better agreement with the measured spectrum for a configuration with much graphite. Detector responses for configurations having  $B_4C$  preceding sodium tended to be overpredicted. Finally, detector responses for Configurations VII (with 30 to 45 cm stainless steel) were slightly underpredicted. Larger differences than those seen here were noted between fine-group and broad-group results when the 61-group library was tested using 1-D mockups containing slabs of steel and sodium<sup>6</sup>. Thus, this slight underprediction is attributed to the broad-group structure.

The results of this analysis have a few implications for shield design analyses.

(1) Analyses using the ENDF  $^{11}B$  cross section set will probably underpredict neutron transmission through  $B_4C$  shields. Though not perfect, the LENDL  $^{11}B$  set is preferable to the ENDF set.

(2) Analyses of  $B_4C$  shields in deep sodium are likely to overpredict neutron transmission through the  $B_4C$  and the sodium that follows.

(3) Fine group calculations may be required for accurate calculation of neutron transmission through thick steel or graphite shields.



APPENDIX A  
EXPERIMENTAL PROGRAM PLAN FOR THE  
JASPER RADIAL SHIELD ATTENUATION EXPERIMENT

## APPENDIX A

### Experimental Program Plan for the JASPER Radial Shield Attenuation Experiment

#### I. Spectrum Modifier (SM) for near core shield designs

- A. SM1 (10.27cm Fe + 9.17cm Al + 2.54cm Boral + 20.32cm Radial Blanket)
1. NE-213 and hydrogen counter measurements on centerline as close as feasible to SM1.
  2. 3-, 5-, 10-in Bonner ball on centerline at same location as NE-213.
  3. 5-in BB horizontal traverse at 30cm behind configuration.
  4. 3-, 5-, 8-, 10-in BB measurements on centerline:
    - a. at 30cm behind configuration
    - b. at 304.8cm from reactor centerline (Foreground and Background)
    - c. at 457.2cm from reactor centerline (Foreground and Background).
  5. INS <sup>3</sup>He BB measurements on centerline:
    - a. at 30cm behind configuration
    - b. at 304.8cm from reactor centerline (Foreground and Background)
    - c. at 457.2cm from reactor centerline (Foreground and Background).

#### II. SM + Stainless Steel and B<sub>4</sub>C combinations (near core shield)

- A. SM1 + 1.27cm Al + 15.24cm SS
1. 5-in BB horizontal traverse at 30cm behind configuration.
  2. 3-, 5-, 8-, 10-in BB measurements on centerline:
    - a. at 30cm behind configuration
    - b. at 304.8cm from reactor centerline (Foreground and Background).

- B. SM1 + 1.27cm Al + 15.24cm SS + 1.27cm Al + 15.24cm B<sub>4</sub>C + 2.54cm SS
1. 3-, 5-, 8-, 10-in BB measurements on centerline:
    - a. at 30cm behind configuration
    - b. at 304.8cm from reactor centerline (Foreground and Background).
- C. SM1 + 1.27cm Al + 15.24cm SS + 1.27cm Al + 15.24cm B<sub>4</sub>C + 2.54cm SS + 1.27cm Al + 10.16cm B<sub>4</sub>C + 5.08cm B<sub>4</sub>C
1. 3-, 5-, 8-, 10-in BB measurements on centerline:
    - a. at 30cm behind configuration
    - b. at 304.8cm from reactor centerline (Foreground and Background).
- D. SM1 + 1.27cm Al + 15.24cm SS + 1.27cm Al + 15.24cm B<sub>4</sub>C + 2.54cm SS + 1.27cm Al + 10.16cm B<sub>4</sub>C + 5.08cm B<sub>4</sub>C + 1.27cm Al + 10.16cm B<sub>4</sub>C + 5.08cm B<sub>4</sub>C
1. NE-213 and hydrogen counter measurements on centerline as close as feasible behind configuration.
  2. 3-, 5-, 10-in BB measurements on centerline at same location as NE-213.
  3. 5-in BB horizontal traverse at 30cm behind configuration.
  4. 3-, 5-, 8-, 10-in BB measurements on centerline:
    - a. at 30cm behind configuration
    - b. at 304.8cm from reactor centerline (Foreground and Background).
  5. INS <sup>3</sup>He BB measurements on centerline:
    - a. at 30cm behind configuration
    - b. at 304.8cm from reactor centerline (Foreground and Background).
- E. SM1 + 1.27cm Al + 15.24cm SS + 1.27cm Al + 15.24cm B<sub>4</sub>C + 2.54cm SS + 1.27cm Al + 10.16cm B<sub>4</sub>C + 5.08cm B<sub>4</sub>C + 1.27cm Al + 10.16cm B<sub>4</sub>C + 5.08cm B<sub>4</sub>C + 30.48cm Na
1. 5-in BB horizontal traverse at 30cm behind configuration.

2. Bare, Cd-covered, 3-, 5-, 8-, 10-in BB measurements on centerline:
  - a. at 30cm behind configuration
  - b. at 304.8cm from reactor centerline (Foreground and Background).
3. Bare detector on centerline at 30cm behind configuration inside partial cadmium enclosure that surrounded the detector except on the side of the last slab in the configuration.
4. Bare detector on centerline at 501.3cm point with cadmium sheet over face of last slab in the configuration.

### III. SM + SS and B<sub>4</sub>C

#### A. SM1 + 10.16cm SS

1. 5-in BB horizontal traverse at 30cm behind configuration.
2. 3-, 5-, 8-, 10-in BB measurements on centerline:
  - a. at 30cm behind configuration
  - b. at 304.8cm from reactor centerline (Foreground and Background).

#### B. SM1 + 10.16cm SS + 5.08cm B<sub>4</sub>C

1. 5-in BB horizontal traverse at 30cm behind configuration.
2. 3-, 5-, 8-, 10-in BB measurements on centerline:
  - a. at 30cm behind configuration
  - b. at 304.8cm from reactor centerline (Foreground and Background).

#### C. SM1 + 20.32cm SS

1. 5-in BB horizontal traverse at 30cm behind configuration.
2. 3-, 5-, 8-, 10-in BB measurements on centerline:
  - a. at 30cm behind configuration
  - b. at 304.8cm from reactor centerline (Foreground and Background).



- D.  $SM1 + 20.32\text{cm SS} + 5.08\text{cm B}_4\text{C}$ 
  - 1. 3-, 5-, 8-, 10-in BB measurements on centerline:
    - a. at 30cm behind configuration
    - b. at 304.8cm from reactor centerline (Foreground and Background).
  
- E.  $SM1 + 20.32\text{cm SS} + 5.08\text{cm B}_4\text{C} + 5.08\text{cm B}_4\text{C}$ 
  - 1. 5-in BB horizontal traverse at 30cm behind configuration.
  - 2. 3-, 5-, 8-, 10-in BB measurements on centerline:
    - a. at 30cm behind configuration
    - b. at 304.8cm from reactor centerline (Foreground and Background).

IV. SM + Graphite and  $B_4C$  (tank type shield reference)

- A.  $SM1 + 1.27\text{cm Al} + 15.24\text{cm SS} + 1.27\text{cm Al} + 10.16\text{cm C} + 5.08\text{cm SS}$ 
  - 1. 5-in BB horizontal traverse at 30cm behind configuration.
  - 2. 3-, 5-, 8-, 10-in BB measurements on centerline:
    - a. at 30cm behind configuration
    - b. at 304.8cm from reactor centerline (Foreground and Background).
  
- B.  $SM1 + 1.27\text{cm Al} + 15.24\text{cm SS} + 1.27\text{cm Al} + 10.16\text{cm C} + 5.08\text{cm SS} + 1.27\text{cm Al} + 10.16\text{cm C} + 5.08\text{cm SS}$ 
  - 1. 3-, 5-, 8-, 10-in BB measurements on centerline:
    - a. at 30cm behind configuration
    - b. at 304.8cm from reactor centerline (Foreground and Background).
  
- C.  $SM1 + 1.27\text{cm Al} + 15.24\text{cm SS} + 1.27\text{cm Al} + 10.16\text{cm C} + 5.08\text{cm SS} + 1.27\text{cm Al} + 10.16\text{cm C} + 5.08\text{cm SS} + 1.27\text{cm Al} + 15.24\text{cm B}_4\text{C} + 2.54\text{cm SS}$ 
  - 1. Ne-213 and hydrogen counter measurements on centerline as close as feasible behind SS.

2. 3-, 5-, 10-in BB measurements on centerline at same location as NE-213.
  3. 5-in BB horizontal traverse at 30cm behind configuration.
  4. 3-, 5-, 8-, 10-in BB measurements on centerline:
    - a. at 30cm behind configuration
    - b. at 304.8cm from reactor centerline (Foreground and Background)
    - c. at 457.2cm from reactor centerline (Foreground and Background).
  5. INS  $^3\text{He}$  BB measurements on centerline:
    - a. at 30cm behind configuration
    - b. at 304.8cm from reactor centerline (Foreground and Background)
    - c. at 457.2cm from reactor centerline (Foreground and Background).
- D. SM1 + 1.27cm Al + 15.24cm SS + 1.27cm Al + 10.16cm C + 5.08cm SS + 1.27cm Al + 10.16cm C + 5.08cm SS + 1.27cm Al + 15.24cm B<sub>4</sub>C + 2.54cm SS + 2.54cm Al + 5.08cm SS
1. 3-, 5-, 8-, 10-in BB measurements on centerline:
    - a. at 30cm behind configuration
    - b. at 457.2cm from reactor centerline (Foreground and Background).
- E. SM1 + 1.27cm Al + 15.24cm SS + 1.27cm Al + 10.16cm C + 5.08cm SS + 1.27cm Al + 10.16cm C + 5.08cm SS + 1.27cm Al + 15.24cm B<sub>4</sub>C + 2.54cm SS + 2.54cm Al + 5.08cm SS + 1.27cm Al + 10.16cm C + 5.08cm SS
1. 3-, 5-, 8-, 10-in BB measurements on centerline:
    - a. at 30cm behind configuration
    - b. at 457.2cm from reactor centerline (Foreground and Background).
- F. SM1 + 1.27cm Al + 15.24cm SS + 1.27cm Al + 10.16cm C + 5.08cm SS + 1.27cm Al + 10.16cm C + 5.08cm SS + 1.27cm Al + 15.24cm B<sub>4</sub>C + 2.54cm SS + 2.54cm Al + 5.08cm SS + 1.27cm Al + 10.16cm C + 5.08cm SS + 1.27cm Al + 10.16cm C + 5.08cm SS

1. 3-, 5-, 8-, 10-in BB measurements on centerline:
    - a. at 30cm behind configuration
    - b. at 457.2cm from reactor centerline (Foreground and Background).
  2. 3-, 5-, 8-, 10-in BB measurements on centerline as close as feasible:
    - a. Foreground (same location as background)
    - b. Background (30.48cm LiH between detector and configuration).
- G. SMI + 1.27cm Al + 15.24cm SS + 1.27cm Al + 10.16cm C + 5.08cm SS + 1.27cm Al + 10.16cm C + 5.08cm SS + 1.27cm Al + 15.24cm B<sub>4</sub>C + 2.54cm SS + 2.54cm Al + 5.08cm SS + 1.27cm Al + 10.16cm C + 5.08cm SS + 1.27cm Al + 10.16cm C + 5.08cm SS + 1.27cm Al + 10.16cm C + 5.08cm SS
1. 3-, 5-, 8-, 10-in BB measurements on centerline as close as feasible:
    - a. Foreground (same location as for background)
    - b. Background (30.48cm LiH between detector and configuration).
  2. INS <sup>3</sup>He BB measurements on centerline as close as feasible:
    - a. Foreground (same location as for background)
    - b. Background (30.48cm LiH between detector and configuration).
- H. SMI + 1.27cm Al + 15.24cm SS + 1.27cm Al + 10.16cm C + 5.08cm SS + 1.27cm Al + 10.16cm C + 5.08cm SS + 1.27cm Al + 15.24cm B<sub>4</sub>C + 2.54cm SS + 2.54cm Al + 5.08cm SS + 1.27cm Al + 10.16cm C + 5.08cm SS + 1.27cm Al + 10.16cm C + 5.08cm SS + 1.27cm Al + 10.16cm C + 5.08cm SS + 5.08cm SS
1. 3-, 5-, 8-, 10-in BB measurements on centerline as close as feasible:
    - a. Foreground (same location as for background)
    - b. Background (30.48cm LiH between detector and configuration).

- I. SM1 + 1.27cm Al + 15.24cm SS + 1.27cm Al + 10.16cm C + 5.08cm SS + 1.27cm Al + 10.16cm C + 5.08cm SS + 1.27cm Al + 15.24cm B<sub>4</sub>C + 2.54cm SS + 2.54cm Al + 5.08cm SS + 1.27cm Al + 10.16cm C + 5.08cm SS + 1.27cm Al + 10.16cm C + 5.08cm SS + 1.27cm Al + 10.16cm C + 5.08cm SS + 5.08cm SS + 30.48cm Na
1. bare, cd-covered, 3-, 5-, 8-, 10-in BB measurements on centerline as close as feasible:
    - a. Foreground (same as for background)
    - b. Background (30.48cm LiH between detector and configuration).
- IA. SM1 + 1.27cm Al + 15.24cm SS + 1.27cm Al + 10.16cm C + 5.08cm SS + 1.27cm Al + 10.16cm C + 5.08cm SS + 1.27cm Al + 5.24cm B<sub>4</sub>C + 2.54cm SS + 2.54cm Al + 5.08cm SS + 1.27cm Al + 10.16cm C + 5.08cm SS + 1.27cm Al + 10.16cm C + 5.08cm SS + 1.27cm Al + 10.16cm C + 5.08cm SS + 5.08cm SS + 30.48cm Na + 30cm Void + 30.48cm Na
1. bare, cd-covered, 3-, 5-, 8-, 10-in BB on centerline in 30cm void.
- J. SM1 + 1.27cm Al + 15.24cm SS + 1.27cm Al + 10.16cm C + 5.08cm SS + 1.27cm Al + 10.16cm C + 5.08cm SS + 1.27cm Al + 15.24cm B<sub>4</sub>C + 2.54cm SS + 2.54cm Al + 5.08cm SS + 1.27cm Al + 10.16cm C + 5.08cm SS + 1.27cm Al + 10.16cm C + 5.08cm SS + 1.27cm Al + 10.16cm C + 5.08cm SS + 5.08cm SS + 61cm Na + 30cm Void + 30.48cm Na
1. bare, cd-covered, 3-, 5-, 8-, 10-in BB on centerline in 30cm void.
  2. INS <sup>3</sup>He BB on centerline in 30cm void.
- K. SM1 + 1.27cm Al + 15.24cm SS + 1.27cm Al + 10.16cm C + 5.08cm SS + 1.27cm Al + 10.16cm C + 5.08cm SS + 1.27cm Al + 15.24cm B<sub>4</sub>C + 2.54cm SS + 2.54cm Al + 5.08cm SS + 1.27cm Al + 10.16cm C + 5.08cm SS + 1.27cm Al + 10.16cm C + 5.08cm SS + 1.27cm Al + 10.16cm C + 5.08cm SS + 5.08cm SS + 91cm Na + 30cm Void + 30.48cm Na
1. bare, cd-covered, 3-, 5-, 8-, 10-in BB on centerline in 30cm void.
- L. SM1 + 1.27cm Al + 15.24cm SS + 1.27cm Al + 10.16cm C + 5.08cm SS + 1.27cm Al + 10.16cm C + 5.08cm SS + 1.27cm Al + 15.24cm B<sub>4</sub>C + 2.54cm SS + 2.54cm Al + 5.08cm SS + 1.27cm Al + 10.16cm C + 5.08cm SS + 1.27cm Al + 10.16cm C + 5.08cm SS + 1.27cm Al + 10.16cm C + 5.08cm SS + 5.08cm SS + 122cm Na + 30cm Void + 30.48cm Na
1. bare, cd-covered, 3-, 5-, 8-, 10-in BB on centerline in 30cm void.

M. SM1 + 1.27cm Al + 15.24cm SS + 1.27cm Al + 10.16cm C + 5.08cm SS + 1.27cm Al + 10.16cm C + 5.08cm SS + 1.27cm Al + 15.24cm B<sub>4</sub>C + 2.54cm SS + 2.54cm Al + 5.08cm SS + 1.27cm Al + 10.16cm C + 5.08cm SS + 1.27cm Al + 10.16cm C + 5.08cm SS + 1.27cm Al + 10.16cm C + 5.08cm SS + 5.08cm SS + 152.4cm Na + 30cm Void + 30.48cm Na

1. bare, cd-covered, 3-, 5-, 8-, 10-in BB on centerline in 30cm void.
2. INS <sup>3</sup>He BB on centerline in 30cm void.

V. SM + SS + B<sub>4</sub>C (IHX Shield)

A. SM2 (10.27cm Fe + 9.17cm Al + 2.54cm Boral + 182.88cm Na)

1. 5-in BB horizontal traverse through midplane at 30cm behind configuration.
2. Bare, cd-covered, 3-, 5-, 8-, 10-in BB measurements on centerline:
  - a. at 30cm behind configuration
  - b. at 501.3cm from reactor centerline (Foreground and Background).
3. Bare detector on centerline at 30cm behind configuration inside partial cadmium enclosure that surrounded the detector except on the side of the last slab in the configuration.
4. Bare detector on centerline at 501.3cm point with cadmium sheet over face of last slab in the configuration.
5. INS <sup>3</sup>He BB measurements on centerline:
  - a. at 30cm behind configuration
  - b. at 501.3cm from reactor centerline (Foreground and Background).

B. SM2 + 5.08cm SS

1. 5-in BB horizontal traverse through midplane at 30cm behind configuration.
2. Bare, cd-covered, 3-, 5-, 8-, 10-in BB measurements on centerline:
  - a. at 30cm behind configuration

- b. at 501.3cm from reactor centerline (Foreground and Background).
  - 3. Bare detector on centerline at 30cm behind configuration inside partial cadmium enclosure that surrounded the detector except on the side of the last slab in the configuration.
  - 4. Bare detector on centerline at 501.3cm point with cadmium sheet over face of last slab in the configuration.
- C. SM2 + 5.08cm SS + 30.48cm Na
  - 1. Bare, cd-covered, 3-, 5-, 8-, 10-in BB measurements on centerline:
    - a. at 30cm behind configuration
    - b. at 501.3cm from reactor centerline (Foreground and Background).
  - 2. Bare detector on centerline at 30cm behind configuration inside partial cadmium enclosure that surrounded the detector except on the side of the last slab in the configuration.
  - 3. Bare detector on centerline at 501.3cm point with cadmium sheet over face of last slab in the configuration.
- D. SM2 + 5.08cm SS + 61cm Na
  - 1. 5-in BB horizontal traverse through midplane at 30cm behind configuration.
  - 2. Bare, cd-covered, 3-, 5-, 8-, 10-in BB measurements on centerline:
    - a. at 30cm behind configuration
    - b. at 501.3cm from reactor centerline (Foreground and Background).
  - 3. Bare detector on centerline at 30cm behind configuration inside partial cadmium enclosure that surrounded the detector except on the side of the last slab in the configuration.
  - 4. Bare detector on centerline at 501.3cm point with cadmium sheet over face of last slab in the configuration.
  - 5. INS  $^3\text{He}$  BB measurements on centerline:
    - a. at 30cm behind configuration

- b. at 501.3cm from reactor centerline (Foreground and Background).
- E. SM2 + 5.08cm B<sub>4</sub>C + 5.08cm SS
  - 1. Bare, cd-covered, 3-, 5-, 8-, 10-in BB measurements on centerline:
    - a. at 30cm behind configuration
    - b. at 501.3cm from reactor centerline (Foreground and Background).
  - 2. Bare detector on centerline at 30cm behind configuration inside partial cadmium enclosure that surrounded the detector except on the side of the last slab in the configuration.
  - 3. Bare detector on centerline at 501.3cm point with cadmium sheet over face of last slab in the configuration.
- F. SM2 + 5.08cm B<sub>4</sub>C + 5.08cm SS + 30.48cm Na
  - 1. Bare, cd-covered, 3-, 5-, 8-, 10-in BB measurements on centerline:
    - a. at 30cm behind configuration
    - b. at 501.3cm from reactor centerline (Foreground and Background).
  - 2. Bare detector on centerline at 30cm behind configuration inside partial cadmium enclosure that surrounded the detector except on the side of the last slab in the configuration.
  - 3. Bare detector on centerline at 501.3cm point with cadmium sheet over face of last slab in the configuration.
- G. SM2 + 5.08cm B<sub>4</sub>C + 5.08cm SS + 61cm Na
  - 1. 5-in BB horizontal traverse through midplane at 30cm behind configuration.
  - 2. Bare, cd-covered, 3-, 5-, 8-, 10-in BB measurements on centerline:
    - a. at 30cm behind configuration
    - b. at 501.3cm from reactor centerline (Foreground and Background).

3. Bare detector on centerline at 30cm behind configuration inside partial cadmium enclosure that surrounded the detector except on the side of the last slab in the configuration.
  4. Bare detector on centerline at 501.3cm point with cadmium sheet over face of last slab in the configuration.
  5. INS  $^3\text{He}$  BB measurements on centerline:
    - a. at 30cm behind configuration
    - b. at 501.3cm from reactor centerline (Foreground and Background).
- H. SM2 + 10.16cm B<sub>4</sub>C + 5.08cm SS
1. Bare, cd-covered, 3-, 5-, 8-, 10-in BB measurements on centerline:
    - a. at 30cm behind configuration
    - b. at 501.3cm from reactor centerline (Foreground and Background).
  2. Bare detector on centerline at 30cm behind configuration inside partial cadmium enclosure that surrounded the detector except on the side of the last slab in the configuration.
  3. Bare detector on centerline at 501.3cm point with cadmium sheet over face of last slab in the configuration.
- I. SM2 + 10.16cm B<sub>4</sub>C + 5.08cm SS + 30.48cm Na
1. Bare, cd-covered, 3-, 5-, 8-, 10-in BB measurements on centerline:
    - a. at 30cm behind configuration
    - b. at 501.3cm from reactor centerline (Foreground and Background).
  2. Bare detector on centerline at 30cm behind configuration inside partial cadmium enclosure that surrounded the detector except on the side of the last slab in the configuration.
  3. Bare detector on centerline at 501.3cm point with cadmium sheet over face of last slab in the configuration.
- J. SM2 + 10.16cm B<sub>4</sub>C + 5.08cm SS + 61cm Na
1. 5-in BB horizontal traverse through midplane at 30cm behind configuration.



2. Bare, cd-covered, 3-, 5-, 8-, 10-in BB measurements on centerline:
  - a. at 30cm behind configuration
  - b. at 501.3cm from reactor centerline (Foreground and Background).
3. Bare detector on centerline at 30cm behind configuration inside partial cadmium enclosure that surrounded the detector except on the side of the last slab in the configuration.
4. Bare detector on centerline at 501.3cm point with cadmium sheet over face of last slab in the configuration.
5. INS  $^3\text{He}$  BB measurements on centerline:
  - a. at 30cm behind configuration
  - b. at 501.3cm from reactor centerline (Foreground and Background).

VI. SM + SS and Graphite (Graphite benchmark)

- A. SM1 (10.27cm Fe + 9.17cm Al + 2.54cm boral + 20.32cm radial blanket) + 1.27cm Al + 15.24cm SS + 10.16cm graphite
  1. NE-213 and hydrogen counter measurements on centerline as close as feasible behind SS.
  2. 3-, 5-, 10-in BB measurements on centerline at same location as NE-213.
  3. 5-in BB horizontal traverse at 30cm behind configuration.
  4. Bare, cd-covered, 3-, 5-, 8-, 10-in BB on centerline:
    - a. at 30cm behind configuration
    - b. at 304.8cm from reactor centerline (Foreground and Background).
  5. Bare detector on centerline at 30cm behind configuration inside partial cadmium enclosure that surrounded the detector except on the side of the last slab in the configuration.
  6. Bare detector on centerline at 304.8cm point with cadmium sheet over face of last slab in the configuration.
  7. INS  $^3\text{He}$  BB measurements on centerline:

- a. at 30cm behind configuration
  - b. at 304.8cm from reactor centerline (Foreground and Background).
- B. SMI + 1.27cm Al + 15.24cm SS + 20.32cm graphite
- 1. 5-in BB horizontal traverse at 30cm behind configuration.
  - 2. Bare, cd-covered, 3-, 5-, 8-, 10-in BB on centerline:
    - a. at 30cm behind configuration
    - b. at 304.8cm from reactor centerline (Foreground and Background).
  - 3. Bare detector on centerline at 30cm behind configuration inside partial cadmium enclosure that surrounded the detector except on the side of the last slab in the configuration.
  - 4. Bare detector on centerline at 304.8cm point with cadmium sheet over face of last slab in the configuration.
- C. SMI + 1.27cm Al + 15.24cm SS + 30.48cm graphite
- 1. Bare, cd-covered, 3-, 5-, 8-, 10-in BB on centerline:
    - a. at 30cm behind configuration
    - b. at 304.8cm from reactor centerline (Foreground and Background).
  - 2. Bare detector on centerline at 30cm behind configuration inside partial cadmium enclosure that surrounded the detector except on the side of the last slab in the configuration.
  - 3. Bare detector on centerline at 304.8cm point with cadmium sheet over face of last slab in the configuration.
- D. SMI + 1.27cm Al + 15.24cm SS + 40.64cm graphite
- 1. 5-in BB horizontal traverse at 30cm behind configuration.
  - 2. Bare, cd-covered, 3-, 5-, 8-, 10-in BB on centerline:
    - a. at 30cm behind configuration
    - b. at 304.8cm from reactor centerline (Foreground and Background).

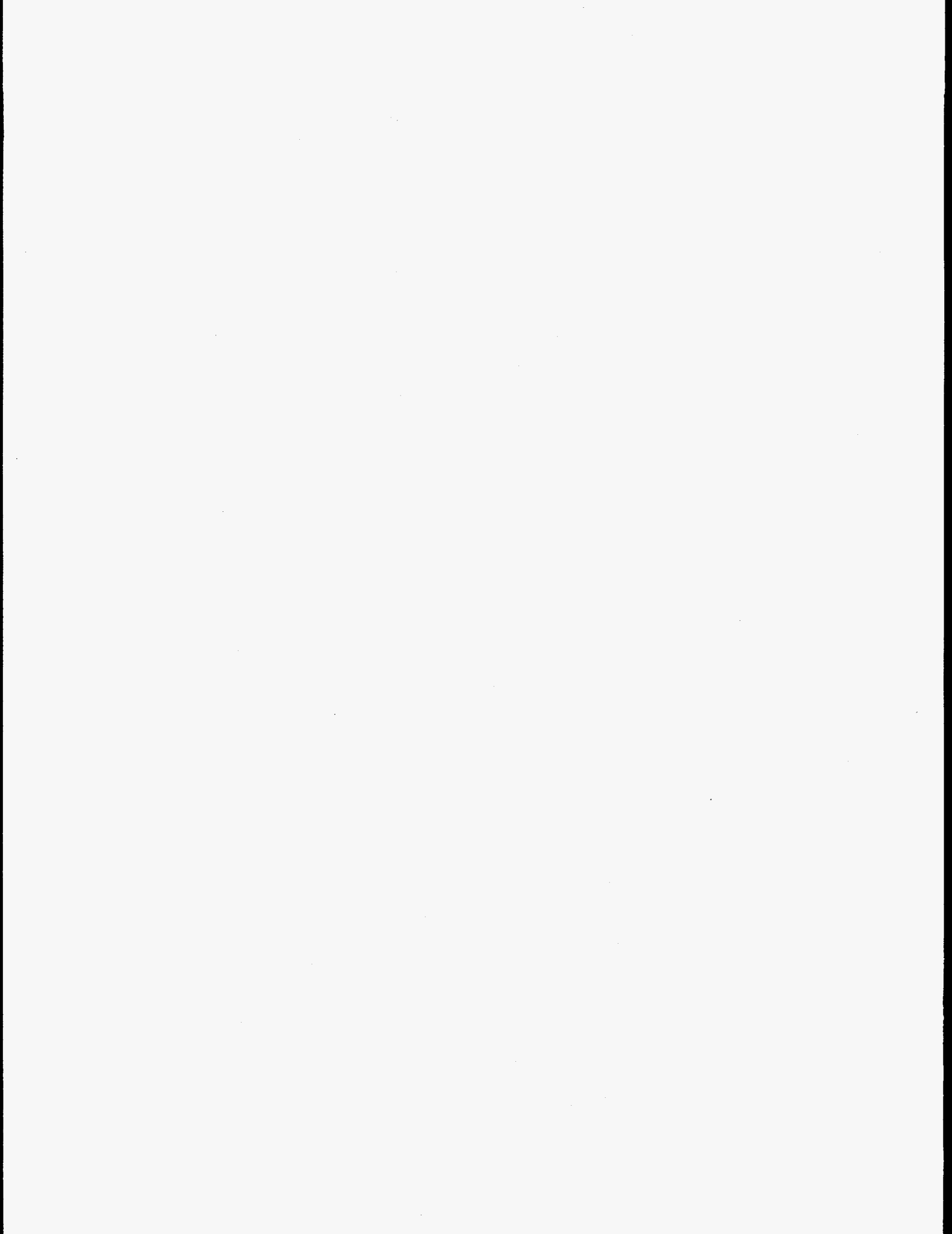
3. Bare detector on centerline at 30cm behind configuration inside partial cadmium enclosure that surrounded the detector except on the side of the last slab in the configuration.
  4. Bare detector on centerline at 304.8cm point with cadmium sheet over face of last slab in the configuration.
  5. INS  $^3\text{He}$  BB measurements on centerline:
    - a. at 30cm behind configuration
    - b. at 304.8cm from reactor centerline (Foreground and Background).
- E. SMI + 1.27cm Al + 15.24cm SS + 50.8cm graphite
1. Bare, cd-covered, 3-, 5-, 8-, 10-in BB on centerline:
    - a. at 30cm behind configuration
    - b. at 304.8cm from reactor centerline (Foreground and Background).
  2. Bare detector on centerline at 30cm behind configuration inside partial cadmium enclosure that surrounded the detector except on the side of the last slab in the configuration.
  3. Bare detector on centerline at 304.8cm point with cadmium sheet over face of last slab in the configuration.
- F. SMI + 1.27cm Al + 15.24cm SS + 60.96cm graphite
1. NE-213 and hydrogen counter measurements on centerline as close as feasible behind SS.
  2. 3-, 5-, 10-in BB measurements on centerline at same location as NE-213.
  3. 5-in BB horizontal traverse at 30cm behind configuration.
  4. Bare, cd-covered, 3-, 5-, 8-, 10-in BB on centerline:
    - a. at 30cm behind configuration
    - b. at 304.8cm from reactor centerline (Foreground and Background).
  5. Bare detector on centerline at 30cm behind configuration inside partial cadmium enclosure that surrounded the detector except on the side of the last slab in the configuration.

6. Bare detector on centerline at 304.8cm point with cadmium sheet over face of last slab in the configuration.
7. INS  $^3\text{He}$  BB measurements on centerline:
  - a. at 30cm behind configuration
  - b. at 304.8cm from reactor centerline (Foreground and Background).

VII. SM + SS and  $\text{B}_4\text{C}$  (near core shield)

- A. SM1 (10.27cm Fe + 9.17cm Al + 2.54cm boron + 20.32cm radial blanket) + 1.27cm Al + 15.24cm SS + 1.27cm Al + 15.24cm SS
  1. 5-in BB horizontal traverse at 30cm behind configuration.
  2. 3-, 5-, 8-, 10-in BB measurements on centerline:
    - a. at 30cm behind configuration
    - b. at 304.8cm from reactor centerline (Foreground and Background).
- B. SM1 + 1.27cm Al + 15.24cm SS + 1.27cm Al + 15.24cm SS + 1.27cm Al + 15.24cm SS
  1. 5-in BB horizontal traverse at 30cm behind configuration.
  2. 3-, 5-, 8-, 10-in BB measurements on centerline:
    - a. at 30cm behind configuration
    - b. at 304.8cm from reactor centerline (Foreground and Background).
- C. SM1 + 1.27cm Al + 15.24cm SS + 1.27cm Al + 15.24cm SS + 1.27cm Al + 15.24cm SS + 1.27cm Al + 15.24cm  $\text{B}_4\text{C}$  + 2.54cm SS
  1. 5-in BB horizontal traverse at 30cm behind configuration.
  2. 3-, 5-, 8-, 10-in BB measurements on centerline:
    - a. at 30cm behind configuration
    - b. at 304.8cm from reactor centerline (Foreground and Background).
  3. INS  $^3\text{He}$  BB measurements on centerline:
    - a. at 30cm behind configuration

- b. at 304.8cm from reactor centerline (Foreground and Background).
- D. SM1 + 1.27cm Al + 15.24cm SS + 1.27cm Al + 15.24cm SS + 1.27cm Al + 15.24cm SS + 1.27cm Al + 15.24cm B<sub>4</sub>C + 1.54cm SS + 30.48cm Na
- 1. Bare, cd-covered, 3-, 5-, 8-, 10-in BB measurements on centerline:
    - a. at 30cm behind configuration
    - b. at 304.8cm from reactor centerline (Foreground and Background).
  - 2. Bare detector on centerline at 30cm behind configuration inside partial cadmium enclosure that surrounded the detector except on the side of the last slab in the configuration.
  - 3. Bare detector on centerline at 304.8cm point with cadmium shell over face of last slab in the configuration.



APPENDIX B  
EXPERIMENTAL CONFIGURATIONS

08

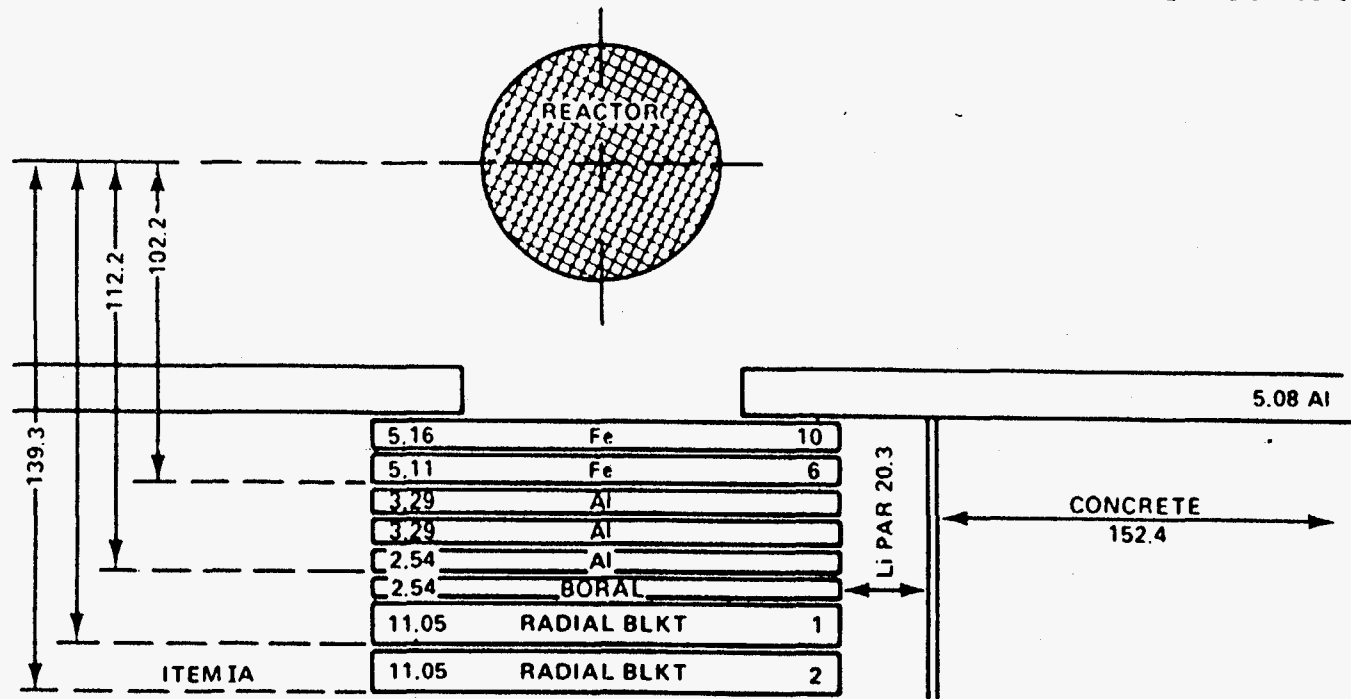


Figure B1. Sketch of the configuration for measurements under section I.A of the experimental program plan.



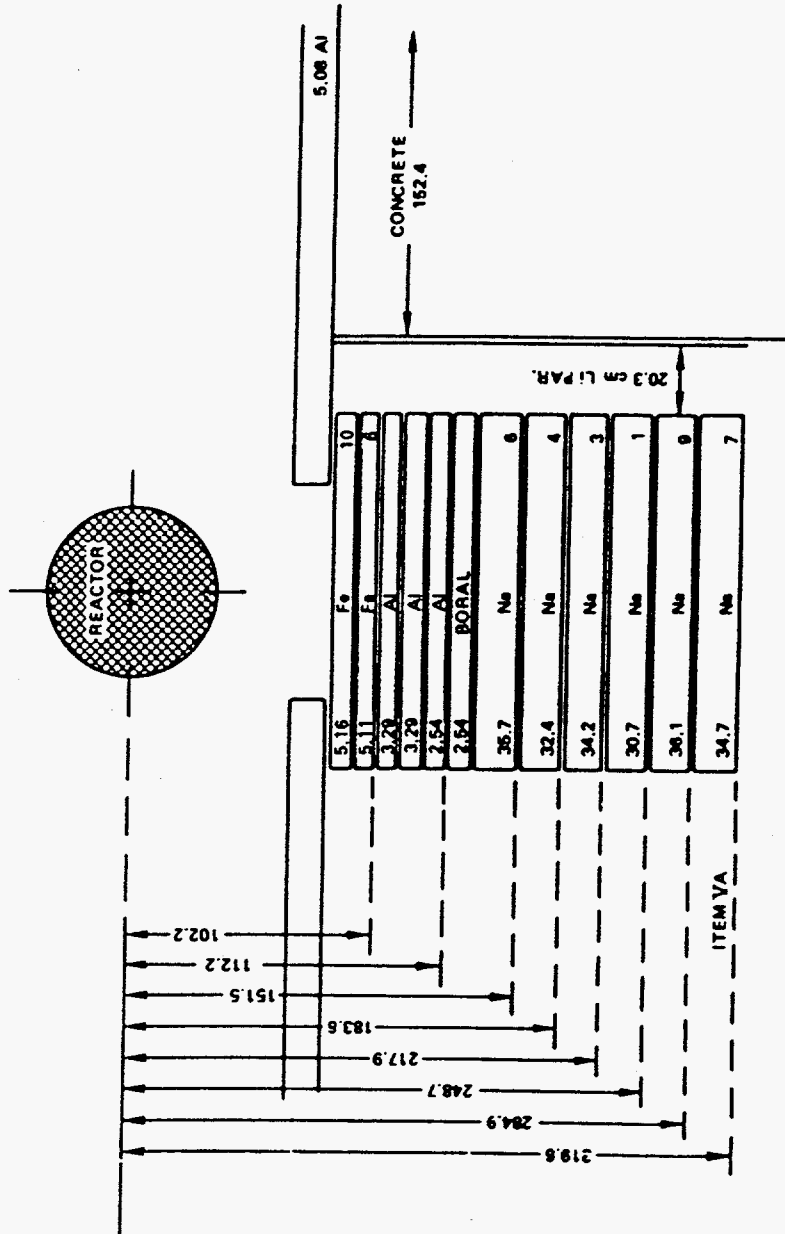


Figure B2. Sketch of the configuration for measurements under section V.A of the experimental program plan.

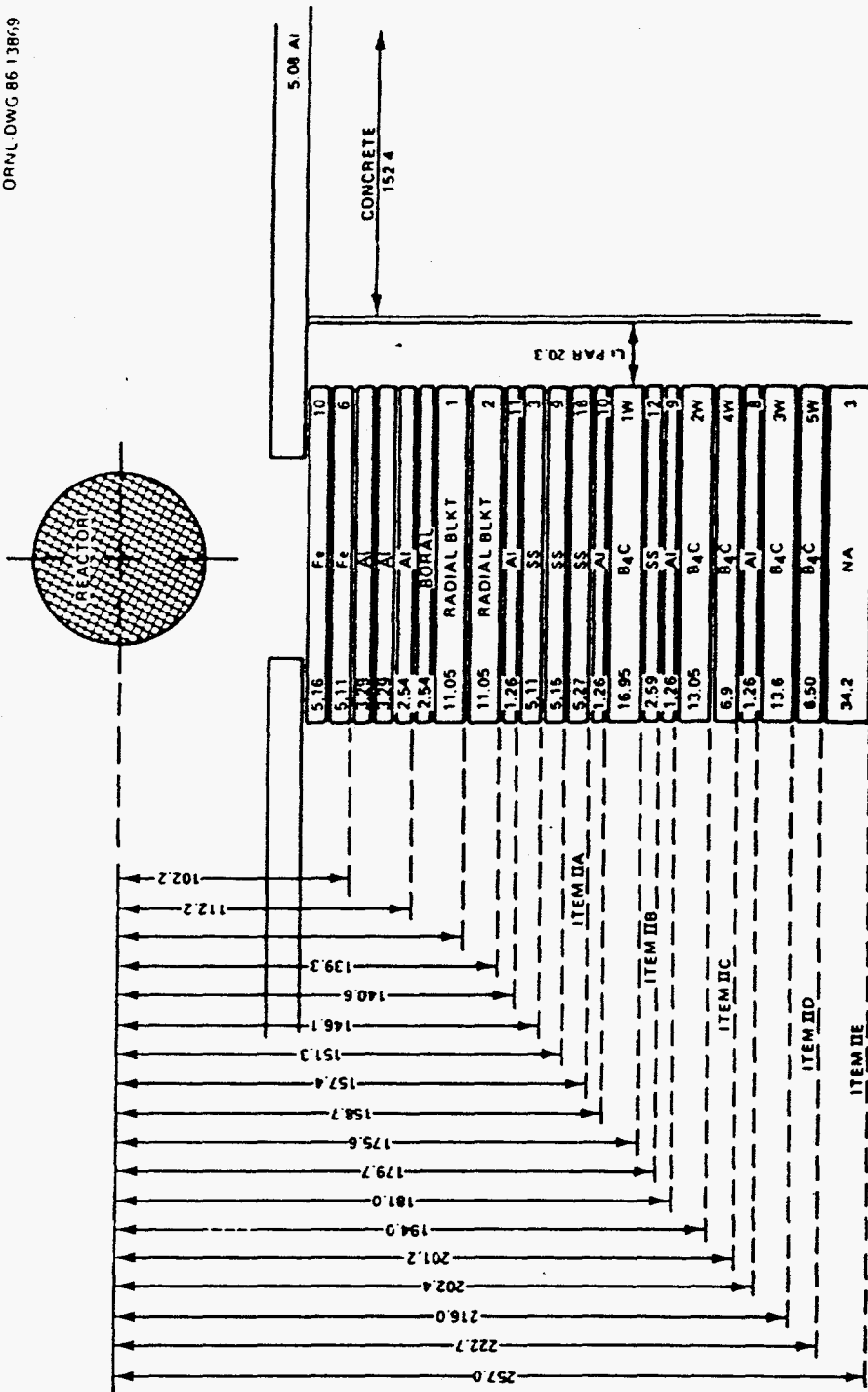


Figure B3. Sketch of the configuration for measurements under sections II.A-C, E and II.D(3-5) of the experimental program plan.

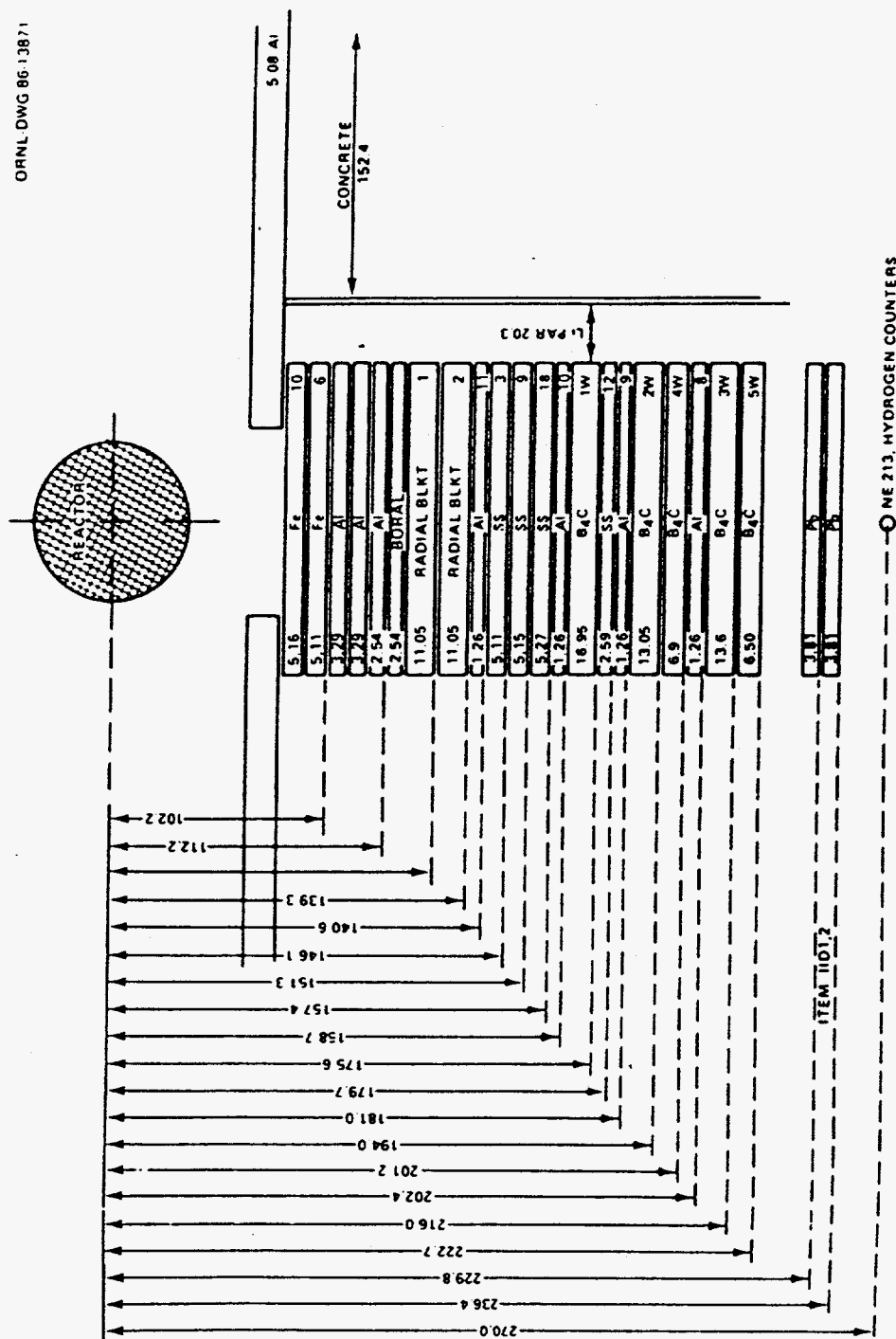
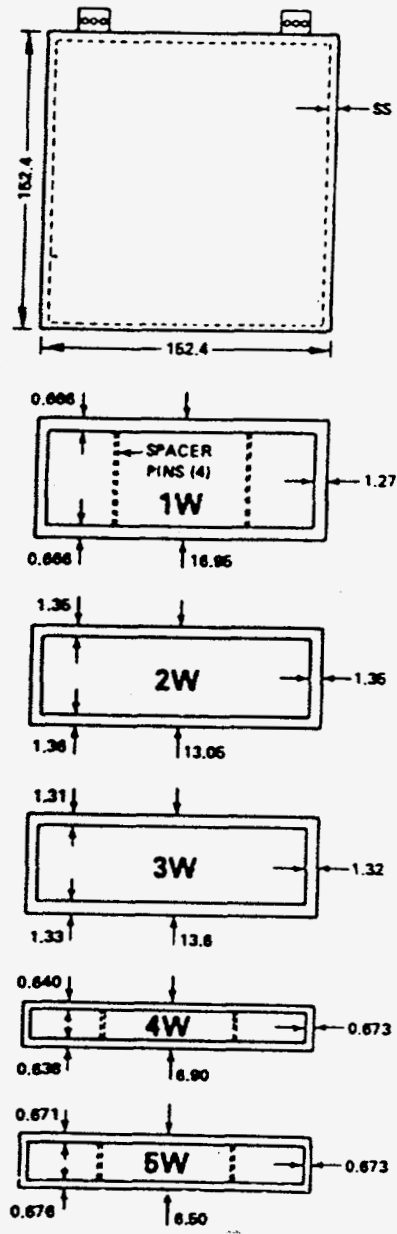


Fig. B4. Sketch of the configuration for measurements under sections II.D (1-2) of the experimental program plan.

**B<sub>4</sub>C CONTAINERS**



(ALL DIMENSIONS ARE IN CENTIMETERS)

Figure B5. Sketches of the stainless steel containers used to form the B<sub>4</sub>C shield slabs.

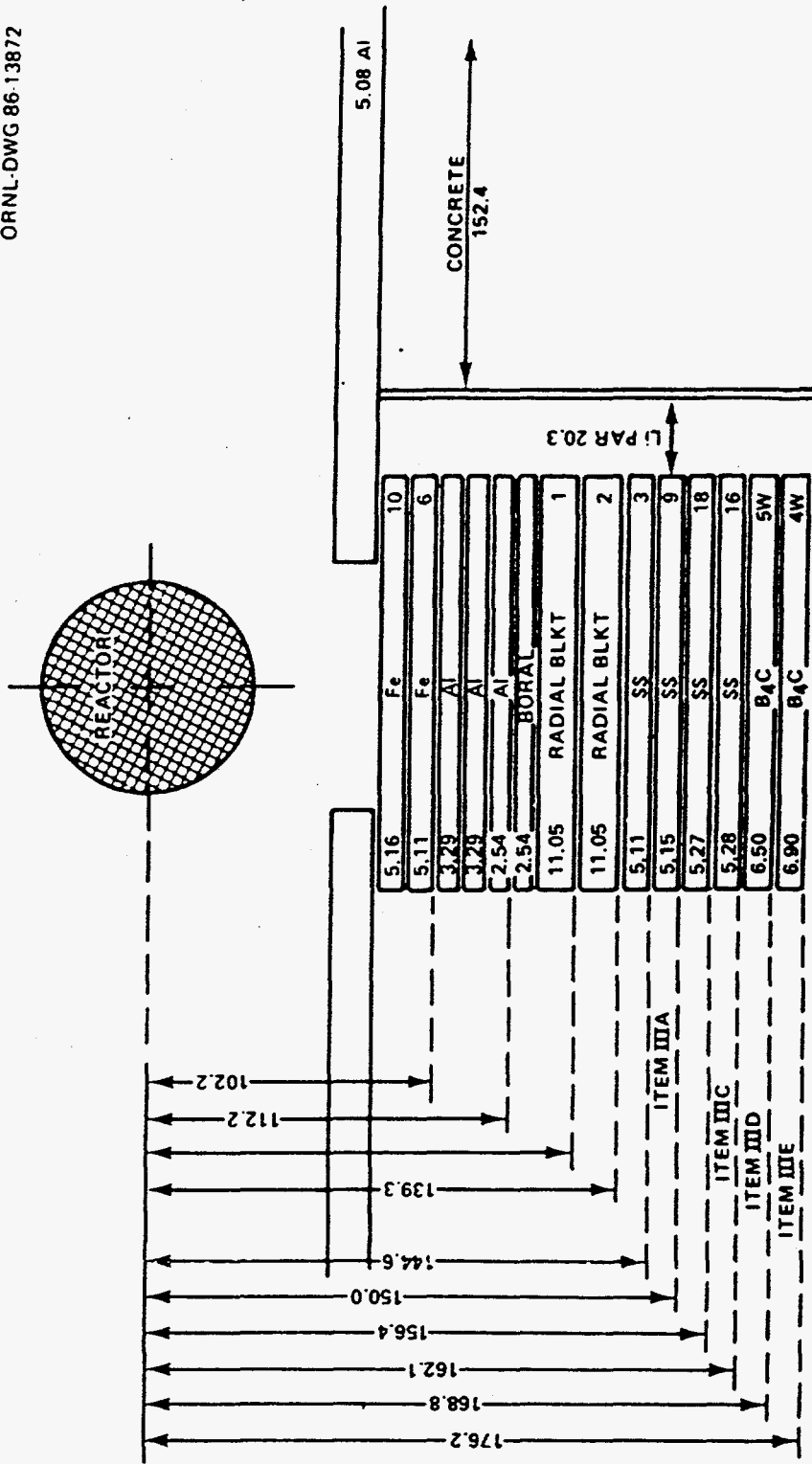


Figure B6. Sketch of the configuration for measurements under sections III.A, C-E of the experimental program plan.

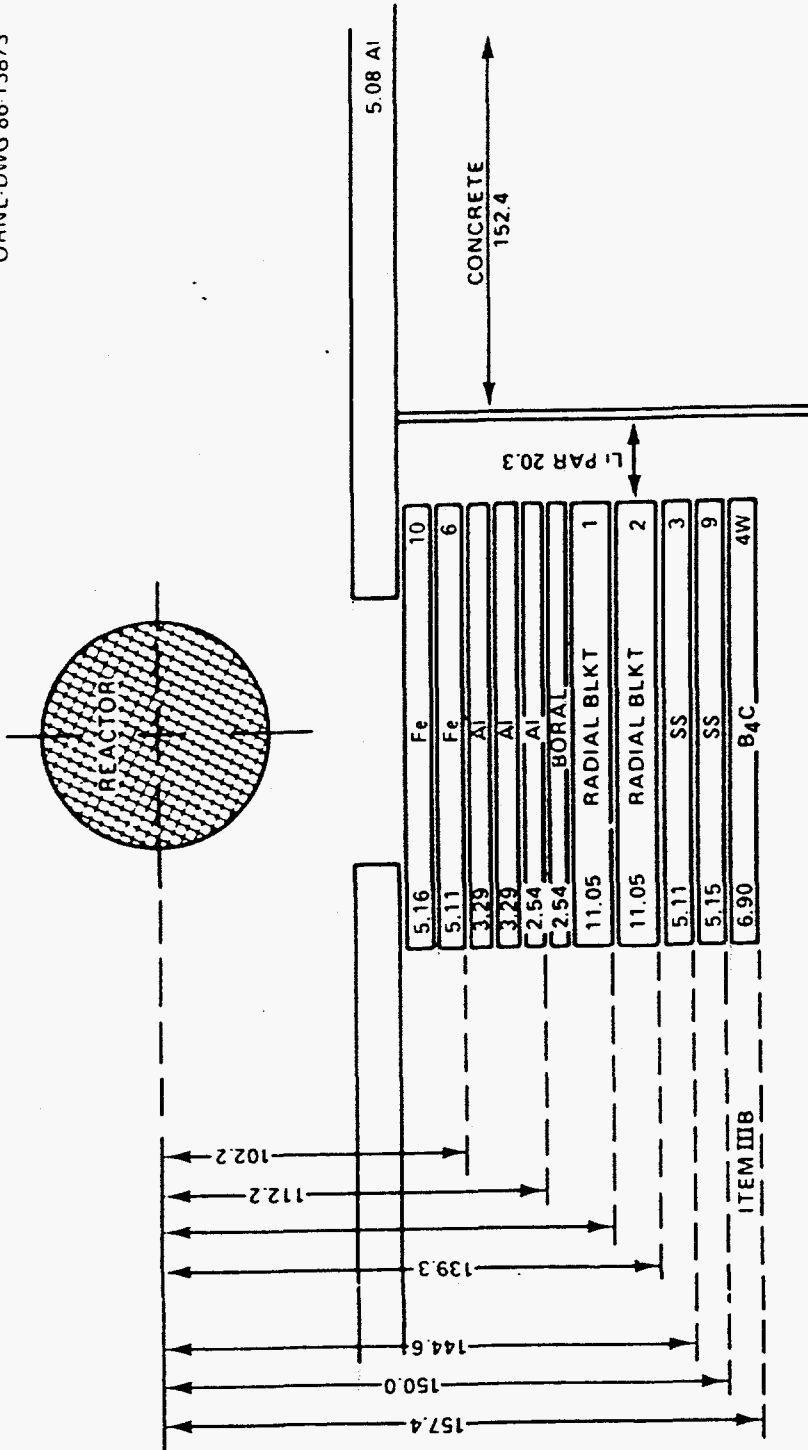


Figure B7. Sketch of the configuration for measurements under section III.B of the experimental program plan.

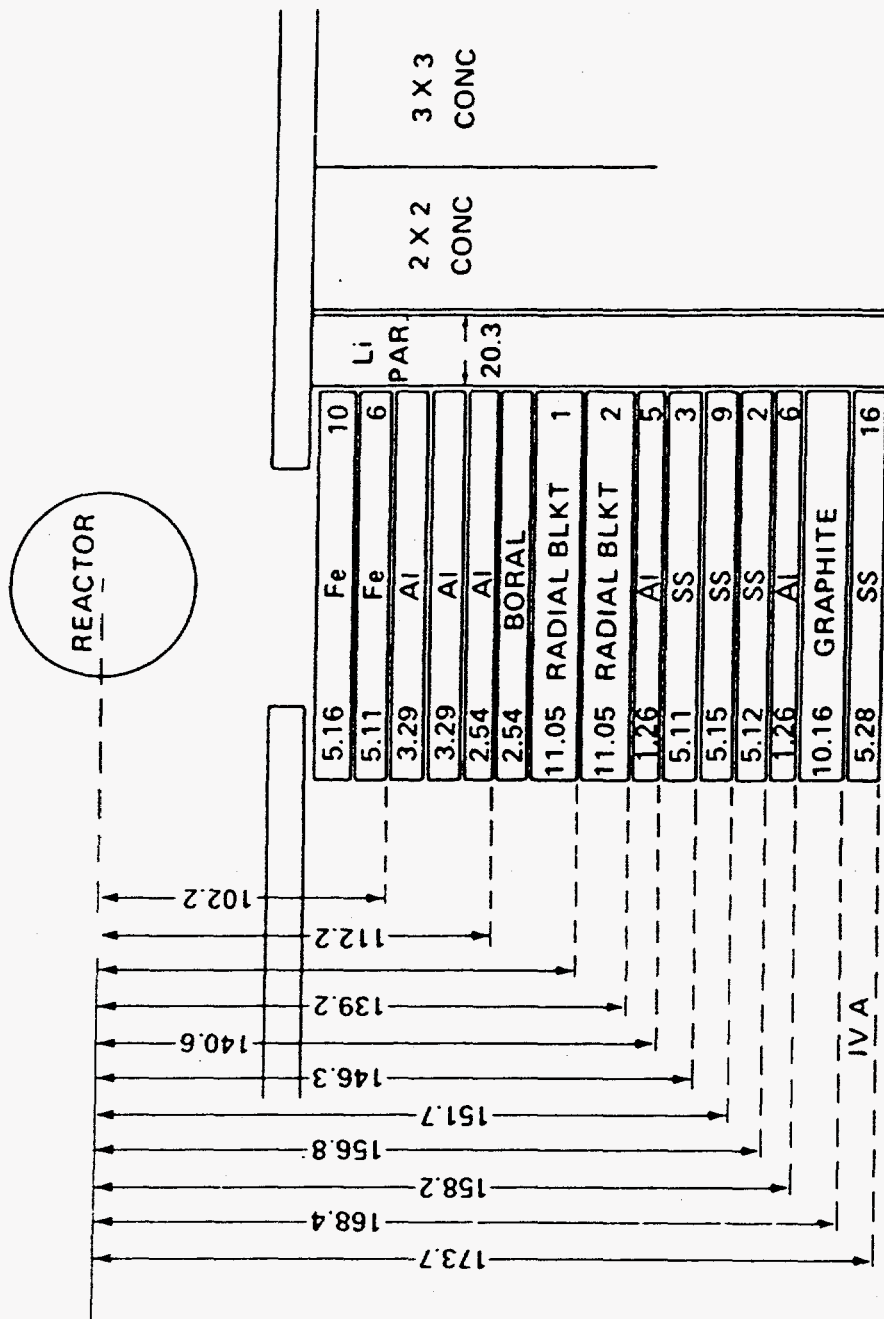


Figure B8. Sketch of the configuration for measurements under section IV.A of the experimental program plan.

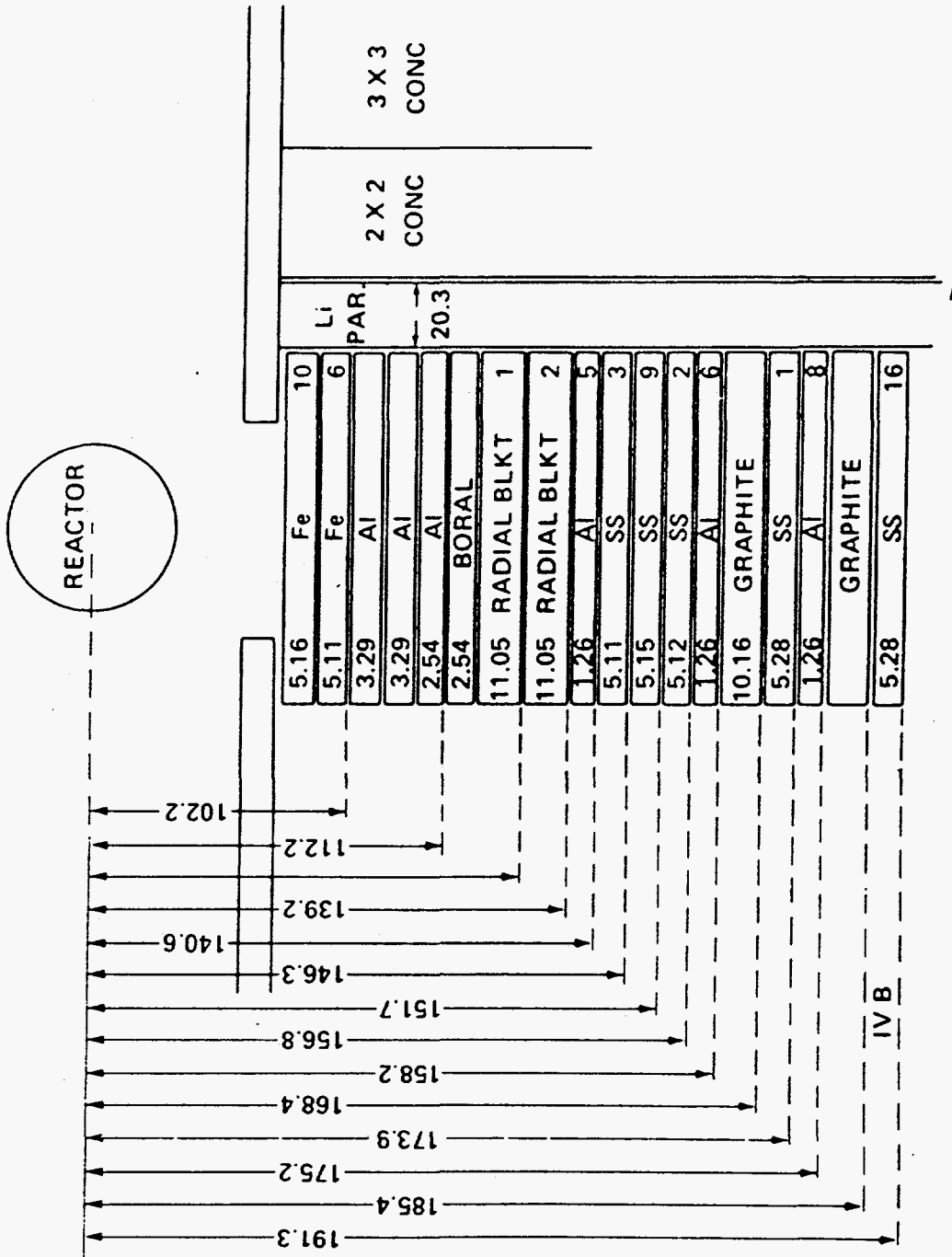


Figure B9. Sketch of the configuration for measurements under section IV.B of the experimental program plan.



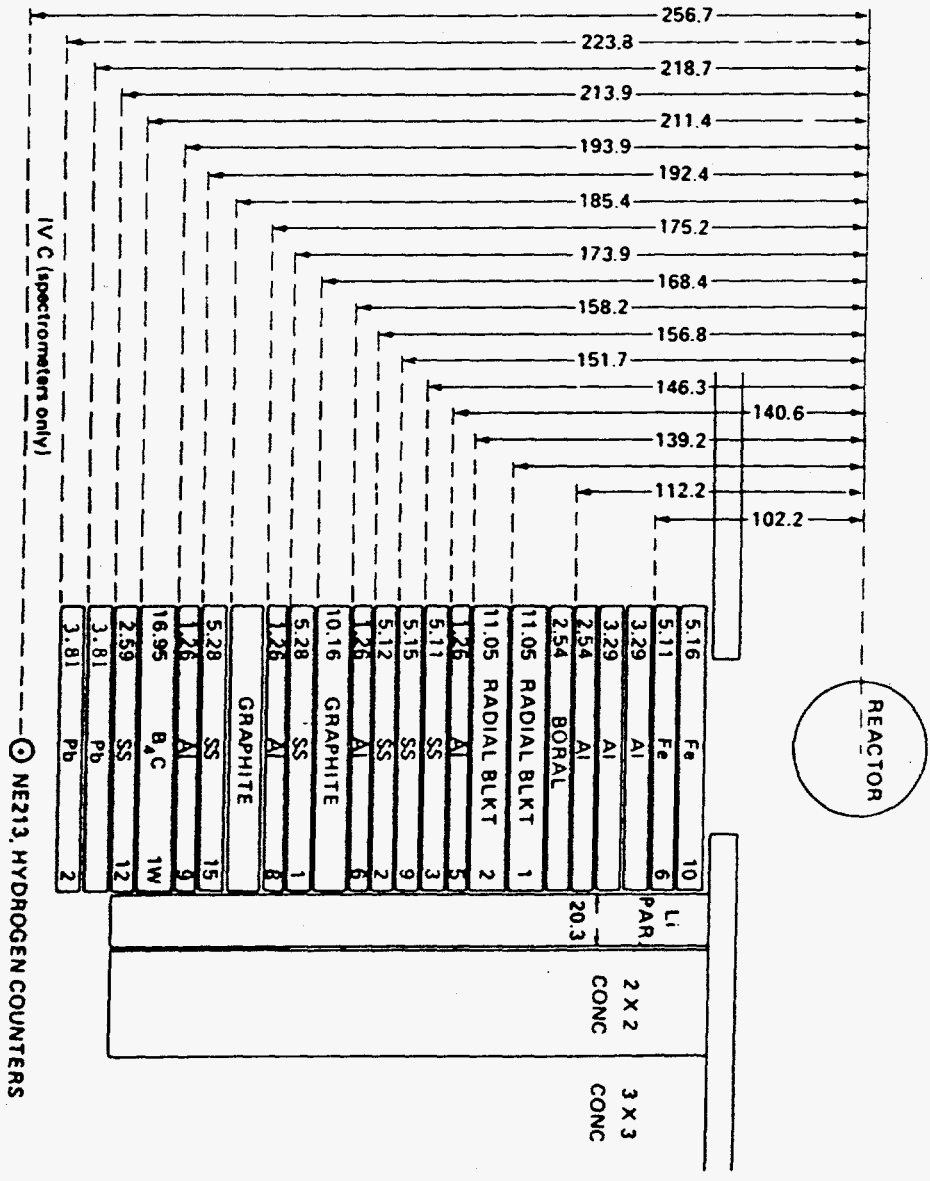


Fig. B10. Sketch of the configuration for measurements under sections IV.C (1-2) of the experimental program plan.

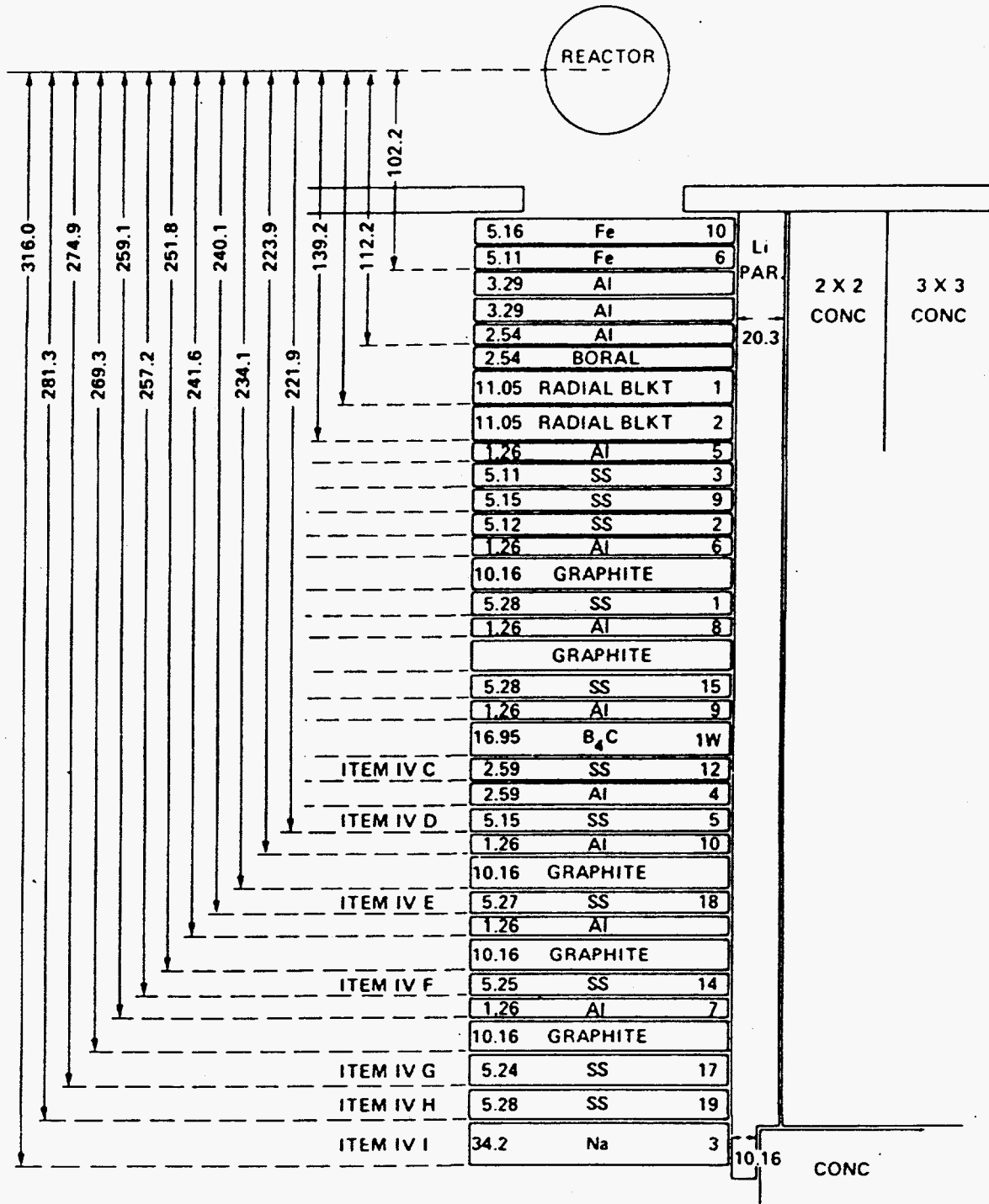


Figure B11. Sketch of the configuration for measurements under sections IV.C(3-5) through IV.I of the experimental program plan.

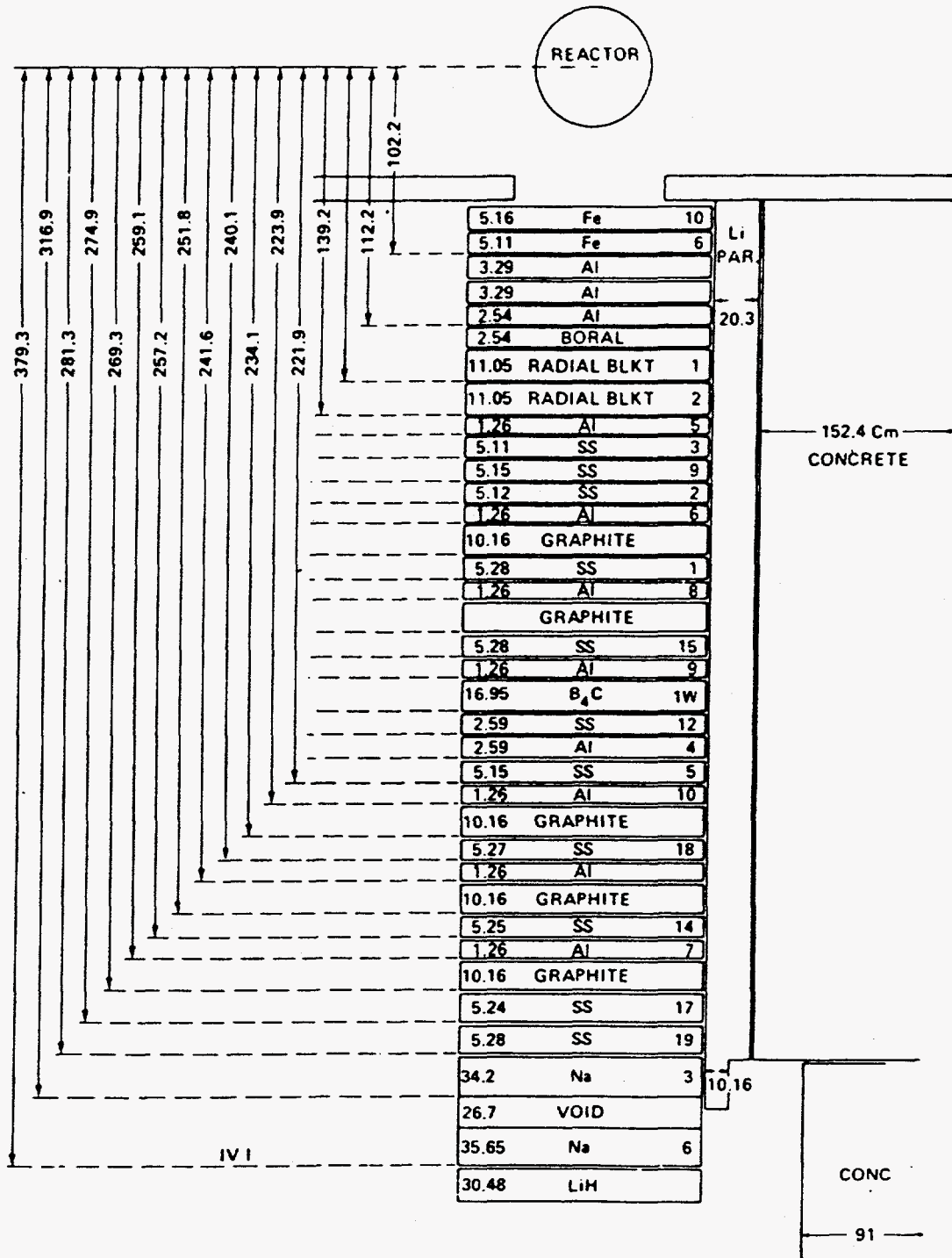


Figure B12. Sketch of the configuration for measurements under section IV.IA of the experimental program plan.

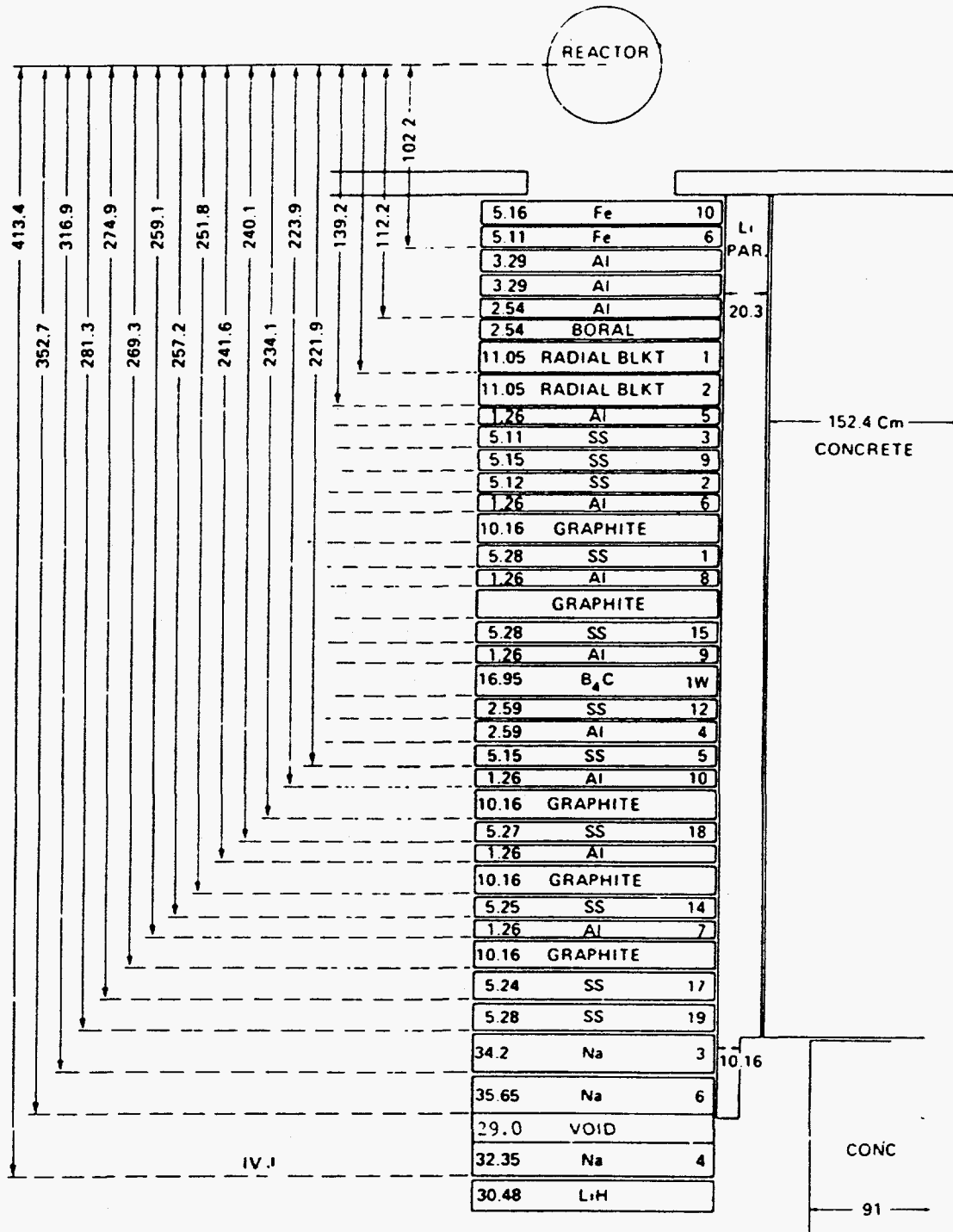


Figure B13. Sketch of the configuration for measurements under section IV.J of the experimental program plan.

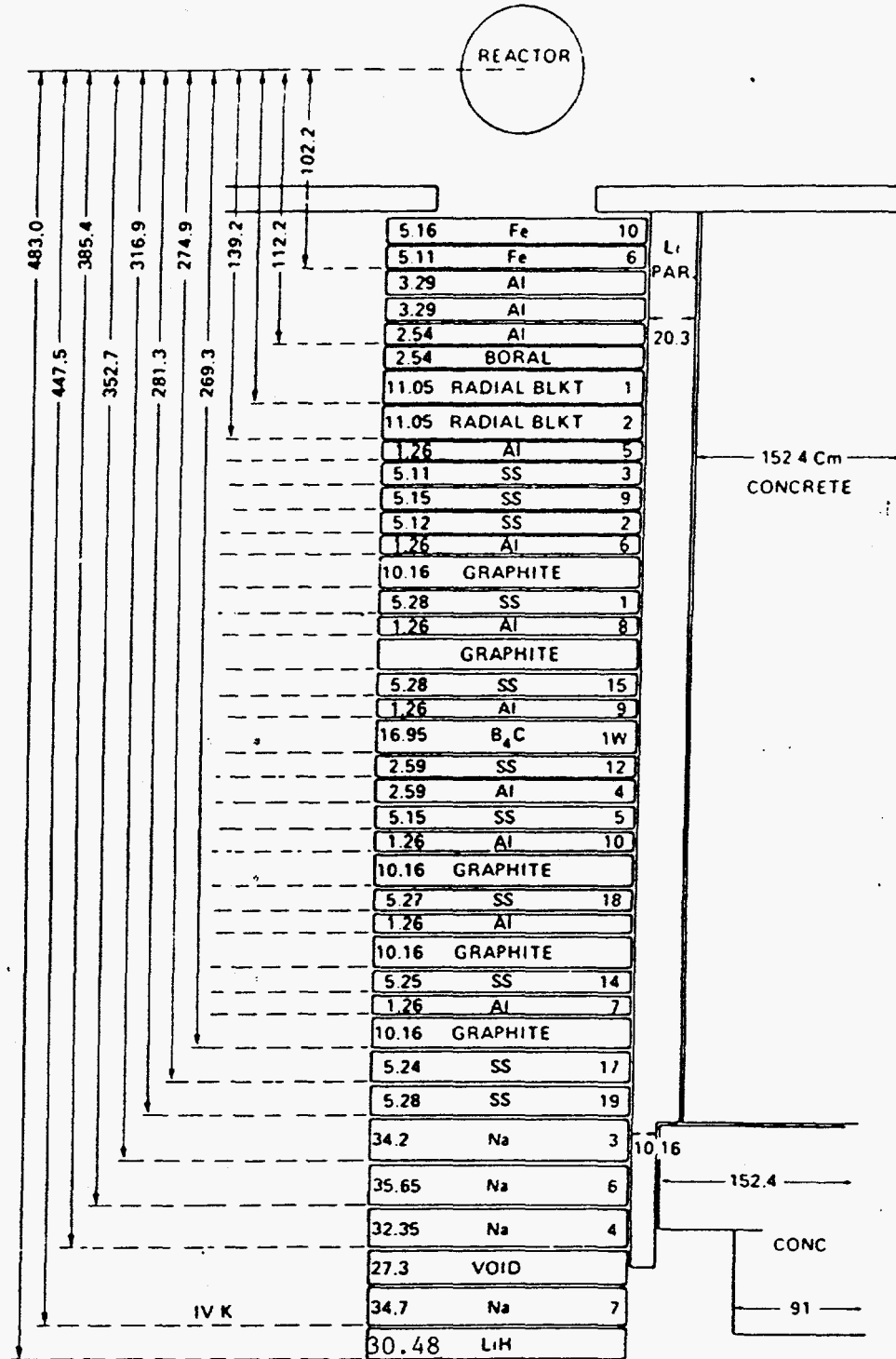


Figure B14. Sketch of the configuration for measurements under section IV.K of the experimental program plan.

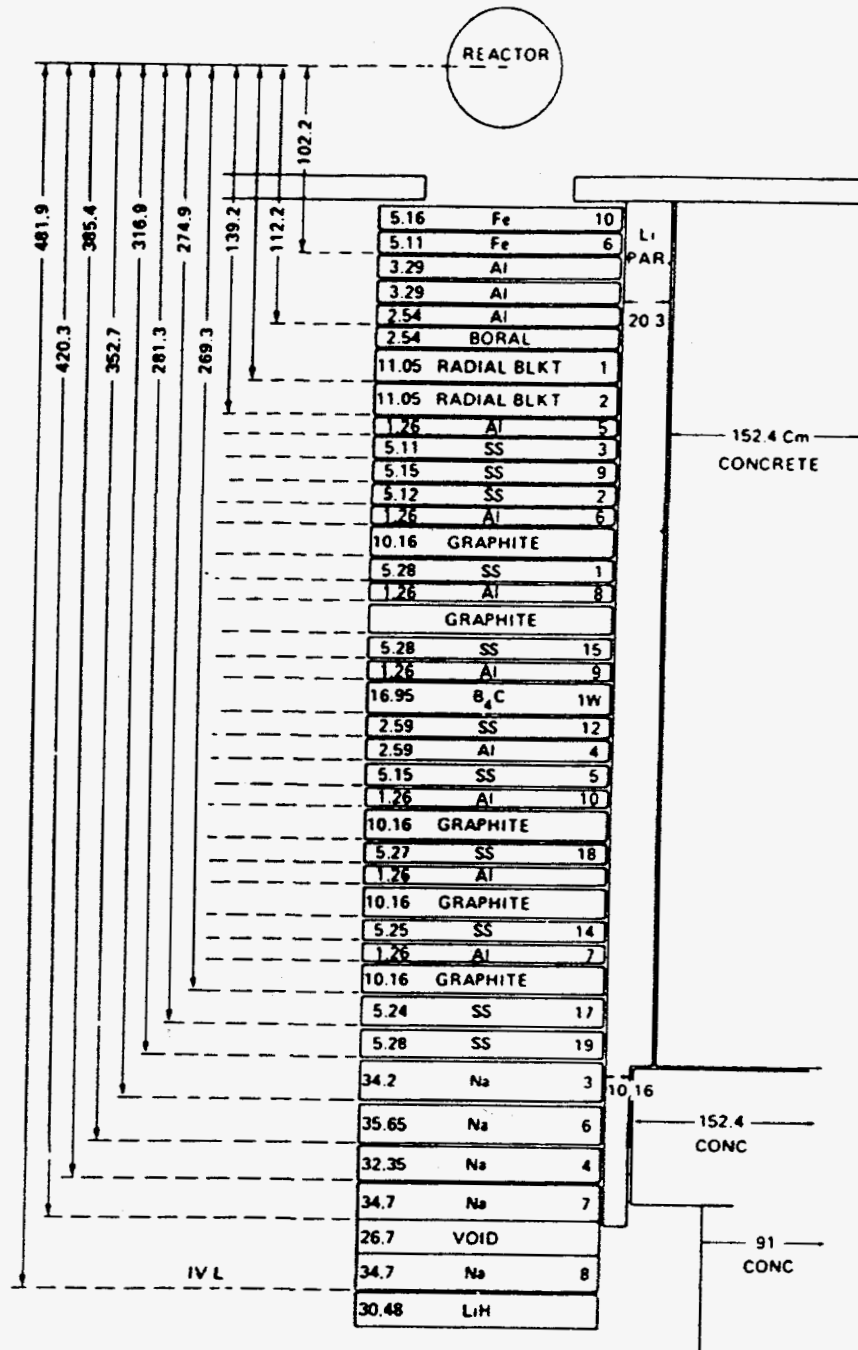


Figure B15. Sketch of the configuration for measurements under section IV.L of the experimental program plan.

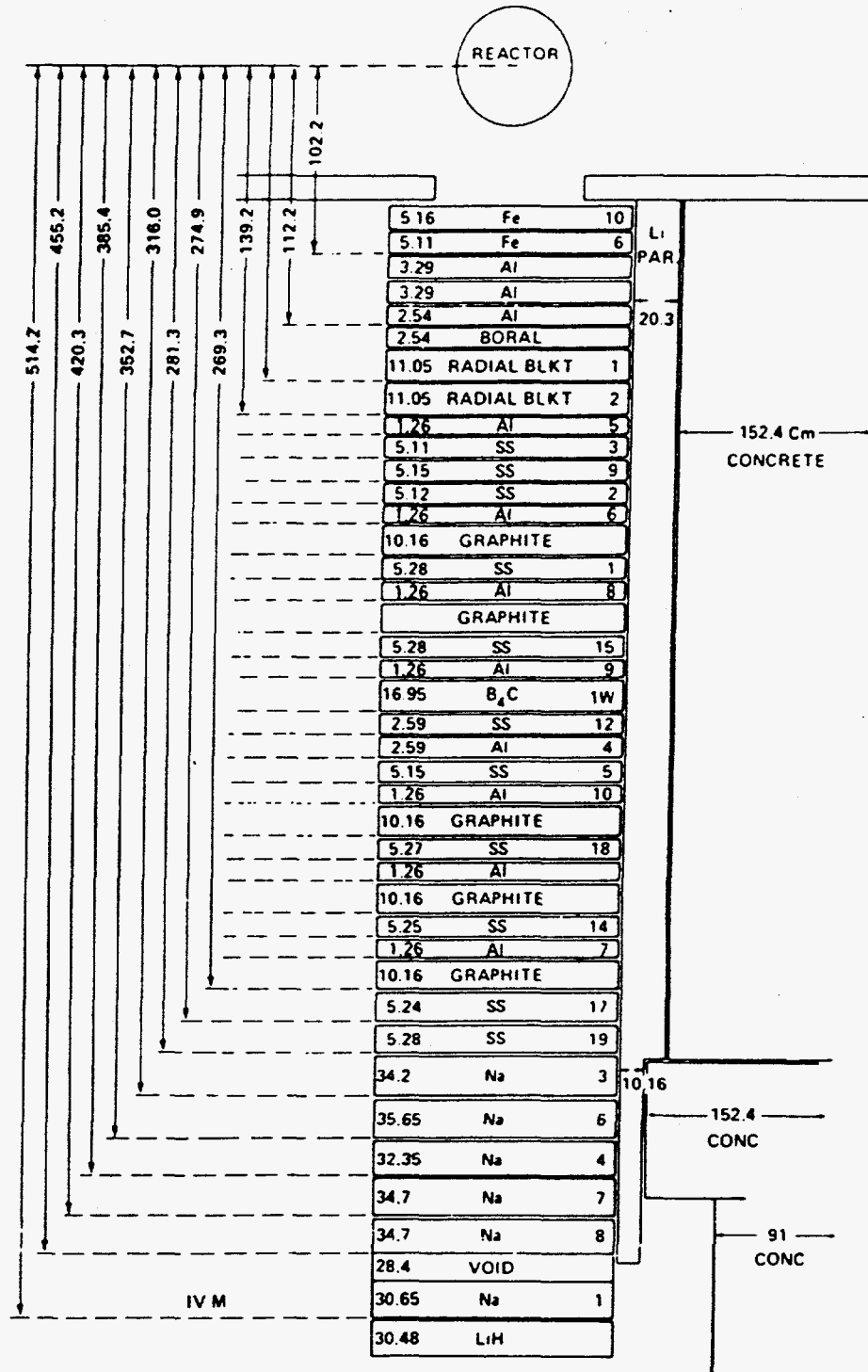


Figure B16. Sketch of the configuration for measurements under section IV.M of the experimental program plan.

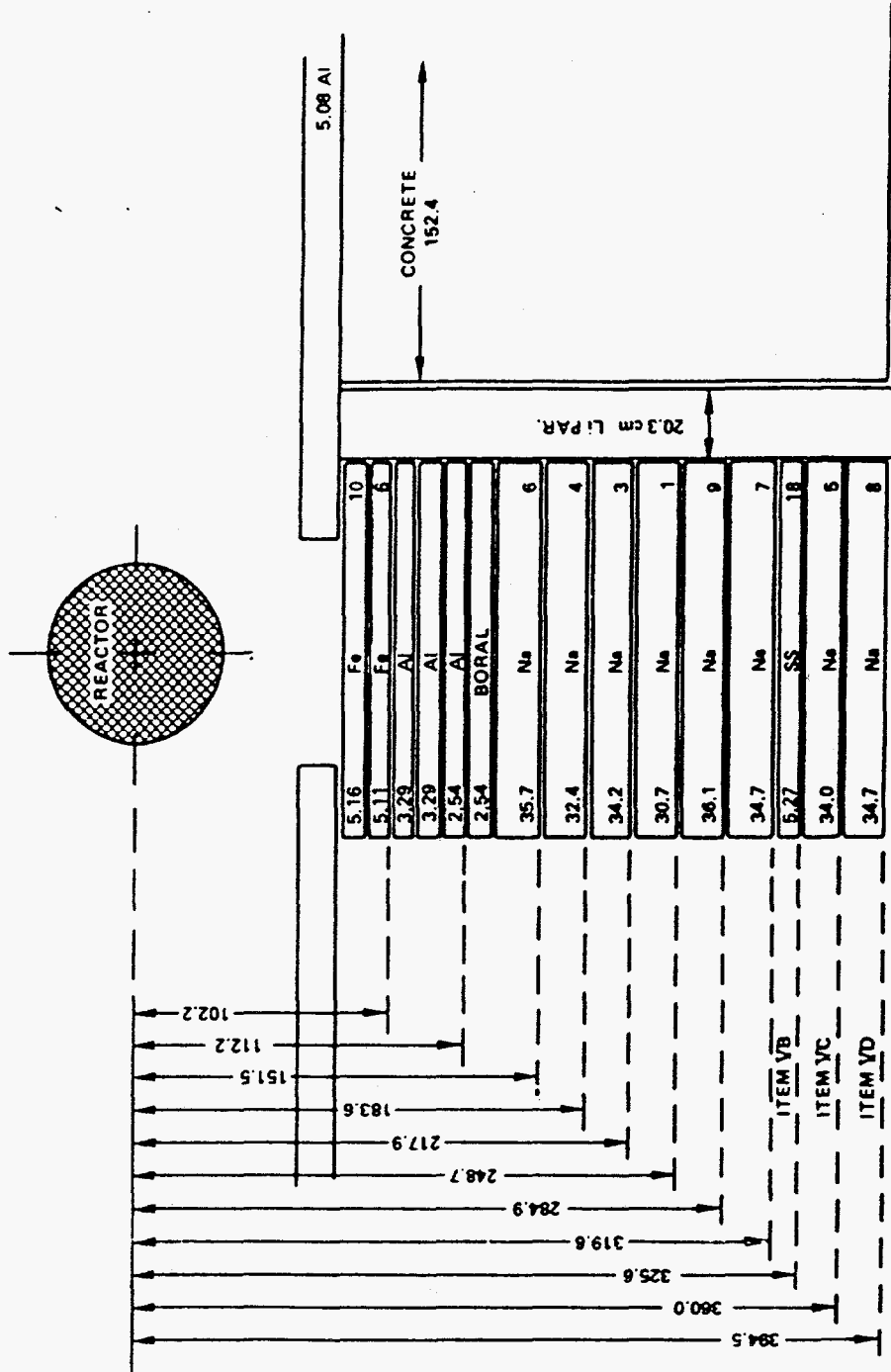


Figure B17. Sketch of the configuration for measurements under sections V.B-D of the experimental program plan.



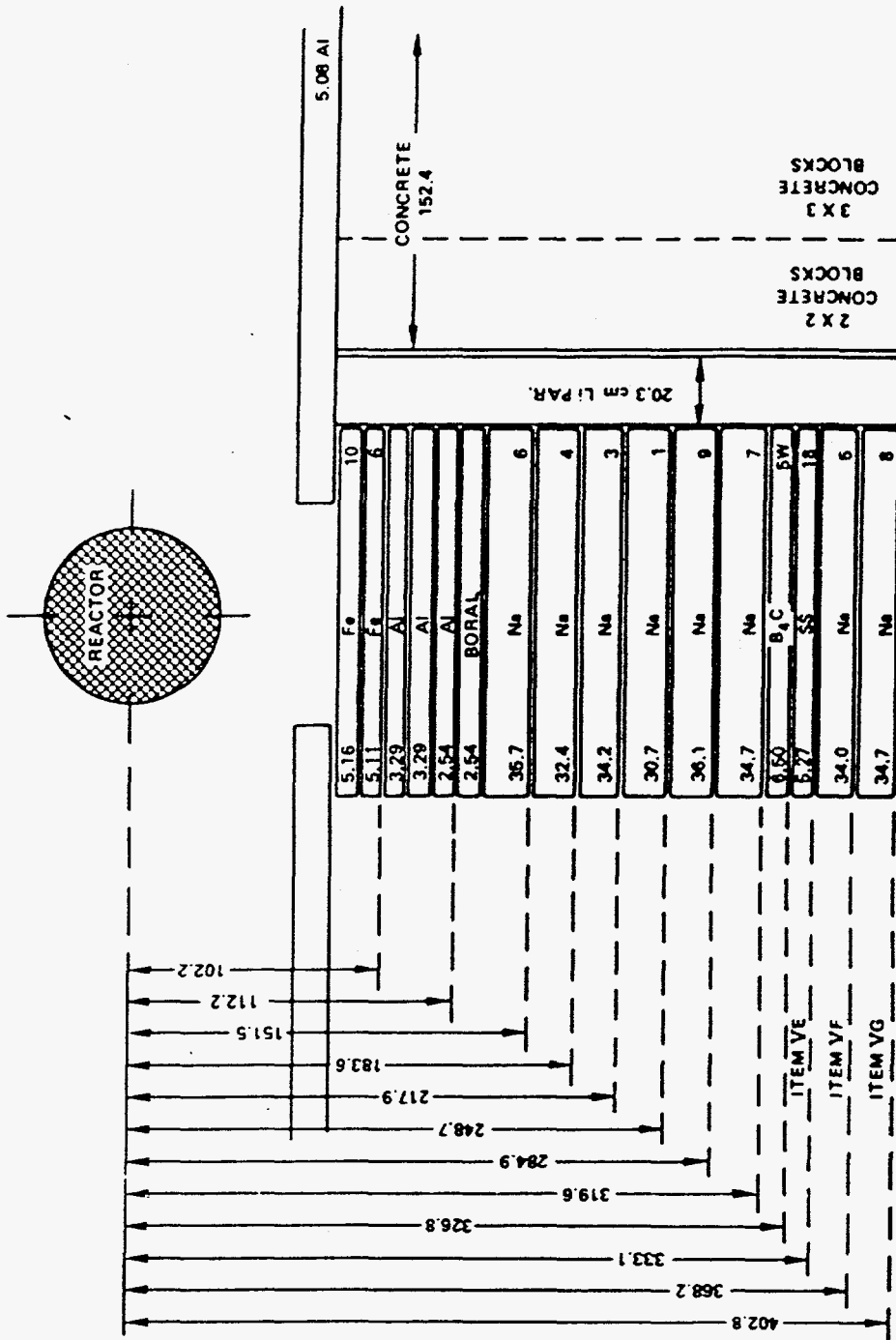


Figure B18. Sketch of the configuration for measurements under sections V.E-G of the experimental program plan.

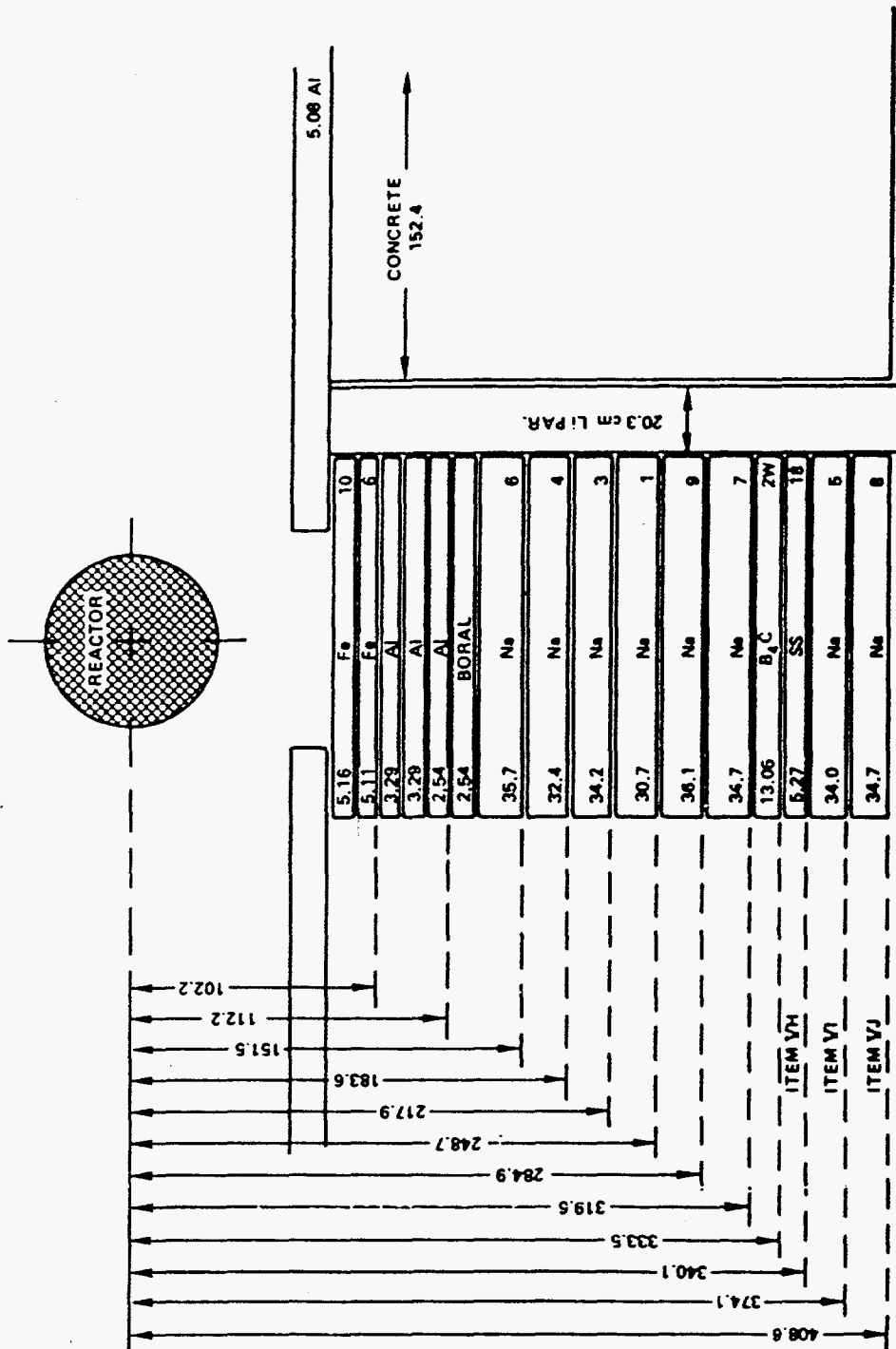


Figure B19. Sketch of the configuration for measurements under sections V.H-J of the experimental program plan.

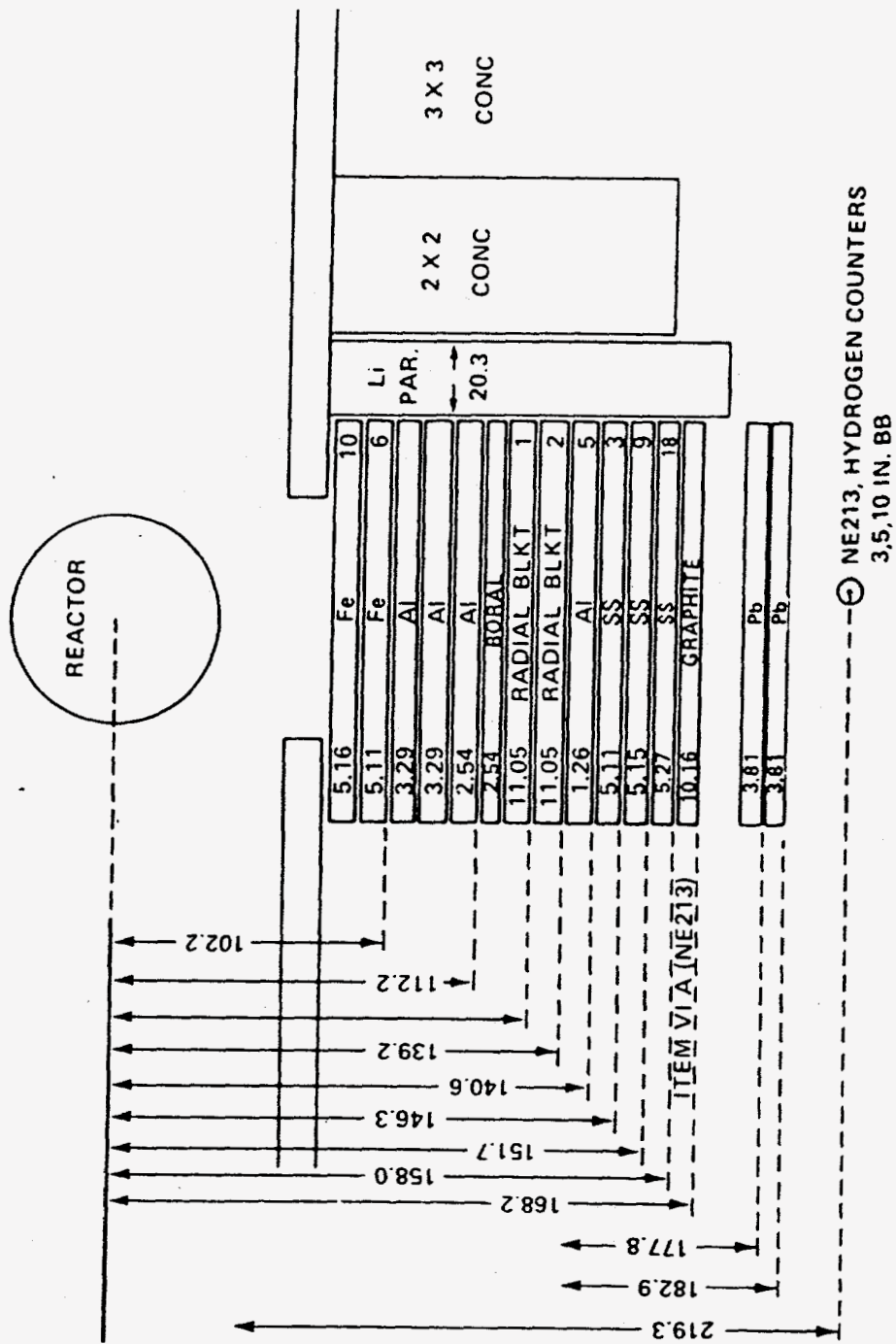


Fig. B20. Sketch of the configuration for measurements under sections IV.A (1-2) of the experimental program plan.

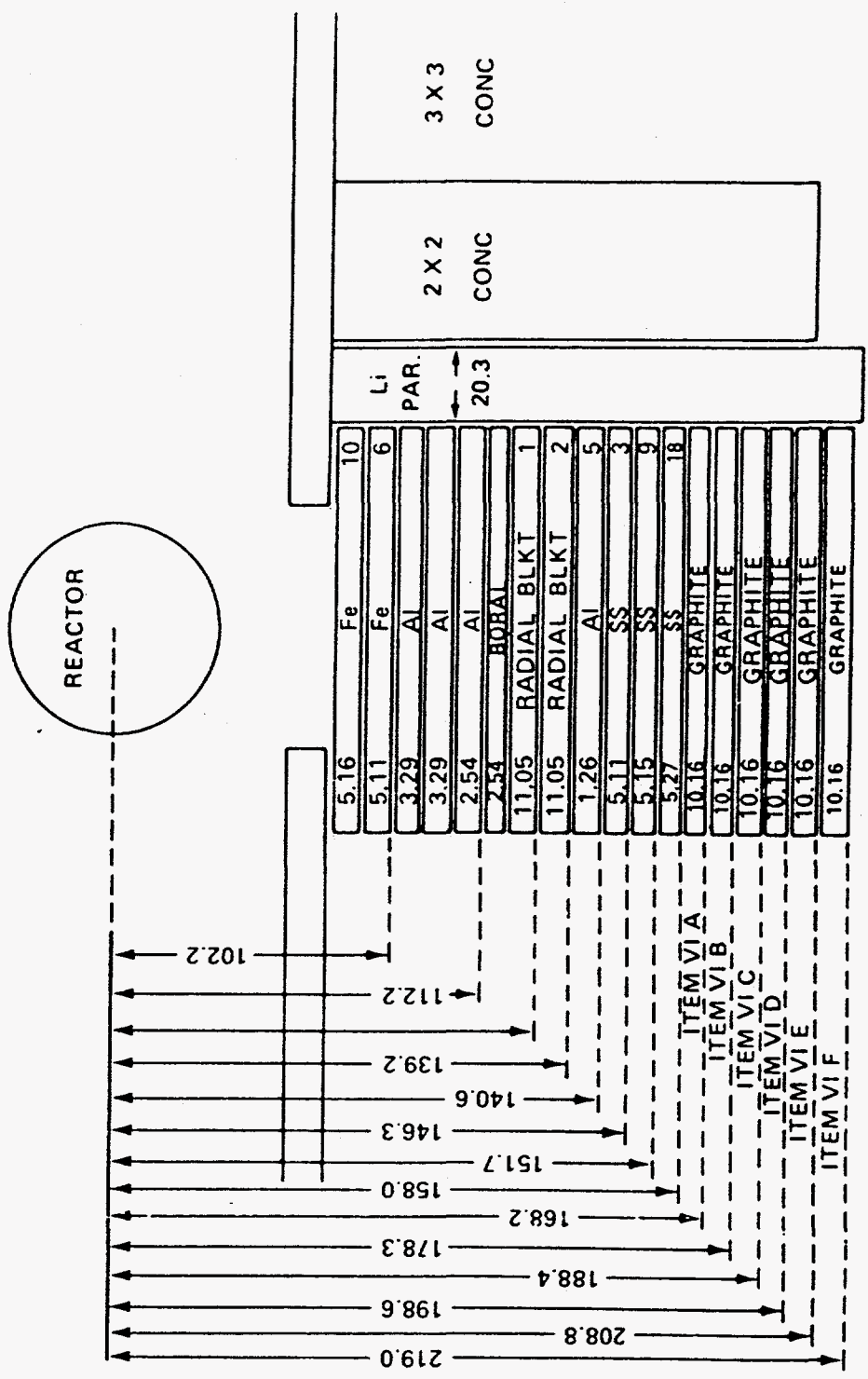


Figure B21. Sketch of the configuration for measurements under sections VI.A(3-5) through VI.E and VI.F(3-5) of the experimental program plan.

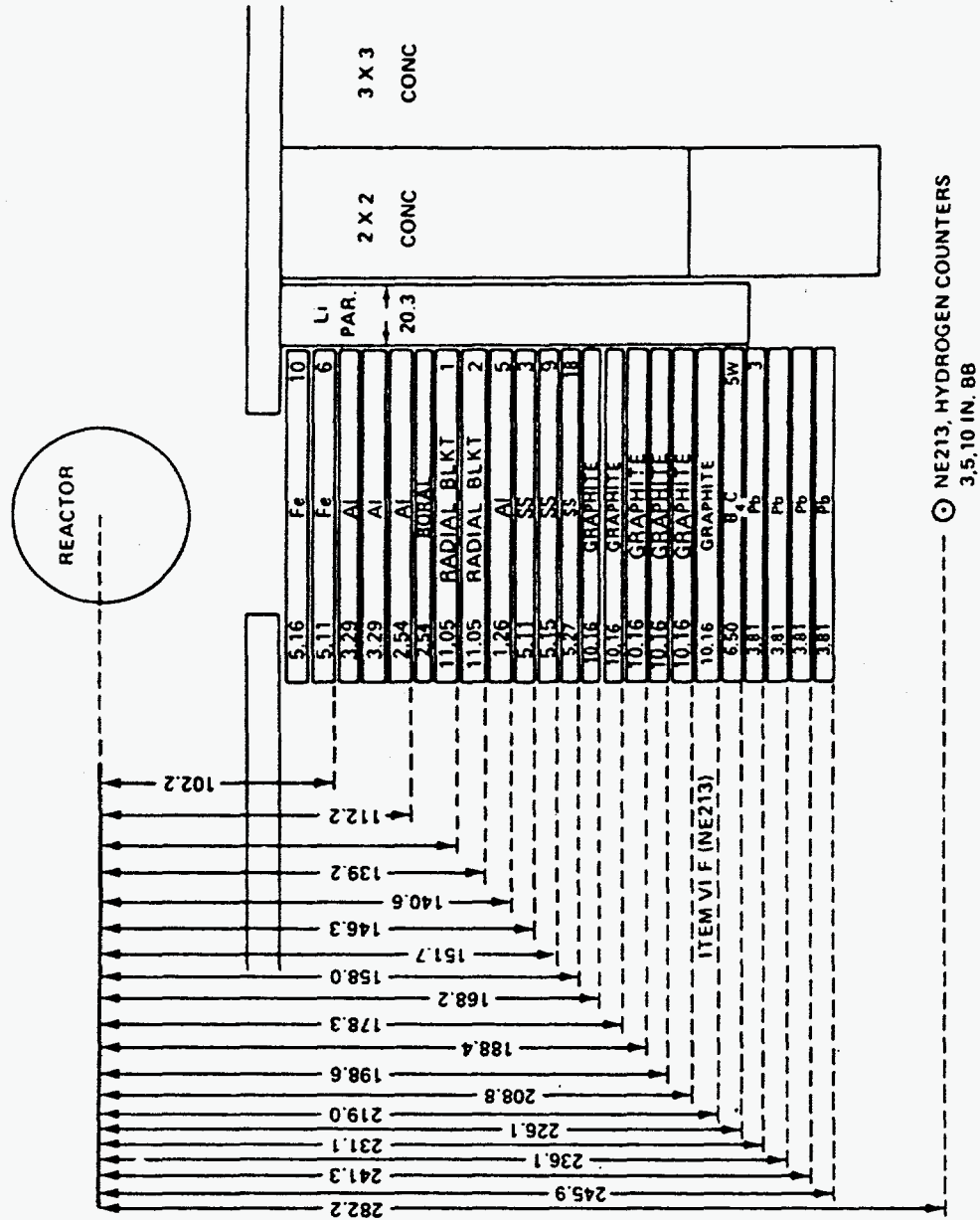


Fig. B22. Sketch of the configuration for measurements under sections VI.F (1-2) of the experimental program plan.

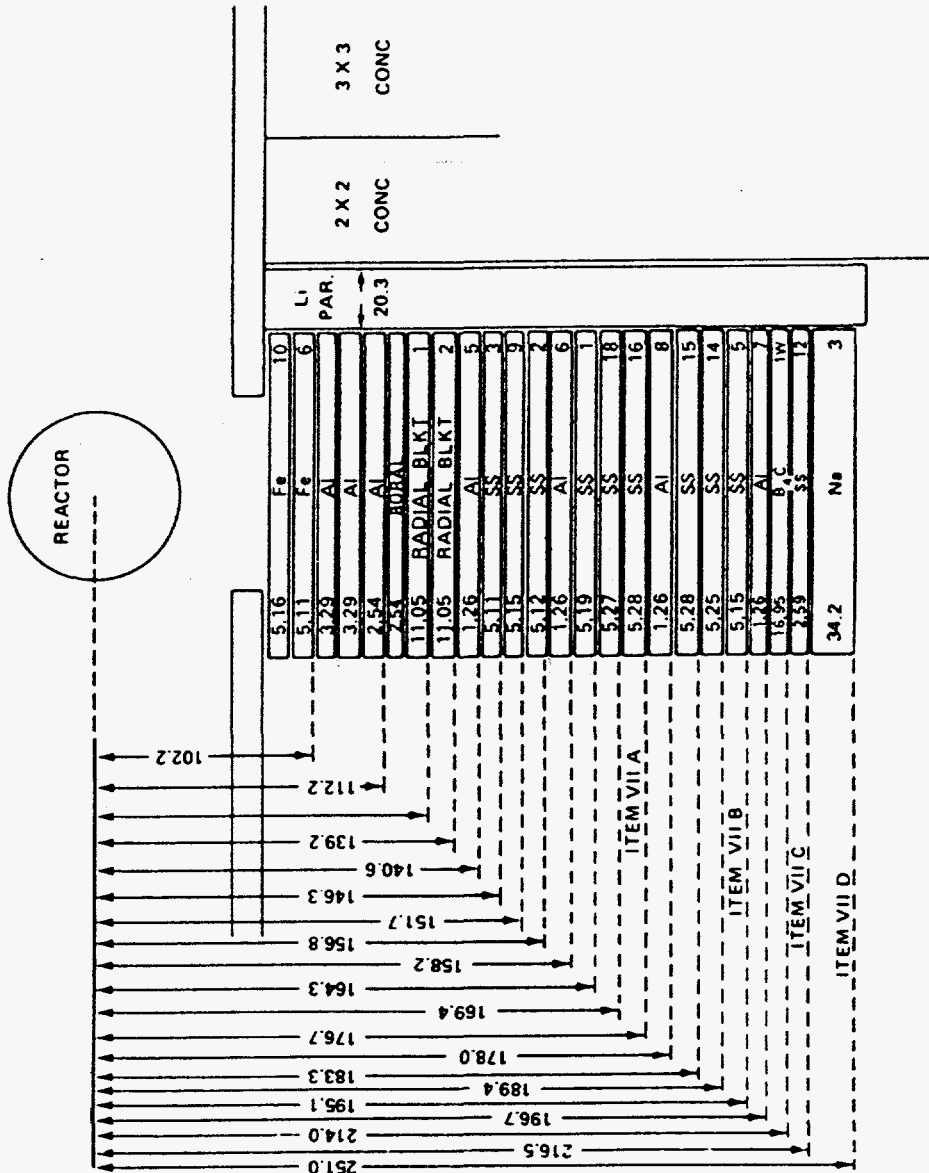


Figure B23. Sketch of the configuration for measurements under sections VII.A-D of the experimental program plan.

APPENDIX C  
ENERGY GROUP STRUCTURES AND MULTIGROUP  
DETECTOR RESPONSE FUNCTIONS USED IN CALCULATIONS

Table C1. 51-Group Response Function for the Bare BF<sub>3</sub> Detector.  
Units are: (Counts · cm<sup>2</sup>/neutron).

Group	Upper Energy (eV)	Response	Group	Upper Energy (eV)	Response
1	1.49200E+07 <sup>a</sup>	6.08293E-05	27	5.24800E+04	1.28557E-03
2	1.22100E+07	9.64387E-05	28	4.08600E+04	1.45530E-03
3	1.00000E+07	1.15173E-04	29	3.18300E+04	1.64764E-03
4	8.18700E+06	1.38946E-04	30	2.47900E+04	1.87795E-03
5	6.70300E+06	1.82038E-04	31	1.90300E+04	2.11134E-03
6	5.48800E+06	1.88700E-04	32	1.50300E+04	2.71548E-03
7	4.49300E+06	1.69184E-04	33	7.10200E+03	3.67985E-03
8	3.67900E+06	1.53397E-04	34	4.30700E+03	4.42658E-03
9	3.01200E+06	1.66163E-04	35	3.35500E+03	5.00872E-03
10	2.46600E-06	1.94736E-04	36	2.61300E+03	5.62130E-03
11	2.01900E+06	2.41792E-04	37	2.03500E+03	6.42654E-03
12	1.65300E+06	1.70912E-04	38	1.58500E+03	7.30401E-03
13	1.35300E+06	1.36139E-04	39	1.23400E+03	8.27696E-03
14	1.10800E+06	1.45402E-04	40	9.61100E+02	1.06452E-02
15	9.07600E+05	1.76148E-04	41	4.54000E+02	1.55501E-02
16	7.42700E+05	2.37209E-04	42	2.14500E+02	2.22467E-02
17	6.08100E+05	3.25078E-04	43	1.01300E+02	3.18797E-02
18	4.97800E+05	3.84333E-04	44	4.78500E+01	4.73209E-02
19	4.07600E+05	3.98219E-04	45	2.26000E+01	7.00329E-02
20	3.33700E+05	4.81773E-04	46	1.06800E+01	1.01495E-01
21	2.73200E+05	6.04378E-04	47	5.04300E+00	1.46607E-01
22	2.23700E+05	6.75572E-04	48	2.38200E+00	2.42090E-01
23	1.83200E+05	7.35003E-04	49	1.12500E+00	3.58920E-01
24	1.50000E+05	7.97585E-04	50	4.14000E-01	5.86870E-01
25	1.22800E+05	8.93137E-04	51 <sup>b</sup>	1.00000E-01	1.11390E+00
26	8.65200E+04	1.08158E-03			

<sup>a</sup>Read as 1.49200 × 10<sup>7</sup>.

<sup>b</sup>Lower energy boundary is 1.0 × 10<sup>-5</sup> eV.



Table C2. 51-Group Response Function for the Cd-Covered BF<sub>3</sub> Detector.  
Units are: (Counts · cm<sup>2</sup>/neutron).

Group	Upper Energy (eV)	Response	Group	Upper Energy (eV)	Response
1	1.49200E+07 <sup>a</sup>	6.08293E-05	27	5.24800E+04	1.28557E-03
2	1.22100E+07	9.64387E-05	28	4.08600E+04	1.45530E-03
3	1.00000E+07	1.15173E-04	29	3.18300E+04	1.64764E-03
4	8.18700E+06	1.38946E-04	30	2.47900E+04	1.87795E-03
5	6.70300E+06	1.82038E-04	31	1.90300E+04	2.11134E-03
6	5.48800E+06	1.88700E-04	32	1.50300E+04	2.71548E-03
7	4.49300E+06	1.69184E-04	33	7.10200E+03	3.67985E-03
8	3.67900E+06	1.53397E-04	34	4.30700E+03	4.42658E-03
9	3.01200E+06	1.66163E-04	35	3.35500E+03	5.00872E-03
10	2.46600E+06	1.94736E-04	36	2.61300E+03	5.62130E-03
11	2.01900E+06	2.41792E-04	37	2.03500E+03	6.42654E-03
12	1.65300E+06	1.70912E-04	38	1.58500E+03	7.30401E-03
13	1.35300E+06	1.36139E-04	39	1.23400E+03	8.27696E-03
14	1.10800E+06	1.45402E-04	40	9.61100E+02	1.06452E-02
15	9.07600E+05	1.76148E-04	41	4.54000E+02	1.55501E-02
16	7.42700E+05	2.37209E-04	42	2.14500E+02	2.22467E-02
17	6.08100E+05	3.25078E-04	43	1.01300E+02	3.18797E-02
18	4.97800E+05	3.84333E-04	44	4.78500E+01	4.73209E-02
19	4.07600E+05	3.98219E-04	45	2.26000E+01	7.00329E-02
20	3.33700E+05	4.81773E-04	46	1.06800E+01	1.01495E-01
21	2.73200E+05	6.04378E-04	47	5.04300E+00	1.46607E-01
22	2.23700E+05	6.75572E-04	48	2.38200E+00	2.07692E-01
23	1.83200E+05	7.35003E-04	49	1.12500E+00	2.28613E-01
24	1.50000E+05	7.97585E-04	50	4.14000E-01	0.0
25	1.22800E+05	8.93137E-04	51 <sup>b</sup>	1.00000E-01	0.0
26	8.65200E+04	1.08158E-03			

<sup>a</sup>Read as 1.49200 × 10<sup>7</sup>.

<sup>b</sup>Lower energy boundary is 1.0 × 10<sup>-5</sup> eV.

Table C3. 51-Group Response Function for the 3-inch Bonner Ball.  
Units are: (Counts · cm<sup>2</sup>/neutron).

Group	Upper Energy (eV)	Response	Group	Upper Energy (eV)	Response
1	1.49200E+07 <sup>a</sup>	3.44697E-03	27	5.24800E+04	2.60266E-01
2	1.22100E+07	4.36754E-03	28	4.08600E+04	2.76680E-01
3	1.00000E+07	5.50543E-03	29	3.18300E+04	2.92975E-01
4	8.18700E+06	6.86545E-03	30	2.47900E+04	3.10526E-01
5	6.70300E+06	9.24691E-03	31	1.90300E+04	3.26311E-01
6	5.48800E+06	1.10365E-02	32	1.50300E+04	3.61419E-01
7	4.49300E+06	1.34925E-02	33	7.10200E+03	4.07614E-01
8	3.67900E+06	1.69481E-02	34	4.30700E+03	4.37120E-01
9	3.01200E+06	2.11136E-02	35	3.35500E+03	4.58520E-01
10	2.46600E+06	2.61091E-02	36	2.61300E+03	4.81026E-01
11	2.01900E+06	3.19911E-02	37	2.03500E+03	5.04895E-01
12	1.65300E+06	3.88334E-02	38	1.58500E+03	5.30163E-01
13	1.35300E+06	4.67591E-02	39	1.23400E+03	5.55102E-01
14	1.10800E+06	5.58187E-02	40	9.61100E+02	6.07197E-01
15	9.07600E+05	6.59898E-02	41	4.54000E+02	6.98568E-01
16	7.42700E+05	7.72060E-02	42	2.14500E+02	7.76309E-01
17	6.08100E+05	8.94341E-02	43	1.01300E+02	7.87411E-01
18	4.97800E+05	1.02508E-01	44	4.78500E+01	8.18827E-01
19	4.07600E+05	1.16211E-01	45	2.26000E+01	9.40470E-01
20	3.33700E+05	1.30279E-01	46	1.06800E+01	1.04548E-00
21	2.73200E+05	1.44609E-01	47	5.04300E+00	1.13841E-00
22	2.23700E+05	1.59106E-01	48	2.38200E+00	1.18444E-00
23	1.83200E+05	1.73572E-01	49	1.12500E+00	8.66930E-01
24	1.50000E+05	1.87950E-01	50	4.14000E-01	0.0
25	1.22800E+05	2.07008E-01	51 <sup>b</sup>	1.00000E-01	0.0
26	8.65200E+04	2.35597E-01			

<sup>a</sup>Read as  $1.49200 \times 10^7$ .

<sup>b</sup>Lower energy boundary is  $1.0 \times 10^{-5}$  eV.

Table C4. 51-Group Response Function for the 5-inch Bonner Ball.  
 Units are: (Counts · cm<sup>2</sup>/neutron).

Group	Upper Energy (eV)	Response	Group	Upper Energy (eV)	Response
1	1.49200E+07 <sup>a</sup>	1.20669E-01	27	5.24800E+04	1.23880E+00
2	1.22100E+07	1.55463E-01	28	4.08600E+04	1.23960E+00
3	1.00000E+07	1.98617E-01	29	3.18300E+04	1.24050E+00
4	8.18700E+06	2.47844E-01	30	2.47900E+04	1.24352E+00
5	6.70300E+06	3.09165E-01	31	1.90300E+04	1.24570E+00
6	5.48800E+06	3.50830E-01	32	1.50300E+04	1.25470E+00
7	4.49300E+06	4.11506E-01	33	7.10200E+03	1.26700E+00
8	3.67900E+06	4.80377E-01	34	4.30700E+03	1.27370E+00
9	3.01200E+06	5.59543E-01	35	3.35500E+03	1.27970E+00
10	2.46600E+06	6.44104E-01	36	2.61300E+03	1.28640E+00
11	2.01900E+06	7.27624E-01	37	2.03500E+03	1.29219E+00
12	1.65300E+06	8.07973E-01	38	1.58500E+03	1.29859E+00
13	1.35300E+06	8.84155E-01	39	1.23400E+03	1.30090E+00
14	1.10800E+06	9.54882E-01	40	9.61100E+02	1.29933E+00
15	9.07600E+05	1.01825E+00	41	4.54000E+02	1.30253E+00
16	7.42700E+05	1.07320E+00	42	2.14500E+02	1.25907E+00
17	6.08100E+05	1.12007E+00	43	1.01300E+02	1.22880E+00
18	4.97800E+05	1.15811E+00	44	4.78500E+01	1.23420E+00
19	4.07600E+05	1.18736E+00	45	2.26000E+01	1.21014E+00
20	3.33700E+05	1.20946E+00	46	1.06800E+01	1.14298E+00
21	2.73200E+05	1.22430E+00	47	5.04300E+00	1.05081E+00
22	2.23700E+05	1.23395E+00	48	2.38200E+00	9.13858E-01
23	1.83200E+05	1.23969E+00	49	1.12500E+00	5.47583E-01
24	1.50000E+05	1.24235E+00	50	4.14000E-01	0.0
25	1.22800E+05	1.24263E+00	51 <sup>b</sup>	1.00000E-01	0.0
26	8.65200E+04	1.24045E+00			

<sup>a</sup>Read as  $1.49200 \times 10^7$ .

<sup>b</sup>Lower energy boundary is  $1.0 \times 10^{-5}$  eV.

Table C5. 51-Group Response Function for the 8-inch Bonner Ball.  
Units are: (Counts · cm<sup>2</sup>/neutron).

Group	Upper Energy (eV)	Response	Group	Upper Energy (eV)	Response
1	1.49200E+07 <sup>a</sup>	4.32326E-01	27	5.24800E+04	6.78782E-01
2	1.22100E+07	5.39892E-01	28	4.08600E+04	6.55690E-01
3	1.00000E+07	6.67276E-01	29	3.18300E+04	6.35525E-01
4	8.18700E+06	7.86134E-01	30	2.47900E+04	6.17751E-01
5	6.70300E+06	9.07779E-01	31	1.90300E+04	6.02962E-01
6	5.48800E+06	9.90159E-01	32	1.50300E+04	5.78139E-01
7	4.49300E+06	1.06950E+00	33	7.10200E+03	5.51763E-01
8	3.67900E+06	1.14892E+00	34	4.30700E+03	5.37200E-01
9	3.01200E+06	1.24834E+00	35	3.35500E+03	5.28644E-01
10	2.46600E-06	1.33619E+00	36	2.61300E+03	5.20655E-01
11	2.01900E+06	1.39025E+00	37	2.03500E+03	5.12425E-01
12	1.65300E+06	1.41070E+00	38	1.58500E+03	5.04734E-01
13	1.35300E+06	1.40779E+00	39	1.23400E+03	4.95599E-01
14	1.10800E+06	1.38561E+00	40	9.61100E+02	4.75849E-01
15	9.07600E+05	1.34711E+00	41	4.54000E+02	4.50639E-01
16	7.42700E+05	1.29614E+00	42	2.14500E+02	4.12817E-01
17	6.08100E+05	1.23801E+00	43	1.01300E+02	4.01933E-01
18	4.97800E+05	1.17527E+00	44	4.78500E+01	3.85773E-01
19	4.07600E+05	1.11077E+00	45	2.26000E+01	3.62755E-01
20	3.33700E+05	1.04936E+00	46	1.06800E+01	3.30363E-01
21	2.73200E+05	9.89847E-01	47	5.04300E+00	2.94706E-01
22	2.23700E+05	9.34578E-01	48	2.38200E+00	2.50431E-01
23	1.83200E+05	8.84631E-01	49	1.12500E+00	1.47241E-01
24	1.50000E+05	8.39704E-01	50	4.14000E-01	0.0
25	1.22800E+05	7.87495E-01	51 <sup>b</sup>	1.00000E-01	0.0
26	8.65200E+04	7.23162E-01			

<sup>a</sup>Read as  $1.49200 \times 10^7$ .

<sup>b</sup>Lower energy boundary is  $1.0 \times 10^{-5}$  eV.

Table C6. 51-Group Response Function for the 10-inch Bonner Ball.  
Units are: (Counts · cm<sup>2</sup>/neutron).

Group	Upper Energy (eV)	Response	Group	Upper Energy (eV)	Response
1	1.49200E+07 <sup>a</sup>	5.78909E-01	27	5.24800E+04	2.69356E-01
2	1.22100E+07	7.00739E-01	28	4.08600E+04	2.57060E-01
3	1.00000E+07	8.39563E-01	29	3.18300E+04	2.46583E-01
4	8.18700E+06	9.46638E-01	30	2.47900E+04	2.37427E-01
5	6.70300E+06	1.04566E+00	31	1.90300E+04	2.29981E-01
6	5.48800E+06	1.10766E+00	32	1.50300E+04	2.17578E-01
7	4.49300E+06	1.12520E+00	33	7.10200E+03	2.04694E-01
8	3.67900E+06	1.14494E+00	34	4.30700E+03	1.97790E-01
9	3.01200E+06	1.18825E+00	35	3.35500E+03	1.93732E-01
10	2.46600E+06	1.21060E+00	36	2.61300E+03	1.89962E-01
11	2.01900E+06	1.18985E+00	37	2.03500E+03	1.86172E-01
12	1.65300E+06	1.13338E+00	38	1.58500E+03	1.82642E-01
13	1.35300E+06	1.06001E+00	39	1.23400E+03	1.78640E-01
14	1.10800E+06	9.77245E-01	40	9.61100E+02	1.70306E-01
15	9.07600E+05	8.90321E-01	41	4.54000E+02	1.59811E-01
16	7.42700E+05	8.03739E-01	42	2.14500E+02	1.45263E-01
17	6.08100E+05	7.22208E-01	43	1.01300E+02	1.53973E-01
18	4.97800E+05	6.47158E-01	44	4.78500E+01	1.47152E-01
19	4.07600E+05	5.79948E-01	45	2.26000E+01	1.37947E-01
20	3.33700E+05	5.22467E-01	46	1.06800E+01	1.25359E-01
21	2.73200E+05	4.72366E-01	47	5.04300E+00	1.11702E-01
22	2.23700E+05	4.29680E-01	48	2.38200E+00	9.48828E-02
23	1.83200E+05	3.93933E-01	49	1.12500E+00	5.57513E-02
24	1.50000E+05	3.63864E-01	50	4.14000E-01	0.0
25	1.22800E+05	3.31235E-01	51 <sup>b</sup>	1.00000E-01	0.0
26	8.65200E+04	2.93774E-01			

<sup>a</sup>Read as  $1.49200 \times 10^7$ .

<sup>b</sup>Lower energy boundary is  $1.0 \times 10^{-5}$  eV.

Table C7. 61-Group Response Function for the Bare BF<sub>3</sub> Detector.  
Units are: (Counts · cm<sup>2</sup>/neutron).

Group	Upper Energy (eV)	Response	Group	Upper Energy (eV)	Response
1	1.49183E+07 <sup>a</sup>	6.08293E-05	32	8.65168E+04	1.08158E-03
2	1.22140E+07	9.63804E-05	33	5.65622E+04	1.08183E-03
3	1.00000E+07	1.15173E-04	34	5.24752E+04	1.35538E-03
4	8.18730E+06	1.38942E-04	35	3.43067E+04	1.56990E-03
5	6.70320E+06	1.82032E-04	36	2.85011E+04	1.64764E-03
6	5.48811E+06	1.88699E-04	37	2.70001E+04	1.64764E-03
7	4.49329E+06	1.69186E-04	38	2.60584E+04	1.64810E-03
8	3.67879E+06	1.53398E-04	39	2.47875E+04	1.87795E-03
9	3.01194E+06	1.66165E-04	40	2.35786E+04	2.00018E-03
10	2.46597E+06	1.94736E-04	41	1.50344E+04	2.71513E-03
11	2.34570E+06	1.94736E-04	42	9.11882E+03	3.19773E-03
12	2.23130E+06	1.94743E-04	43	5.53084E+03	3.95969E-03
13	2.01897E+06	2.41790E-04	44	3.70744E+03	4.71797E-03
14	1.65299E+06	1.70912E-04	45	3.03539E+03	5.00935E-03
15	1.35335E+06	1.36184E-04	46	2.61259E+03	5.62130E-03
16	1.10803E+06	1.45472E-04	47	2.24867E+03	5.62257E-03
17	9.07180E+05	1.76148E-04	48	2.03468E+03	6.86570E-03
18	7.42735E+05	2.37194E-04	49	1.23410E+03	9.46083E-03
19	6.08101E+05	3.25077E-04	50	7.48518E+02	1.06452E-02
20	5.23397E+05	3.25078E-04	51	4.53999E+02	1.55501E-02
21	4.97870E+05	3.87073E-04	52	2.75364E+02	1.89013E-02
22	3.87742E+05	4.31607E-04	53	1.67017E+02	2.22467E-02
23	3.01974E+05	4.81773E-04	54	1.01301E+02	3.18796E-02
24	2.98491E+05	4.81773E-04	55	4.78512E+01	4.73204E-02
25	2.97211E+05	4.81773E-04	56	2.26033E+01	7.00402E-02
26	2.94518E+05	4.81773E-04	57	1.06770E+01	1.01495E-01
27	2.73237E+05	6.04295E-04	58	5.04348E+00	1.46601E-01
28	2.23708E+05	6.75630E-04	59	2.38237E+00	2.42070E-01
29	1.83156E+05	7.35095E-04	60	1.12535E+00	3.58887E-01
30	1.49956E+05	7.97690E-04	61 <sup>b</sup>	4.13994E-01	1.04347E+00
31	1.22773E+05	8.93156E-04			

<sup>a</sup>Read as 1.49183 × 10<sup>7</sup>.

<sup>b</sup>Lower energy boundary is 1.0 × 10<sup>-5</sup> eV.

Table C8. 61-Group Response Function for the Cd-Covered BF<sub>3</sub> Detector.  
Units are: (Counts · cm<sup>2</sup>/neutron).

Group	Upper Energy (eV)	Response	Group	Upper Energy (eV)	Response
1	1.49183E+07 <sup>a</sup>	6.08293E-05	32	8.65168E+04	1.08158E-03
2	1.22140E+07	9.63804E-05	33	5.65622E+04	1.08183E-03
3	1.00000E+07	1.15173E-04	34	5.24752E+04	1.35538E-03
4	8.18730E+06	1.38942E-04	35	3.43067E+04	1.56990E-03
5	6.70320E+06	1.82032E-04	36	2.85011E+04	1.64764E-03
6	5.48811E+06	1.88699E-04	37	2.70001E+04	1.64764E-03
7	4.49329E+06	1.69186E-04	38	2.60584E+04	1.64810E-03
8	3.67879E+06	1.53398E-04	39	2.47875E+04	1.87795E-03
9	3.01194E+06	1.66165E-04	40	2.35786E+04	2.00018E-03
10	2.46597E+06	1.94736E-04	41	1.50344E+04	2.71513E-03
11	2.34570E+06	1.94736E-04	42	9.11882E+03	3.19773E-03
12	2.23130E+06	1.94743E-04	43	5.53084E+03	3.95969E-03
13	2.01897E+06	2.41790E-04	44	3.70744E+03	4.71797E-03
14	1.65299E+06	1.70912E-04	45	3.03539E+03	5.00935E-03
15	1.35335E+06	1.36184E-04	46	2.61259E+03	5.62130E-03
16	1.10803E+06	1.45472E-04	47	2.24867E+03	5.62257E-03
17	9.07180E+05	1.76148E-04	48	2.03468E+03	6.86570E-03
18	7.42735E+05	2.37194E-04	49	1.23410E+03	9.46083E-03
19	6.08101E+05	3.25077E-04	50	7.48518E+02	1.06452E-02
20	5.23397E+05	3.25078E-04	51	4.53999E+02	1.55501E-02
21	4.97870E+05	3.87073E-04	52	2.75364E+02	1.89013E-02
22	3.87742E+05	4.31607E-04	53	1.67017E+02	2.22467E-02
23	3.01974E+05	4.81773E-04	54	1.01301E+02	3.18796E-02
24	2.98491E+05	4.81773E-04	55	4.78512E+01	4.73204E-02
25	2.97211E+05	4.81773E-04	56	2.26033E+01	7.00402E-02
26	2.94518E+05	4.81773E-04	57	1.06770E+01	1.01495E-01
27	2.73237E+05	6.04295E-04	58	5.04348E+00	1.46601E-01
28	2.23708E+05	6.75630E-04	59	2.38237E+00	2.07679E-01
29	1.83156E+05	7.35095E-04	60	1.12535E+00	2.28603E-01
30	1.49956E+05	7.97690E-04	61 <sup>b</sup>	4.13994E-01	0.0
31	1.22773E+05	8.93156E-04			

<sup>a</sup>Read as 1.49183 × 10<sup>7</sup>.

<sup>b</sup>Lower energy boundary is 1.0 × 10<sup>-5</sup> eV.

Table C9. 61-Group Response Function for the 3-inch Bonner Ball.  
Units are: (Counts · cm<sup>2</sup>/neutron).

Group	Upper Energy (eV)	Response	Group	Upper Energy (eV)	Response
1	1.49183E+07 <sup>a</sup>	3.44697E-03	32	8.65168E+04	2.35597E-01
2	1.22140E+07	4.36603E-03	33	5.65622E+04	2.35627E-01
3	1.00000E+07	5.50542E-03	34	5.24752E+04	2.67017E-01
4	8.18730E+06	6.86520E-03	35	3.43067E+04	2.86389E-01
5	6.70320E+06	9.24655E-03	36	2.85011E+04	2.92975E-01
6	5.48811E+06	1.10363E-02	37	2.70001E+04	2.92975E-01
7	4.49329E+06	1.34927E-02	38	2.60584E+04	2.93010E-01
8	3.67879E+06	1.69485E-02	39	2.47875E+04	3.10526E-01
9	3.01194E+06	2.11139E-02	40	2.35786E+04	3.18793E-01
10	2.46597E+06	2.61091E-02	41	1.50344E+04	3.61398E-01
11	2.34570E+06	2.61091E-02	42	9.11882E+03	3.84520E-01
12	2.23130E+06	2.61100E-02	43	5.53084E+03	4.18671E-01
13	2.01897E+06	3.19913E-02	44	3.70744E+03	4.47832E-01
14	1.65299E+06	3.88334E-02	45	3.03539E+03	4.58543E-01
15	1.35335E+06	4.67488E-02	46	2.61259E+03	4.81026E-01
16	1.10803E+06	5.58410E-02	47	2.24867E+03	4.81064E-01
17	9.07180E+05	6.59897E-02	48	2.03468E+03	5.17541E-01
18	7.42735E+05	7.72032E-02	49	1.23410E+03	5.81143E-01
19	6.08101E+05	8.94339E-02	50	7.48518E+02	6.07197E-01
20	5.23397E+05	8.94340E-02	51	4.53999E+02	6.98568E-01
21	4.97870E+05	1.05238E-01	52	2.75364E+02	7.37472E-01
22	3.87742E+05	1.21833E-01	53	1.67017E+02	7.76309E-01
23	3.01974E+05	1.30279E-01	54	1.01301E+02	7.87411E-01
24	2.98491E+05	1.30279E-01	55	4.78512E+01	8.18826E-01
25	2.97211E+05	1.30279E-01	56	2.26033E+01	9.40486E-01
26	2.94518E+05	1.30279E-01	57	1.06770E+01	1.04548E+00
27	2.73237E+05	1.44599E-01	58	5.04348E+00	1.13840E+00
28	2.23708E+05	1.59121E-01	59	2.38237E+00	1.18443E+00
29	1.83156E+05	1.73593E-01	60	1.12535E+00	8.67016E-01
30	1.49956E+05	1.87971E-01	61 <sup>b</sup>	4.13994E-01	0.0
31	1.22773E+05	2.07011E-01			

<sup>a</sup>Read as  $1.49183 \times 10^7$ .

<sup>b</sup>Lower energy boundary is  $1.0 \times 10^{-5}$  eV.



Table C10. 61-Group Response Function for the 5-inch Bonner Ball.  
Units are: (Counts · cm<sup>2</sup>/neutron).

Group	Upper Energy (eV)	Response	Group	Upper Energy (eV)	Response
1	1.49183E+07 <sup>a</sup>	1.20669E-01	32	8.65168E+04	1.24045E+00
2	1.22140E+07	1.55406E-01	33	5.65622E+04	1.24045E+00
3	1.00000E+07	1.98617E-01	34	5.24752E+04	1.23913E+00
4	8.18730E+06	2.47835E-01	35	3.43067E+04	1.24014E+00
5	6.70320E+06	3.09156E-01	36	2.85011E+04	1.24050E+00
6	5.48811E+06	3.50826E-01	37	2.70001E+04	1.24050E+00
7	4.49329E+06	4.11506E-01	38	2.60584E+04	1.24051E+00
8	3.67879E+06	4.80385E-01	39	2.47875E+04	1.24352E+00
9	3.01194E+06	5.59548E-01	40	2.35786E+04	1.24466E+00
10	2.46597E+06	6.44104E-01	41	1.50344E+04	1.25469E+00
11	2.34570E+06	6.44104E-01	42	9.11882E+03	1.26085E+00
12	2.23130E+06	6.44116E-01	43	5.53084E+03	1.26951E+00
13	2.01897E+06	7.27626E-01	44	3.70744E+03	1.27670E+00
14	1.65299E+06	8.07973E-01	45	3.03539E+03	1.27971E+00
15	1.35335E+06	8.84056E-01	46	2.61259E+03	1.28640E+00
16	1.10803E+06	9.55019E-01	47	2.24867E+03	1.28641E+00
17	9.07180E+05	1.01825E+00	48	2.03468E+03	1.29539E+00
18	7.42735E+05	1.07318E+00	49	1.23410E+03	1.30011E+00
19	6.08101E+05	1.12007E+00	50	7.48518E+02	1.29933E+00
20	5.23397E+05	1.12007E+00	51	4.53999E+02	1.30253E+00
21	4.97870E+05	1.16393E+00	52	2.75364E+02	1.28078E+00
22	3.87742E+05	1.19619E+00	53	1.67017E+02	1.25907E+00
23	3.01974E+05	1.20946E+00	54	1.01301E+02	1.22880E+00
24	2.98491E+05	1.20946E+00	55	4.78512E+01	1.23420E+00
25	2.97211E+05	1.20946E+00	56	2.26033E+01	1.21012E+00
26	2.94518E+05	1.20946E+00	57	1.06770E+01	1.14298E+00
27	2.73237E+05	1.22429E+00	58	5.04348E+00	1.05082E+00
28	2.23708E+05	1.23395E+00	59	2.38237E+00	9.13886E-01
29	1.83156E+05	1.23969E+00	60	1.12535E+00	5.47689E-01
30	1.49956E+05	1.24235E+00	61 <sup>b</sup>	4.13994E-01	0.0
31	1.22773E+05	1.24263E+00			

<sup>a</sup>Read as  $1.49183 \times 10^7$ .

<sup>b</sup>Lower energy boundary is  $1.0 \times 10^{-5}$  eV.

Table C11. 61-Group Response Function for the 8-inch Bonner Ball.  
 Units are: (Counts · cm<sup>2</sup>/neutron).

Group	Upper Energy (eV)	Response	Group	Upper Energy (eV)	Response
1	1.49183E+07 <sup>a</sup>	4.32326E-01	32	8.65168E+04	7.23162E-01
2	1.22140E+07	5.39716E-01	33	5.65622E+04	7.23108E-01
3	1.00000E+07	6.67276E-01	34	5.24752E+04	6.69284E-01
4	8.18730E+06	7.86112E-01	35	3.43067E+04	6.43675E-01
5	6.70320E+06	9.07761E-01	36	2.85011E+04	6.35525E-01
6	5.48811E+06	9.90151E-01	37	2.70001E+04	6.35525E-01
7	4.49329E+06	1.06950E+00	38	2.60584E+04	6.35489E-01
8	3.67879E+06	1.14893E+00	39	2.47875E+04	6.17751E-01
9	3.01194E+06	1.24834E+00	40	2.35786E+04	6.10005E-01
10	2.46597E+06	1.33619E+00	41	1.50344E+04	5.78153E-01
11	2.34570E+06	1.33619E+00	42	9.11882E+03	5.64949E-01
12	2.23130E+06	1.33620E+00	43	5.53084E+03	5.46305E-01
13	2.01897E+06	1.39025E+00	44	3.70744E+03	5.32917E-01
14	1.65299E+06	1.41070E+00	45	3.03539E+03	5.28635E-01
15	1.35335E+06	1.40779E+00	46	2.61259E+03	5.20655E-01
16	1.10803E+06	1.38552E+00	47	2.24867E+03	5.20642E-01
17	9.07180E+05	1.34711E+00	48	2.03468E+03	5.08575E-01
18	7.42735E+05	1.29615E+00	49	1.23410E+03	4.85726E-01
19	6.08101E+05	1.23801E+00	50	7.48518E+02	4.75849E-01
20	5.23397E+05	1.23801E+00	51	4.53999E+02	4.50639E-01
21	4.97870E+05	1.16242E+00	52	2.75364E+02	4.31711E-01
22	3.87742E+05	1.08623E+00	53	1.67017E+02	4.12817E-01
23	3.01974E+05	1.04936E+00	54	1.01301E+02	4.01933E-01
24	2.98491E+05	1.04936E+00	55	4.78512E+01	3.85773E-01
25	2.97211E+05	1.04936E+00	56	2.26033E+01	3.62747E-01
26	2.94518E+05	1.04936E+00	57	1.06770E+01	3.30363E-01
27	2.73237E+05	9.89887E-01	58	5.04348E+00	2.94710E-01
28	2.23708E+05	9.34528E-01	59	2.38237E+00	2.50440E-01
29	1.83156E+05	8.84565E-01	60	1.12535E+00	1.47271E-01
30	1.49956E+05	8.39646E-01	61 <sup>b</sup>	4.13994E-01	0.0
31	1.22773E+05	7.87488E-01			

<sup>a</sup>Read as 1.49183 × 10<sup>7</sup>.

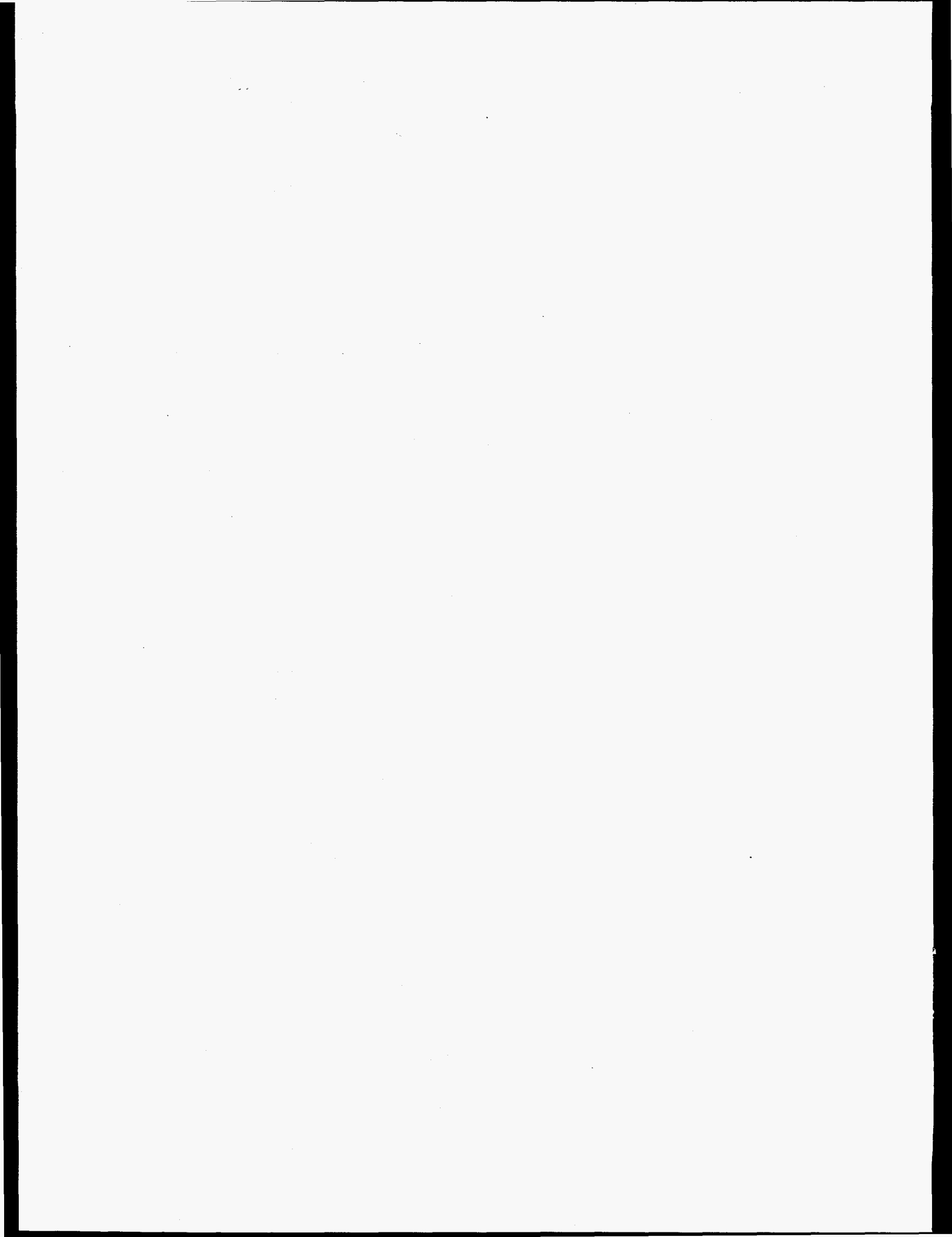
<sup>b</sup>Lower energy boundary is 1.0 × 10<sup>-5</sup> eV.

Table C12. 61-Group Response Function for the 10-inch Bonner Ball.  
Units are: (Counts · cm<sup>2</sup>/neutron).

Group	Upper Energy (eV)	Response	Group	Upper Energy (eV)	Response
1	1.49183E+07 <sup>a</sup>	5.78909E-01	32	8.65168E+04	2.93774E-01
2	1.22140E+07	7.00540E-01	33	5.65622E+04	2.93744E-01
3	1.00000E+07	8.39563E-01	34	5.24752E+04	2.64298E-01
4	8.18730E+06	9.46618E-01	35	3.43067E+04	2.50817E-01
5	6.70320E+06	1.04564E+00	36	2.85011E+04	2.46583E-01
6	5.48811E+06	1.10765E+00	37	2.70001E+04	2.46583E-01
7	4.49329E+06	1.12520E+00	38	2.60584E+04	2.46564E-01
8	3.67879E+06	1.14494E+00	39	2.47875E+04	2.37427E-01
9	3.01194E+06	1.18825E+00	40	2.35786E+04	2.33527E-01
10	2.46597E+06	1.21060E+00	41	1.50344E+04	2.17585E-01
11	2.34570E+06	1.21060E+00	42	9.11882E+03	2.11135E-01
12	2.23130E+06	1.21060E+00	43	5.53084E+03	2.02107E-01
13	2.01897E+06	1.18985E+00	44	3.70744E+03	1.95759E-01
14	1.65299E+06	1.13338E+00	45	3.03539E+03	1.93728E-01
15	1.35335E+06	1.06010E+00	46	2.61259E+03	1.89962E-01
16	1.10803E+06	9.77055E-01	47	2.24867E+03	1.89956E-01
17	9.07180E+05	8.90321E-01	48	2.03468E+03	1.84405E-01
18	7.42735E+05	8.03759E-01	49	1.23410E+03	1.74474E-01
19	6.08101E+05	7.22208E-01	50	7.48518E+02	1.70306E-01
20	5.23397E+05	7.22208E-01	51	4.53999E+02	1.59811E-01
21	4.97870E+05	6.33772E-01	52	2.75364E+02	1.52531E-01
22	3.87742E+05	5.56978E-01	53	1.67017E+02	1.45263E-01
23	3.01974E+05	5.22467E-01	54	1.01301E+02	1.53973E-01
24	2.98491E+05	5.22467E-01	55	4.78512E+01	1.47152E-01
25	2.97211E+05	5.22467E-01	56	2.26033E+01	1.37944E-01
26	2.94518E+05	5.22467E-01	57	1.06770E+01	1.25359E-01
27	2.73237E+05	4.72399E-01	58	5.04348E+00	1.11704E-01
28	2.23708E+05	4.29645E-01	59	2.38237E+00	9.48862E-02
29	1.83156E+05	3.93889E-01	60	1.12535E+00	5.57627E-02
30	1.49956E+05	3.63828E-01	61 <sup>b</sup>	4.13994E-01	0.0
31	1.22773E+05	3.31231E-01			

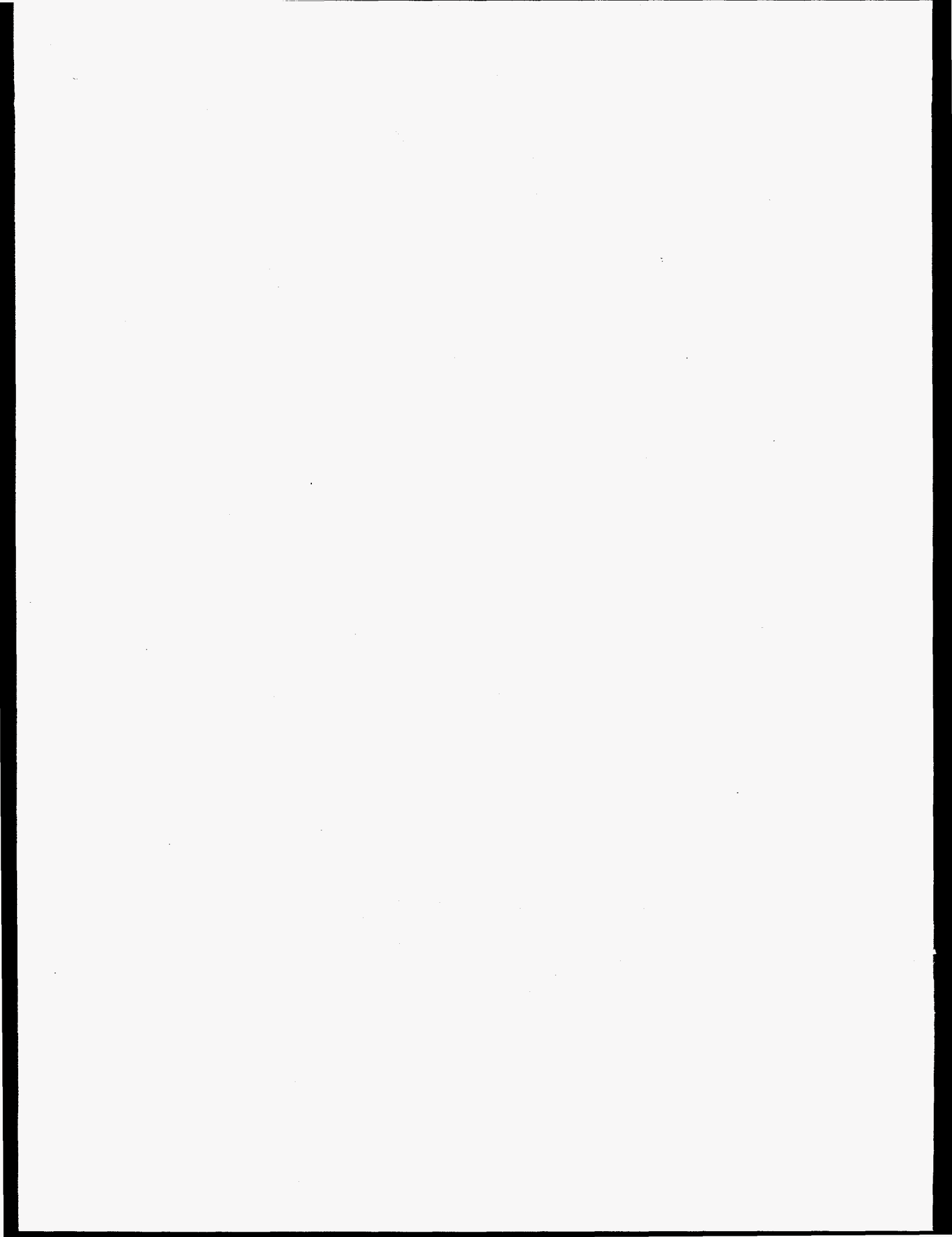
<sup>a</sup>Read as  $1.49183 \times 10^7$ .

<sup>b</sup>Lower energy boundary is  $1.0 \times 101^{-5}$  eV.



## REFERENCES

1. F. J. Muckenthaler et al., "Measurements for the JASPER Program Radial Shield Attenuation Experiment," ORNL/TM-10371, May 1987.
2. W. A. Rhoades and R. L. Childs, "An Updated Version of the DOT 4 One- and Two-Dimensional Neutron/Photon Transport Code," ORNL-5851, July 1982.
3. W. W. Engle, Jr., "A User's Manual for ANISN: A One-Dimensional Discrete Ordinates Transport Code with Anisotropic Scattering," Union Carbide Nuclear Division Report K-1693, 1967.
4. D. E. Bartine, F. R. Mynatt, and E. M. Oblow, SWANLAKE, "A Computer Code Utilizing ANISN Radiation Transport Calculations for Cross Section Sensitivity Analysis," ORNL/TM-3809, May 1973.
5. R. E. Maerker et al., "Final Report on a Benchmark Experiment for Neutron Transport in Thick Sodium," ORNL-4880, 1974.
6. C. Y. Fu and D. T. Ingersoll, "VELM61 and VELM22: Multigroup Cross-Section Libraries for Sodium-Cooled Reactor Shield Analysis," ORNL/TM-10302, April 1987.
7. C. Y. Fu and D. M. Hetrick, "Update of ENDF/B-V Mod-3 Iron: Neutron-Producing Reaction Cross Sections and Energy-Angle Correlations," ORNL/TM-9964 (ENDF-341), July 1986.
8. R. E. Maerker et al., "Response Functions for Bonner Ball Neutron Detectors," ORNL/TM-3451, 1971.
9. W. W. Engle, Jr., "AMP (Activity Manipulation Program)," ORNL/TM-5296, Union Carbide Corp., Oak Ridge National Lab., June 1975.
10. R. E. Maerker and F. J. Muckenthaler, "The Absolute Neutron Spectrum Emerging Through the Large Beam Collimator from the TSR-II Reactor at the Tower Shielding Facility," ORNL/TM-5183, 1976.
11. C. O. Slater, "Analysis of the ORNL/TSF Alternate Shielding Materials Experiment," ORNL/TM-10183, April 1987.
12. F. J. Muckenthaler et al., "Measurements for the LMR Alternate Shielding Materials Experiment," ORNL/TM-9977, October 1986.



## INTERNAL DISTRIBUTION

- |     |                    |        |                               |
|-----|--------------------|--------|-------------------------------|
| 1.  | B. R. Appleton     | 21.    | F. R. Mynatt                  |
| 2.  | Y. Y. Azmy         | 22-26. | J. V. Pace, III               |
| 3.  | J. M. Barnes       | 27.    | W. A. Rhoades                 |
| 4.  | B. L. Broadhead    | 28.    | R. W. Roussin                 |
| 5.  | J. A. Bucholz      | 29.    | R. T. Santoro                 |
| 6.  | T. J. Burns        | 30.    | A. Shono                      |
| 7.  | R. L. Childs       | 31-35. | C. O. Slater                  |
| 8.  | J. D. Drischler    | 36.    | M. S. Smith                   |
| 9.  | M. B. Emmett       | 37.    | R. R. Spencer                 |
| 10. | W. W. Engle, Jr.   | 38.    | J. S. Tang                    |
| 11. | C. Y. Fu           | 39.    | R. C. Ward                    |
| 12. | L. B. Holland      | 40.    | J. D. White                   |
| 13. | F. J. Homan        | 41.    | J. E. White                   |
| 14. | J. L. Hull         | 42.    | L. R. Williams                |
| 15. | H. J. Hunter       | 43.    | EPMD Reports Office           |
| 16. | D. T. Ingersoll    | 44-45. | Laboratory Records Department |
| 17. | J. O. Johnson      | 46.    | Laboratory Records, ORNL-RC   |
| 18. | R. A. Lillie       | 47.    | Document Reference Section    |
| 19. | R. E. Maerker      | 48.    | Central Research Library      |
| 20. | F. J. Muckenthaler | 49.    | ORNL Patent Section           |

## EXTERNAL DISTRIBUTION

50. Office of the Assistant Manager for Energy Research and Development, Department of Energy, Oak Ridge Operations, P.O. Box 2001, Oak Ridge, TN 37831-6269
- 51-62. Office of Scientific and Technical Information, P.O. Box 62, Oak Ridge, TN 37831
63. L. F. Blankner, Energy Research and Development, DOE-OR, P.O. Box 2008, Oak Ridge, TN 37831-6269
64. R. W. Brockett, Harvard University, Pierce Hall, 29 Oxford Street, Cambridge, MA 02138
65. L. L. Carter, Westinghouse Hanford Company, 400 Area Trailer 1, P.O. Box 1970, Richland, WA 99352
66. K. Chatani, Power Reactor and Nuclear Fuel Development Corporation, 4002 Narita-Cho, O-Arai-Machi, Ibaraki-Ken, 311-13, Japan
67. R. K. Disney, Westinghouse Electric Company, P.O. Box 158, Madison, PA 15663

68. J. J. Dorning, Department of Nuclear Engineering and Engineering Physics, Reactor Facility, University of Virginia, Charlottesville, VA 22903-2442
69. P. B. Hemmig, Safety and Physics Branch, Office of Technology Support Programs, DOE-Washington, Washington, DC 20585
70. J. E. Leiss, Rt. 2, Box 142C, Broadway, VA 22815
71. Professor Neville Moray, University of Illinois, Dept. of Mechanical and Ind. Engineering, 1206 West Green Street, Urbana, IL 61801
72. M. F. Wheeler, Department of Mathematics, Rice University, Post Office Box 1892, Houston, Texas 77251
73. K. Takahashi, Power Reactor and Nuclear Fuel Development Corporation, Sankaido Building, 9-13, 1-Chrome, Minato-Ku, Tokyo, Japan
74. M. Tsutsumi, Power Reactor and Nuclear Fuel Development Corporation-Washington, Suite 715, 2600 Virginia Avenue NW, Washington, DC 20037
- 75-149. Given distribution as shown in DOE/OSTI-4500-R75, LMFBR-Reactor Core Systems, UC-535'